NREL/SR-520-23942 • UC Category: 1270

Photovoltaic Module Energy Rating Procedure

Final Subcontract Report

C.M. Whitaker and J.D. Newmiller
Endecon Engineering
San Ramon, California

NREL technical monitor: B. Kroposki

National Renewable Energy Laboratory
1617 Cole Boulevard
Golden, Colorado 80401-3393
A national laboratory of
the U.S. Department of Energy
Managed by Midwest Research Institute
for the U.S. Department of Energy
under Contract No. DE-AC36-83CH10093

Prepared under Subcontract No. AAI-4-14192-01

January 1998

NOTICE

Available to DOE and DOE contractors from:
Office of Scientific and Technical Information (OSTI)
P.O. Box 62
Oak Ridge, TN 37831
Prices available by calling (423) 576-8401

Available to the public from:
National Technical Information Service (NTIS)
U.S. Department of Commerce
5285 Port Royal Road
Springfield, VA 22161
(703) 487-4650

Printed on paper containing at least 50% wastepaper, including 20% postconsumer waste

Acknowledgments

The authors wish to express their gratitude to all of the individuals who provided ideas, support, and guidance to this project. The following people deserve special recognition. Benjamin Kroposki of NREL performed most of the outdoor measurements, compiled data from a number of sources, made sure the data got to us, and took the torch at the end of the project. Daryl Myers of NREL provided irradiance model code, evaluated the NSRDB data and selected the reference days. Keith Emery of NREL oversaw most of the indoor measurements and provided code and guidance for the spectral and incidence angle models. Laxmi Mrig of NREL was the project manager and TRC Chairman. Jerry Anderson of Sunset Technologies provided one of the performance models as well as a number of great ideas that have been incorporated in this procedure. Tim Townsend of Endecon Engineering and Howard Wenger of Pacific Energy Group also provided a good deal of useful input and feedback.

We would also like to thank the members of the Technical Review Committee for their interest, knowledge, guidance, and patience. The members of the TRC were:

Scott Albright
Jerry Anderson
Gobind Atmaram
Moneer Azzam
Joe Burdick
Eric Daniels
Alan Delahoy
Steve Durand
Pete Eckert
Sam Edwards
Keith Emery
Brian Farmer
Vahan Garboushian
Subhendu Guha
Robert Hammond
Mandy Herner
Steve Hogan
Neil Kaminar
David King
Ben Kroposki
Leslie Libby
Alex Maish
Laxmi Mrig
Daryl Myers
Mark O'Neill
Don Osborn
Carl Osterwald
Miles Russell
Mike Stern
Chuck Whitaker
John Wohlgemuth
Teddy Zhou

Table of Contents

Section **Page**

Table of Contents (cont.)

Section **Page**

Table of Contents (cont.)

Section **Page**

Table of Contents (cont.)

Section **Page**

1. INTRODUCTION

In May 1994, the National Renewable Energy Laboratory (NREL) initiated an effort to develop a consensus-based approach to rating photovoltaic modules. This new approach was intended to address the limitations of the de-facto standard module power rating at Standard Test Conditions (STC[1]). Using technical input from a number of sources and under the guidance of an industry-based Technical Review Committee, the approach described in this document was developed.

This document describes testing and computation procedures used to generate a photovoltaic Module Energy Rating (MER). The MER consists of 10 estimates the amount of energy a single module of a particular type (make and model) will produce in one day. Module energy values are calculated for each of 5 different sets of weather conditions (defined by location and date), and 2 load-types. Since reproduction of these exact testing conditions in the field or laboratory is not feasible, limited testing and modeling procedures and assumptions are specified.

1.1 Background

Presently, manufacturers supply a module's rating (power, open circuit voltage, short circuit current, peak power voltage and current) at STC, the module's Nominal Operating Cell Temperature (NOCT[2]), and possibly voltage and current temperature coefficients. With these parameters, a user can translate the module rating to another set of conditions. Translation accuracy is strongly dependent on the translation range and on equation complexity.

Pacific Gas and Electric Company and others found that most PV modules mounted outdoors rarely, if ever, produce their rated power. This discrepancy is due, in large part, to the fact that under high irradiance conditions (>500 W/m^2), PV modules typically operate much hotter than the 25°C cell temperature specified by STC. Based on this experience, systems procured by the Photovoltaics for Utility Scale Applications (PVUSA) project are rated at PVUSA Test Conditions (PTC[3]), which are more indicative

---

[1] STC: 1000 W/m^2 irradiance with an Air Mass 1.5 spectrum and 25°C cell temperature.

[2] NOCT: 800 W/m^2 irradiance, 1 m/s wind speed, 20°C ambient temperature, single module, open circuited.

[3] PTC: 1000 W/m^2 irradiance, 1 m/s wind speed, and 20°C ambient temperature.

than STC of peak performance conditions in many other locations. By specifying ambient conditions rather than module conditions, PTC also allows for a more realistic comparison of modules and array designs with different thermal characteristics.

While PTC is a step in the right direction, a single point rating does not account for variations in performance with changing conditions. Specifically, different technologies have different temperature coefficients (change of electrical output due to changes in device temperature), thermal characteristics (change in device temperature due to changes in ambient conditions), spectral response characteristics, and solar angle of incidence response characteristics.

The need for something beyond an STC power rating goes back at least 15 years to Gay's [1,2] AM/PM approach. Reference [2] accurately describes the issues that need to be addressed. AM/PM is simply the module energy produced for a standard day as defined by profiles of irradiance, ambient temperature, and air mass. Through AM/PM, Gay was trying to characterize the module's thermal response to ambient conditions and its power production as a function of light intensity, spectral content and module temperature.

Ideally, a performance rating should allow the user to compare not only similar products from different manufacturers, but different technologies as well, and should provide a realistic performance measure for the installation region. The ideal rating would provide values that could be used by designers to quickly generate first-cut system designs. The information necessary to convey the module rating would be simple enough to be included on the module's label. The procedure for generating the rating would be well defined and repeatable. Because the rating predicts performance for real operating conditions, the industry would be compelled to optimize their cell and module designs for real conditions rather than for STC. However, because the conditions really are representative, the rating would not unduly tax the industry. Rather, it might show that one technology works best in one climate region, but not as well in another region. Finally, because the rating accurately describes a module's performance, the method would be unanimously accepted by the general PV community including manufacturers, installers, users, and researchers. In summary, the rating should:

- provide relative comparison of different manufacturers and technologies
- provide realistic performance for the contemplated site

- be easy to use, simple to convey, and accurate
- have the blessing of the PV community

1.2 Approach

As stated above, the module energy rating is based on modeled performance under give sets of weather conditions and two load types.

The five sets of weather conditions provide the basic range of environmental conditions anticipated for typical uses of PV modules in the US, and allow for comparison of module performance under a wide variety of conditions. The National Solar Resource Database (NSRDB) was selected as the source of the weather data. By doing so, entire daily weather profiles can be specified simply by indicating a city name and a location.

Two load types are assumed, corresponding to the two most common loads connected to PV modules: maximum power tracking for grid-tied applications and fixed voltage for battery charging.

For purposes of rating comparison, a 14.4-Volt (V) operating voltage per battery (2.4 V/battery-cell) is assumed. The 14.4 V value may be divided by the recommended number of modules and multiplied by the recommended number of batteries to obtain a fixed voltage for purposes of rating. If the manufacturer does not recommend this module for battery application, then the modules need not be rated for fixed voltage. It is assumed that no charge regulation occurs; that is, the module operates at 14.4 V whenever there is sufficient sun.

The information presented here is the results of the combined efforts of Endecon Engineering, the National Renewable Energy Laboratory, and Sunset Technology, as well as the members of the Technical Review Committee (TRC). The 35 TRC members represent PV manufacturers, system integrators, government and academic researchers and industry consultants. This group guided the technical and philosophical approach and reviewed results.

The following sections describe the MER computations and the corresponding module testing procedures to obtain the module-specific input data.

2. MODULE ENERGY RATING COMPUTATION

The Module Energy Rating consists of measuring module characteristics, defining sets of weather and load conditions, and estimating module performance under those conditions. This section describes the last of these three processes. The selection of performance estimating (modeling) tools must be completed first as they define which weather parameters and which module characteristics are necessary.

Based on the experience of the project team and the guidance of the TRC, five modeling areas were considered essential to adequately estimate module performance:

1) *Irradiance*: estimating the magnitudes of the various components of sunlight striking the module

2) *Thermal*: estimating the module temperature based on module characteristics and weather conditions

3) *Spectral*: estimating the response of the module to changes in the solar spectrum

4) *Optical*: accounting for optical effects, such as reflection loss at high angles of solar incidence

5) *Power*: estimating module output based on a characterization of the module, and the defined weather data and the results of the other models

Figure 2-1 shows conceptually the flow of data and the relationships between the various models. We will start at the right side of the diagram and work our way to the left. First, the algorithms used in each of the computational process (the circles in Figure 2-1) are described. Next, the input variables (the rectangles in the figure) required for each process are presented.

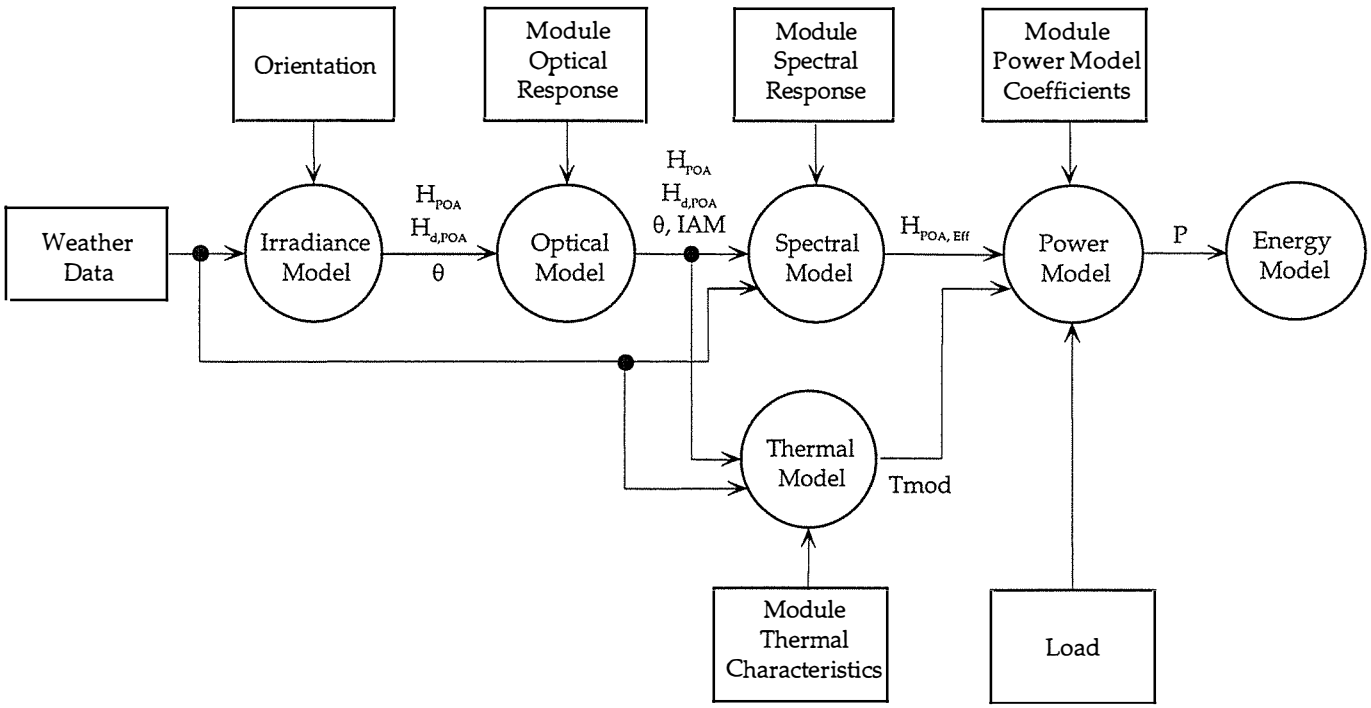

Figure 2-1 Model Flow Diagram

2.1 Algorithms

This section discusses the computation processes shown in Figure 2-1. The model inputs are described in the next section.

2.1.1 Energy Computation

Energy is computed from the daily power production curves by numerical integration according to the following formula (Euler integration):

$$E = \Delta t \cdot \sum_{i=1}^{n} P_i \qquad (2\text{-}1)$$

where

E = Module output energy (Wh)

Δt = Data sampling interval (hours)

P_i = Power at the ith sample time (W)

This method is as accurate for daily power integration as trapezoidal integration would be, because the power at the beginning and end of the interval (midnight) is zero.

2.1.2 DC Power Model

The power output of the module is computed from the plane-of-array irradiance (adjusted for spectral and incidence-angle effects), the module temperature, and appropriate coefficients. Ultimately, this methodology will specify only one power model. Each model is required to estimate power output for maximum power operation and ampere-hours for fixed voltage operating conditions. Five models have been investigated: linear (Myers), interpolation, Anderson, Blaesser, and the lumped four-parameter model.

The first model is a simple linear-fit model that only depends on irradiance. This model is included to help estimate the value of the refinements used in the other power and minor effects models.

The second model uses the raw data supplied by the module characterization process (a matrix of IV curves dependent on irradiance and temperature) and extracts appropriate maximum power and fixed voltage points for each irradiance/temperature combination. The resulting two tables are used to linearly interpolate the power behavior as desired.

The third and fourth models use translation models (developed by J. Anderson and G. Blaesser, respectively) to translate an IV curve taken at reference irradiance and temperature conditions to the actual conditions.

The fifth model is the only analytical model that was investigated. Suggested by T. Townsend, this model described the module as a single, lumped diode and a series resistance.

The following sections describe these models in more detail.

2.1.2.1 Linear Irradiance-Only (Myers) Model

This model was proposed by D. Myers of NREL. Myers noted that the errors inherent in the measurement of the input parameters to various power models might be larger than the magnitude of the contributions of any parameters other than irradiance. His proposal is to use the following equation:

$$P = a \cdot H + b \tag{2-2}$$

where

P = power out of module (W)

H = Plane-of-array irradiance (W/m^2)

a, b = Least-squares fit coefficients (m^2, W)

using field measured data as the basis for determining the a and b coefficients. Field measured data must be used because the effect of irradiance on module temperature in field conditions must be included in the coefficients for this equation to work best.

Note that this model does not predict the shape of the IV curve at all. Therefore, this model will only be compared to the other models for the maximum power case.

2.1.2.2 Interpolation Model

Determining model coefficients for a module often requires data from an irradiance/temperature cross-sensitivity test where module IV curves are measured under various controlled irradiance and temperature conditions. Rather than calculating performance coefficients, the interpolation model uses the sensitivity data directly. It does not attempt to simplify or fit any particular equation to the data; rather, it uses the actual maximum power and fixed voltage points from the test as a table to interpolate into. The interpolation scheme used is bilinear interpolation, as described in [Press, et. al., 1986]. Assuming the tabular data for both the maximum power and the fixed voltage cases are obtained at the same combinations of irradiance and temperature, the equations are:

$$\begin{aligned} P_{\max}(H, T_m) = {} & (1-t)\cdot(1-u)\cdot P_{\max(j,k)} \\ & + t\cdot(1-u)\cdot P_{fv(j+1,k)} \\ & + t\cdot u\cdot P_{\max(j+1,k+1)} \\ & + (1-t)\cdot u\cdot P_{\max(j,k+1)} \end{aligned} \tag{2-3}$$

$$\begin{aligned} I_{fv}(H, T_m) = {} & (1-t)\cdot(1-u)\cdot I_{fv(j,k)} \\ & + t\cdot(1-u)\cdot I_{fv(j+1,k)} \\ & + t\cdot u\cdot I_{fv(j+1,k+1)} \\ & + (1-t)\cdot u\cdot I_{fv(j,k+1)} \end{aligned} \tag{2-4}$$

$$t = \frac{H - H_{(j)}}{H_{(j+1)} - H_{(j)}} \tag{2-5}$$

$$u = \frac{T_m - T_{m(k)}}{T_{m(k+1)} - T_{m(k)}} \tag{2-6}$$

where

H = the irradiance at which the output power is desired

T_m = the module temperature at which the output power is desired

$P_{max(n,m)}$ = the maximum power output corresponding to the nth value of irradiance and the mth value of temperature

$I_{fv(n,m)}$ = the fixed voltage current output corresponding to the nth value of irradiance and the mth value of temperature

j = the index of the largest tested irradiance value less than H

k = the index of the largest tested temperature value less than T_m

t,u = H and T_m interpolation grid fraction, respectively

2.1.2.3 Anderson Model

Jerry Anderson of Sunset Technology has offered the following IV curve translation equations as modifications to those under development in IEEE SCC21 [Anderson, 1994].

$$I_{2i} = I_{1i} \frac{I_{sc2}}{I_{sc1}} \tag{2-7}$$

$$V_{2i} = V_{1i} \frac{V_{oc2}}{V_{oc1}} \tag{2-8}$$

$$\frac{I_{sc2}}{I_{sc1}} = \frac{H_2/H_1}{1 + \alpha(T_1 - T_2)} \tag{2-9}$$

$$\frac{V_{oc2}}{V_{oc1}} = \frac{1}{\left[1 + \beta(T_1 - T_2)\right] \times \left[1 + \delta \ln(H_1/H_2)\right]} \tag{2-10}$$

where

I = current (A)

H = irradiance (W/m^2)

V = voltage (V)

T = module temperature, (C)

α = temperature coefficient for current (C^{-1})

β = temperature coefficient for voltage (C^{-1})

δ = irradiance coefficient for voltage (unitless)

and where subscripts

sc = short circuit

oc = open circuit

1,2 = at conditions 1 or 2

i = i^{th} point on the IV curve

Coefficients α, β, and δ are determined experimentally, and are normalized at condition 2. Cell or module temperature is needed, as no conversion from ambient conditions is provided. Each point on an IV curve measured at conditions 1 are translated to conditions 2 using equations (2-7) and (2-8). Short circuit current and open circuit voltage are converted directly with equations (2-9) and (2-10); peak power is found by applying the translations to the maximum power point of the reference IV curve.

Note that the equations are not symmetric; that is, if the reference and target conditions are exchanged in the equations, the appropriate values for the coefficients will be different. Anderson argues that the difference between these two versions of the coefficients is small (<1%) for reasonable translations.

2.1.2.4 Blaesser Model

Gerd Blaesser of the European Solar Test Institute (ESTI) in Ispra Italy, introduced a slightly different approach [Blaesser, 1995] than Anderson. The basic equations are:

$$I_r = I\left(H_{1,r} / H_1\right) \tag{2-11}$$

$$V_r = V + DV \tag{2-12}$$

$$i_r = I_r / I_{sc,r}\,, \qquad i = I / I_{sc}\,,$$
$$v_r = V_r / V_{oc,r}\,, \qquad v = V / V_{oc}\,, \qquad Dv = DV / V_{oc,r} \tag{2-13}$$

$$V = V_r - Dv \cdot V_{oc,r} \tag{2-14}$$

$$i = i_r \tag{2-15}$$

$$v = \left(v_r - Dv\right) / \left(1 - Dv\right) \tag{2-16}$$

$$Dv = a \cdot \ln\left(H_{I,r} / H_I\right) + b\left(T_{amb} - T_I\right) + c \cdot H_I \tag{2-17}$$

$$FF = FF_r \frac{v_m}{v_{m,r}} = \frac{FF_r}{v_{m,r}} \frac{\left(v_{m,r} - Dv\right)}{\left(1 - Dv\right)} \tag{2-18}$$

$$P_m = V_{oc} I_{sc} \cdot FF \tag{2-19}$$

where

I	=	current, A
i	=	normalized current
H	=	irradiance, W/m²
V	=	voltage, V
v	=	normalized voltage
a, b, c	=	coefficients
T	=	temperature (ambient or cell), C
FF	=	fill factor
P	=	power, W

and where subscripts

I	=	in-plane (for irradiance)
r	=	at reference conditions
amb	=	ambient (temperature)
m	=	at maximum power point

and no subscript implies measured values.

Like α, β, and δ in the Anderson equations, coefficients a, b, and c are determined experimentally (default values: a = 0.06, b = 0.004°C^{-1}, and c=0.12 m²/kW) and equations (2-17), (2-16), (2-18), (2-11), and (2-14) are used to calculate Dv, v_m, FF, Isc, and Voc at the new conditions given values of V_{oc}, V_m, I_{sc}, and I_m at some initial conditions. A new peak power may be computed using (2-19).

Specifically, the maximum power may be computed using:

$$P_m = I_{m,r} \cdot \frac{H_I}{H_{I,r}} \cdot \left(V_{m,r} - Dv \cdot V_{oc,r}\right) \tag{2-20}$$

The fixed voltage current may be computed by translating the entire reference IV curve to the specified conditions and interpolating, but this process is computation intensive. A more computationally efficient alternative is to translate the fixed voltage from the specified conditions to the reference conditions, interpolate to find the corresponding reference current, and translating that value back to the specified conditions. That is,

$$I_{fv} = I_{fv,r} \cdot \frac{H_I}{H_{I,r}} \tag{2-21}$$

$$I_{fv,r} = \frac{I_{j+1,r} - I_{j,r}}{V_{j+1,r} - V_{j,r}} \cdot \left(V_{fv,r} - V_{j,r}\right) + I_{j,r} \tag{2-22}$$

$$V_{fv,r} = V_{fv} + Dv \cdot V_{oc,r} \tag{2-23}$$

and where subscripts

j = index of IV pair whose voltage is the maximum value less than $V_{fv,r}$

j+1 = index of IV pair whose voltage is the minimum value greater than $V_{fv,r}$

The Blaesser approach assumes a current multiplier equal to the ratio of measured and reference irradiance (ignoring temperature effects) and a voltage offset proportional to the natural log of the irradiance ratio (direct effect of irradiance on voltage), a delta T and a constant irradiance term (relating module voltage to irradiance). The model is conveniently based on ambient temperature but converts to (or from) a cell temperature. Wind speed could be added as a term to equation (2-17) though Blaesser says it doesn't improve the model. This model was derived based on the need to translate field data (where ambient temperature is much easier to measure than module temperature) to STC.

2.1.2.5 Lumped Four Parameter (L4P) Model

The L4P model is derived from an electrical model of a single-bandgap solar cell; specifically, a light-induced current source in parallel with a single diode and series resistance. This model has been discussed by Townsend (1989), Kreith (1978) and

briefly by Rauschenbach (1980). This model is sometimes modeled with an additional shunt resistance; this form of the model is considered more appropriate for a-Si devices.

The defining equations for this model are:

$$V = \frac{\gamma \cdot k \cdot T_c}{q} \cdot \ln\left(\frac{I_L - I}{I_0 \cdot NCP} + 1\right) - I \cdot R_s \tag{2-24}$$

$$I_L = \frac{H}{H_{ref}} \cdot \left[I_{L,ref} + \mu_{ISC} \cdot \left(T_c - T_{c,ref}\right)\right] \tag{2-25}$$

$$\gamma = A \cdot NCS \tag{2-26}$$

where

V	=	Voltage on translated IV curve, as a function of current I (A)
I	=	Current on translated IV curve (A)
I_L	=	Light-induced current (A)
$I_{L,ref}$	=	Light-induced current at reference conditions (A)
I_0	=	Reverse saturation current (A)
T_c	=	Cell temperature (C)
$T_{c,ref}$	=	Cell temperature at reference conditions (C)
H	=	Irradiance (W/m^2)
H_{ref}	=	Irradiance at reference conditions (W/m^2)
μ_{ISC}	=	Short circuit current temperature sensitivity (A/C)
R_s	=	Series resistance (Ω)
γ	=	Multi-cell diode ideality factor (unitless)
A	=	Single-cell diode ideality factor (unitless)
NCS	=	number of cells in series
NCP	=	number of cells in parallel
k	=	Boltzmann constant ($1.380622*10^{-23}$)
q	=	Electron charge constant ($1.6021917*10^{-19}$)

The four parameters for this model are I_L, I_0, γ, and R_s. Of these four, one is trivial to obtain, while the remaining three are not. $I_{L,ref}$ may be simply approximated by $I_{sc,ref}$. Townsend offers several techniques for obtaining the remaining parameters using conventional module characterization parameters and reference curve characteristics.

One "simplified" method he offered involves solving for an intermediate parameter Λ using peak power current and voltage and short circuit current and open circuit voltage, using this to obtain γ, R_s and I_0 as follows:

$$\Lambda = \frac{\frac{I_{sc}}{I_{sc}-I_{mp}} + \ln\left(1-\frac{I_{mp}}{I_{sc}}\right)}{2 \cdot V_{mp} - V_{oc}} \tag{2-27}$$

$$\gamma = \frac{q}{\Lambda \cdot k \cdot T_c} \tag{2-28}$$

$$R_s = \frac{\frac{1}{\Lambda} \cdot \ln\left(1-\frac{I_{mp}}{I_{sc}}\right) + V_{oc} - V_{mp}}{I_{mp}} \tag{2-29}$$

$$I_0 = \frac{I_{sc}}{NCP} \cdot \exp\left(-\Lambda \cdot V_{oc}\right) \tag{2-30}$$

where

I_{sc} = Short circuit current (A)
V_{oc} = Open circuit voltage (V)
I_{mp} = Current at maximum power point of curve (A)
V_{mp} = Voltage at maximum power point of curve (V)

Townsend indicated that this technique sometimes yields "unrealistic" results, and offered an alternative solution technique that iteratively computes the voltage/temperature sensitivity $\mu_{VOC,A}$ from R_s until the "known" value of μ_{VOC} is obtained, thus, indirectly obtaining the correct value for R_s. The equations for this approach are:

$$\Lambda = \frac{\ln\left(1-\frac{I_{mp}}{I_{sc}}\right)}{R_s \cdot I_{mp} - V_{oc} + V_{mp}} \tag{2-31}$$

$$\mu_{VOC,A} = \frac{\gamma \cdot k}{q} \cdot \left[\ln\left(\frac{I_{sc}}{I_0}\right) + \frac{T_c \cdot \mu_{ISC}}{I_{sc}} - 3 - \frac{q \cdot \varepsilon_G \cdot NCS}{\gamma \cdot k \cdot T_c} \right] \tag{2-32}$$

where

ε_G = Bandgap energy (1.12 for silicon)

and I_0 and γ are computed as in the "simplified" method. Unfortunately, for our exploratory tests this technique yielded "unrealistic" negative resistances. These results appear to reflect the low sensitivity of the I-V curve measurements to the parameters of interest; and conversely, the high sensitivity of the parameters on the I-V curve measurements. For example, the uncertainties in I_0 and R_s due to uncertainties in the I-V curve measurements are greater than the values of I_0 and R_s.

Two drawbacks to this approach have been suggested: namely, the restriction to application to single bandgap devices; and the difficulty of estimating the parameters accurately. The difficulty of estimating the parameters accurately is of concern because the model behavior is fairly strongly dependent on these values. Both the fact that the model behavior is so sensitive and that the resistance estimates are sensitive to measurement error in the testing procedure suggest that this model may not produce repeatable results.

Because of the difficulty encountered in obtaining reasonable estimates of the model parameters, this model was not compared to the other models. Further investigation into the reasons why the parameters were so difficult to obtain could either allow this model to be used, or perhaps provide insight into difficulties observed with other models. For example, it is possible that a non-linear curve fitting algorithm could be applied that would tend to be less sensitive to random experimental error by more fully utilizing the test data. In addition, this model may be a good basis for extension to multi-bandgap devices, should detailed models be required for them.

2.1.3 Spectral Model

The spectral model has two major components. First, the spectral model simulates irradiance spectra appropriate to the specified weather conditions for each time interval. These spectra are then combined with a measured module spectral response function to obtain an equivalent AM1.5 broadband irradiance value for input to the power model.

This modeling approach ignores the dependence of the IV curve shape on the incident spectral distribution. While this dependence may be an issue for multi-bandgap devices, it is not an issue for most PV technology currently in production. None of the empirical power models investigated here or suggested by the Technical Review Committee (TRC) handle the spectral IV-curve-shape effect, so our approach represents

a practical compromise. Some analytical models have been proposed [Emery and Osterwald, 1988] that could handle these shape effects, but no practical module testing procedures have been developed yet to obtain the appropriate model parameters.

The general approach used is to compute the ratio of two weighted-average spectral responses (SR) of the module: the numerator SR weighted with the actual (simulated) spectrum, and the denominator SR weighted with the ASTM E892 (AM1.5) spectrum to which the laboratory tests are referenced. This approach has been discussed by Emery and Osterwald (1988), King and Hansen (1991), and Seaman (1981).

In order to make adjustments based on field and test spectra, these spectra need to be available. Since these data are very rare, a model is used to estimate the spectrum corresponding to the weather data set. To accomplish this, the model uses the station pressure, dewpoint temperature, solar geometry, diffuse horizontal and plane-of-array (broadband) irradiances, and the beam (broadband) irradiance. In addition, a fixed dataset is required that contains the extraterrestrial spectrum, typical clear sky spectral absorption characteristics, and a set of empirically derived spectral cloud-cover model coefficients. The standard (AM1.5) testing spectrum is required for the effective irradiance calculation.

The spectral model chosen is that implemented by the SEDES2 code by Nann and Bakenfelder (described by Nann and Riordan (1991)), which is in turn derived from the SPCTRL2 model by Bird and Riordan (1986) with an empirically derived modifier added to account for cloud cover. The cloud cover modifier is a function of wavelength, air mass, and the ratio of the actual broadband global horizontal irradiance to the predicted clear-sky wavelength.

The major steps that are used in the SEDES2 model are estimation of clear-sky spectra (direct and diffuse horizontal), estimation of the (potentially) cloudy-sky spectra, magnitude normalization and estimation of plane-of-array diffuse spectra, and estimation of the effective irradiance. These topics are covered in the following sections in reverse order, to emphasize results and required inputs in a "top-down" manner. For discussion of the origins of, assumptions in, and derivations of these equations, refer to the papers described above.

2.1.3.1 Effective Irradiance

The effective (usable) irradiance for a specific module is given by

$$H_{POA,Eff} = SCF \cdot IAM \cdot H_{POA} \quad (2\text{-}33)$$

where

IAM = incidence angle modifier (see page 34)

H_{POA} = plane-of-array irradiance (see page 37)

and the spectral correction factor, *SCF*, is given by

$$SCF = \frac{\left(\frac{\int SR(\lambda)\cdot H_{POA}(\lambda)d\lambda}{\int H_{POA}(\lambda)d\lambda}\right)}{\left(\frac{\int SR(\lambda)\cdot H_{std}(\lambda)d\lambda}{\int H_{std}(\lambda)d\lambda}\right)} \quad (2\text{-}34)$$

where

λ = irradiance wavelength (μm)

$SR(\lambda)$ = spectral response of the module (A/W)

$H_{POA}(\lambda)$ = plane-of-array irradiance spectrum ($W/m^2/\mu m$)

$H_{std}(\lambda)$ = standard (ASTM E892 AM1.5 irradiance spectrum) ($W/m^2/\mu m$).

The integrals may be evaluated using Euler numerical integration. This computation is simplified if all of these functions of wavelength (represented as explicit arrays of data rather than as closed-form formulas) are evaluated at the same wavelengths.

2.1.3.2 Normalization and Incident Surface Translation

The spectrum generated by the SEDES2 model does not contain exactly the same broadband power as the measured (input) irradiances do. This is because cloud cover modifiers change the shape of the clear-sky spectrum based solely on wavelength and the broadband measured-to-predicted irradiance ratio. That is, for each wavelength the magnitude is multiplied by a coefficient that does not depend on the rest of the actual (or estimated) spectrum. Since the coefficients are derived from actual data, they may be expected to work reasonably well as long as the colors in view of the site being simulated are similar to those where the data for the coefficients were obtained. This is not an entirely unreasonable assumption, but we have observed a 3-7 percent difference between the integrated SEDES2 spectrum and the input broadband irradiance.

Assuming the cloud cover modifiers do in fact improve the shape of the estimated actual spectrum, the magnitude of the modified spectrum should be corrected to agree with the broadband irradiance before it is used. However, for the purposes of the Module Energy Rating (MER), the shape of the spectrum is all that is needed. As long as the broadband irradiance is not substituted for the integrated spectrum in the *SCF* calculation, the scaling makes no difference.

To obtain global plane-of-array spectral irradiance from direct normal and diffuse horizontal spectral irradiances, the diffuse spectral distributions are assumed to be isotropic. That is, the color is isotropic while intensity may not be. This reduces the problem to a simple scaling computation, as follows:

$$H_{POA}(\lambda) = H_d(\lambda) \cdot \cos(\theta) + H_{s,POA}(\lambda) \tag{2-35}$$

$$H_{s,POA}(\lambda) = H_{s,H}(\lambda) \cdot \frac{H_{s,POA}}{H_{s,H}} \tag{2-36}$$

where

$H_d(\lambda)$ = direct (beam) spectral irradiance ($W/m^2/\mu m$)

$H_{s,POA}(\lambda)$ = scattered (diffuse) plane-of-array spectral irradiance ($W/m^2/\mu m$)

$H_{s,H}(\lambda)$ = scattered (diffuse) horizontal spectral irradiance ($W/m^2/\mu m$)

$H_{s,POA,meas}$ = scattered (diffuse) broadband plane-of-array irradiance (W/m^2), measured or estimated using Perez model

$H_{s,H,meas}$ = scattered (diffuse) broadband horizontal irradiance (W/m^2), measured

θ = incidence angle (page 36)

2.1.3.3 Estimated Spectrum with Cloud-Cover

To account for the most general weather conditions, the SEDES2 model estimates the spectral irradiance using:

$$H_d(\lambda) = H_{d,clear}(\lambda) \cdot CCM(\lambda, NGH, z) \tag{2-37}$$

$$H_{s,H}(\lambda) = H_{s,H,clear}(\lambda) \cdot CCM(\lambda, NGH, z) \tag{2-38}$$

$$CCM(\lambda, NGH, z) = (A1(\lambda) + \frac{A2(\lambda)}{\cos(z)}) + (B1(\lambda) + \frac{B2(\lambda)}{\cos(z)}) \cdot NGH + (C1(\lambda) + \frac{C2(\lambda)}{\cos(z)}) \cdot NGH^2 \quad (2\text{-}39)$$

where

$H_{d,clear}(\lambda)$	=	direct clear sky spectrum (page 20)
$H_{s,H,clear}(\lambda)$	=	scattered horizontal clear sky spectrum (page 20)
NGH	=	normalized global horizontal insolation (page 21)
z	=	sun zenith angle (see page 35)
$CCM(\lambda,NGH,z)$	=	cloud cover modifier function
$A1(\lambda)$, $A2(\lambda)$, $B1(\lambda)$, $B2(\lambda)$, $C1(\lambda)$, $C2(\lambda)$	=	cloud cover coefficients (Tables 2-1, 2-2)

Table 2-1. SEDES2 Cloud Cover Modifier Coefficients

λ	$A1(\lambda)$	$A2(\lambda)$	$B1(\lambda)$	$B2(\lambda)$	$C1(\lambda)$,	$C2(\lambda)$
320	1.285724	0.306791	-0.29613	-0.58516	0.020632	0.20915
330	1.235103	0.262007	-0.28377	-0.53864	0.010728	0.206493
340	1.206166	0.250204	-0.25258	-0.51989	0.004315	0.204614
350	1.139737	0.242676	-0.19222	-0.49821	-0.01184	0.201329
360	1.091643	0.244214	-0.13386	-0.48722	-0.0272	0.200767
370	1.033731	0.251496	-0.07915	-0.48133	-0.04285	0.202966
380	0.997179	0.243862	-0.0655	-0.45039	-0.03607	0.191915
390	0.997948	0.227502	-0.08976	-0.40715	-0.01039	0.17371
400	0.990572	0.205403	-0.12091	-0.35735	0.018082	0.152083
410	0.984024	0.193105	-0.13671	-0.32748	0.034395	0.140702
420	0.971385	0.177868	-0.15584	-0.29288	0.051752	0.127548
430	0.97645	0.159398	-0.18434	-0.25421	0.072127	0.112706
440	0.973204	0.142079	-0.20773	-0.21836	0.088689	0.098569
450	0.979785	0.129315	-0.22806	-0.19197	0.103365	0.08717
460	0.98578	0.119208	-0.24438	-0.1714	0.117445	0.076708
470	0.99861	0.109176	-0.26163	-0.15113	0.132599	0.066066
480	1.005317	0.099677	-0.27866	-0.13004	0.147219	0.055762
490	1.019677	0.089575	-0.30482	-0.10709	0.16626	0.045127
500	1.024404	0.080517	-0.32229	-0.0875	0.179513	0.036474
510	1.031585	0.069067	-0.34795	-0.06441	0.196865	0.025472
520	1.049367	0.056443	-0.38233	-0.04055	0.218811	0.013729
530	1.063939	0.046316	-0.40907	-0.02121	0.236117	0.004201
540	1.071553	0.0383	-0.42769	-0.00587	0.248413	-0.00299
550	1.070387	0.031852	-0.43045	0.004491	0.251829	-0.00768
560	1.062834	0.026342	-0.41879	0.011999	0.246651	-0.01046
570	1.045843	0.024689	-0.37226	0.009432	0.223078	-0.00801
580	1.037469	0.023472	-0.33927	0.008971	0.207507	-0.0069
590	1.026083	0.023298	-0.3141	0.008151	0.195734	-0.00518
600	1.040383	0.015681	-0.34917	0.024337	0.218887	-0.01426
610	1.05082	0.006659	-0.38518	0.041762	0.241564	-0.02411
620	1.051636	0.000294	-0.39171	0.051032	0.246386	-0.02902
630	1.040294	-0.00264	-0.36449	0.050866	0.230633	-0.02769
640	1.04091	-0.00243	-0.35577	0.051709	0.225536	-0.02653
650	1.040678	-0.00316	-0.34746	0.053757	0.221069	-0.02611
660	1.065054	-0.00775	-0.38644	0.068596	0.246247	-0.0347
670	1.081709	-0.0102	-0.40061	0.077291	0.257483	-0.04034
680	1.077241	-0.00697	-0.36968	0.071587	0.240555	-0.03716
690	1.040409	-0.00413	-0.28523	0.052308	0.187536	-0.02455
700	1.016405	-0.00067	-0.23359	0.036039	0.150176	-0.01227
710	1.006519	-0.00416	-0.21335	0.030742	0.130581	-0.00725
720	1.015005	-0.00986	-0.20643	0.033451	0.120013	-0.00709
730	1.11212	-0.03985	-0.3703	0.086799	0.198931	-0.03506
740	1.259638	-0.07938	-0.63633	0.167885	0.336038	-0.08023
750	1.359701	-0.10681	-0.82757	0.227298	0.435026	-0.11411
760	1.364134	-0.10886	-0.84101	0.233641	0.440063	-0.11907
770	1.413504	-0.12491	-0.91952	0.262684	0.480399	-0.13497
780	1.472111	-0.14378	-1.00406	0.291321	0.524579	-0.14918
790	1.460142	-0.14248	-0.96339	0.280995	0.499939	-0.14149
800	1.397082	-0.12613	-0.83251	0.242547	0.428312	-0.11892
810	1.303223	-0.09812	-0.64065	0.184689	0.325405	-0.08646
820	1.231193	-0.08347	-0.50422	0.149742	0.253542	-0.06661
830	1.278968	-0.09801	-0.59564	0.179143	0.30194	-0.08288
840	1.394604	-0.12999	-0.82226	0.248595	0.42466	-0.12262
850	1.48684	-0.15767	-1.02211	0.309727	0.533828	-0.15811
860	1.533058	-0.17332	-1.12535	0.343352	0.589583	-0.17738
870	1.54842	-0.17691	-1.14042	0.350555	0.597075	-0.18138

Table 2-1. SEDES2 Cloud Cover Modifier Coefficients (cont.)

λ	$A1(\lambda)$	$A2(\lambda)$	$B1(\lambda)$	$B2(\lambda)$	$C1(\lambda)$,	$C2(\lambda)$
880	1.509161	-0.16271	-1.02979	0.319605	0.536668	-0.1636
890	1.398192	-0.1247	-0.77108	0.242984	0.400871	-0.1215
900	1.176119	-0.06824	-0.34215	0.120864	0.176265	-0.05349
910	0.986845	-0.01315	0.01589	0.015608	-0.00784	0.003255
920	0.830406	0.03159	0.284686	-0.06127	-0.14019	0.042905
930	0.611229	0.097008	0.607703	-0.15086	-0.28158	0.08258
940	0.369127	0.137444	0.920399	-0.22796	-0.42836	0.122108
950	0.306382	0.132255	1.017929	-0.25108	-0.50619	0.144856
960	0.427639	0.084802	0.85788	-0.20327	-0.46987	0.132757
970	0.650115	0.034501	0.600522	-0.12507	-0.37126	0.097659
980	0.843689	-0.01411	0.352464	-0.04375	-0.26576	0.058199
990	1.018712	-0.05584	0.115209	0.032978	-0.16069	0.01951
1000	1.110714	-0.08242	-0.02662	0.08182	-0.09732	-0.00507
1010	1.158305	-0.09845	-0.10842	0.111704	-0.0598	-0.02013
1020	1.187785	-0.10971	-0.17215	0.13436	-0.02617	-0.03236
1030	1.216623	-0.12039	-0.24681	0.157773	0.018206	-0.04635
1040	1.242954	-0.13007	-0.3248	0.179514	0.068458	-0.06071
1050	1.242954	-0.13007	-0.3248	0.179514	0.068458	-0.06071

The cloud cover coefficients describe how the actual spectrum tends to deviate from the clear sky spectrum for each wavelength as the air mass (approximated by 1/cos(z)) and normalized global horizontal irradiance vary. These coefficients were derived from measured data using statistical analyses as described by Nann and Riordan, 1991.

2.1.3.4 Estimated Clear Sky Spectrum

The clear sky spectrum may be estimated by computing the absorption and scattering effects of the atmosphere on the (relatively constant) extraterrestrial spectrum using local weather conditions as input. However, the non-isotropic field of view and non-uniform atmospheric conditions (that are not reflected in the *local* weather conditions, but may affect the light as it passes through the atmosphere) significantly reduce the accuracy of this approach. If the atmosphere is assumed to behave as a neutral density filter (spectrally independent scaling), then the first cut estimate of the spectral irradiance may be "corrected" by scaling it back to the measured broadband irradiance. Any errors in spectral shape introduced by this assumption may be assumed to be corrected by the empirically derived cloud cover modifier. Thus, the clear sky horizontal scattered (diffuse) spectra $H_{s,H,clear}(\lambda)$ and the direct (beam) spectra $H_{d,clear}(\lambda)$ may be computed using the equations:

$$H_{s,H,clear}(\lambda) = \left(H_{d,est}(\lambda) \cdot \cos(z) + H_{s,H,est}(\lambda)\right) \cdot NGH - H_{d,clear}(\lambda) \qquad (2\text{-}40)$$

$$H_{d,clear}(\lambda) = H_{d,est}(\lambda) \cdot NDIR \qquad (2\text{-}41)$$

where the *est* subscript indicates first cut spectral estimates from the extraterrestrial spectrum (assumed constant) affected by atmospheric absorptance, scattering and reflection as described below. The normalized direct and global horizontal irradiances NDIR and NGH represent scaling factors to convert the magnitudes of the first cut estimates to match the broadband measurements:

$$NDIR = \frac{H_{H,meas} - H_{s,H,meas}}{H_{d,est} \cdot \cos(z)} \tag{2-42}$$

$$NGH = \frac{H_{H,meas}}{H_{s,H,est} + H_{d,est} \cdot \cos(z)} \tag{2-43}$$

where

$H_{H,meas}$ = global horizontal broadband measured irradiance (W/m^2)

$H_{s,H,meas}$ = scattered (diffuse) horizontal broadband measured irradiance (W/m^2)

and the estimated broadband irradiances are given by:

$$H_{s,H,est} = \int H_{s,H,est}(\lambda) d\lambda \tag{2-44}$$

$$H_{d,est} = \int H_{d,est}(\lambda) d\lambda \tag{2-45}$$

The first-cut direct irradiance spectra are obtained by multiplying the estimated extraterrestrial spectrum by the transmittances of the optically significant components of the atmosphere:

$$H_{d,est}(\lambda) = H_{exo}(\lambda) \cdot T_r(\lambda) \cdot T_a(\lambda) \cdot T_w(\lambda) \cdot T_o(\lambda) \cdot T_u(\lambda) \tag{2-46}$$

where the extraterrestrial spectrum is a standard spectrum modified in intensity as a function of the time of year:

$$H_{exo}(\lambda) = H_0(\lambda) \cdot \begin{pmatrix} 1.00011 \cdots \\ +0.034221 \cdot \cos(\alpha_D) + 0.00128 \cdot \sin(\alpha_D) \cdots \\ +0.000719 \cdot \cos(2\alpha_D) + 0.000077 \cdot \sin(2\alpha_D) \end{pmatrix} \tag{2-47}$$

where $H_0(\lambda)$ is given in Table 2-2, and α_D is the day angle given on page 35.

The transmittances due to Rayleigh scattering ($T_r(\lambda)$), aerosols ($T_a(\lambda)$), water vapor ($T_w(\lambda)$), ozone ($T_o(\lambda)$), and uniform gases ($T_u(\lambda)$) are given by:

$$T_r(\lambda) = \exp\left(\frac{-m_p}{\lambda^4 \cdot \left(115.6406 - \frac{1.3366}{\lambda^2}\right)}\right) \tag{2-48}$$

$$T_a(\lambda) = \exp\left(-\tau_a(\lambda) \cdot m\right) \tag{2-49}$$

$$T_w(\lambda) = \exp\left(\frac{-0.2385 \cdot A_w(\lambda) \cdot W \cdot m}{\left(1 + 20.07 \cdot A_w(\lambda) \cdot W \cdot m\right)^{0.45}}\right) \tag{2-50}$$

$$T_o(\lambda) = \exp(-A_o(\lambda) \cdot O3 \cdot m_o) \tag{2-51}$$

$$T_u(\lambda) = \exp\left(\frac{-1.41 \cdot A_u(\lambda) \cdot m}{\left(1 + 118.3 \cdot A_u(\lambda) \cdot m\right)^{0.45}}\right) \tag{2-52}$$

where

m = air mass (page 37)

m_p = pressure-corrected air mass ($= m \cdot \frac{P}{1013}$)

$A_w(\lambda)$ = absorption spectrum of water (given in Table 2-2)

$A_o(\lambda)$ = absorption spectrum of ozone (given in Table 2-2)

$A_u(\lambda)$ = absorption spectrum of uniform gases (given in Table 2-2)

and the aerosol spectral turbidity ($\tau_a(\lambda)$), water amount (W), ozone amount (O3) and ozone mass (m_O) are estimated using:

$$\tau_a(\lambda) = \beta \cdot \lambda^{-\alpha} \tag{2-53}$$

$$W = \exp\left(0.06930 \cdot T_{dewpt} - 0.0756\right) \tag{2-54}$$

$$O3 = 0.001 \cdot \left(235 + \sin\left(1.28 \cdot \tfrac{\pi}{180} \cdot \phi\right)^2 \cdot \left[\begin{array}{c} 150\ldots \\ +40 \cdot \sin\left(0.9865 \cdot \tfrac{\pi}{180} \cdot \left(N_{day} - 30\right)\right)\ldots \\ +20 \cdot \sin\left(3 \cdot \tfrac{\pi}{180} \cdot \theta_{O3}\right) \end{array} \right] \right) \tag{2-55}$$

$$m_o = \frac{1 + RR}{\sqrt{\cos(z)^2 + 2 \cdot RR}} \tag{2-56}$$

where

α = Exponent for rural aerosol turbidity model (=1.14)

β = scaling factor for rural aerosol turbidity model (= $\frac{0.27}{0.5^{-\alpha}}$)

T_{dewpt} = dewpoint temperature (Celsius)

N_{day} = day of year (1 = January 1)

ϕ = latitude of location (degrees in northern hemisphere)

θ_{O3} = adjusted longitude in degrees east of Greenwich. If negative (west of meridian), then no adjustment. If positive, then add 20 degrees.

RR = height of ozone layer in earth radii (=22/6370)

When the dewpoint temperature must be estimated from ambient temperature and relative humidity, the following formulas were used in SEDES2:

$$T_{dewpt} = \begin{cases} \frac{5}{9} \cdot \left(39.98 + 24.83 \cdot \ln\left(P_w\right) + 0.8927 \cdot \ln\left(P_w\right)^2\right) & ; T_{amb} < 0 \\ \frac{5}{9} \cdot \left(47.047 + 30.579 \cdot \ln\left(P_w\right) + 1.8893 \cdot \ln\left(P_w\right)^2\right) & ; T_{amb} \geq 0 \end{cases} \quad (2\text{-}57)$$

$$P_w = \frac{RH}{100} \cdot P_{ws} \quad (2\text{-}58)$$

$$P_{ws} = 0.02953 \cdot 10^{8.42926609 - \frac{1827.17843}{T_{amb}+273.15} - \frac{71208.271}{(T_{amb}+273.15)^2}} \quad (2\text{-}59)$$

where

T_{amb} = ambient temperature (Celsius)

P_{ws} = water vapor saturation pressure (in-Hg)

RH = relative humidity (percent)

The diffuse horizontal estimated spectrum ($H_{s,H,est}(\lambda)$) may be computed with:

$$H_{s,H,est}(\lambda) = C_s(\lambda) \cdot \left(H_r(\lambda) + H_a(\lambda) + H_g(\lambda)\right) \quad (2\text{-}60)$$

$$C_s(\lambda) = \begin{cases} (\lambda + 0.55)^{1.8} & ; \lambda < 0.45 \\ 1 & ; \lambda \geq 0.45 \end{cases} \quad (2\text{-}61)$$

where

$C_s(\lambda)$ = adjustment factor for short wavelength light

and

$$H_r(\lambda) = \tfrac{1}{2} \cdot H_{exo}(\lambda) \cdot \cos(z) \cdot T_o(\lambda) \cdot T_u(\lambda) \cdot T_w(\lambda) \cdot T_{aa}(\lambda) \cdot \left(1 - T_r(\lambda)^{0.95}\right) \quad (2\text{-}62)$$

$$H_a(\lambda) = H_{exo}(\lambda) \cdot \cos(z) \cdot T_o(\lambda) \cdot T_u(\lambda) \cdot T_w(\lambda) \cdot T_{aa}(\lambda) \cdot T_r(\lambda)^{1.5} \cdot \left(1 - T_{as}(\lambda)\right) \cdot F_s(z) \quad (2\text{-}63)$$

$$H_g(\lambda) = \frac{r_s(\lambda) \cdot r_g(\lambda)}{1 - r_s(\lambda) \cdot r_g(\lambda)} \cdot \left(H_{d,est}(\lambda) \cdot \cos(z) + H_r(\lambda) + H_a(\lambda)\right) \quad (2\text{-}64)$$

where

$H_r(\lambda)$ = Rayleigh scattering diffuse component ($W/m^2/\mu m$)
$H_a(\lambda)$ = aerosol scattering diffuse component ($W/m^2/\mu m$)
$H_g(\lambda)$ = ground-reflected scattering diffuse component ($W/m^2/\mu m$)
$r_s(\lambda)$ = sky reflectivity
$r_g(\lambda)$ = ground albedo (assumed constant = 0.2)
$T_o(\lambda)$ = ozone transmittance
$T_u(\lambda)$ = uniform gasses transmittance
$T_w(\lambda)$ = water vapor transmittance
$T_{aa}(\lambda)$ = transmittance due to aerosol absorptance
$T_{as}(\lambda)$ = transmittance due to aerosol scattering
$T_r(\lambda)$ = Rayleigh transmittance
$F_s(z)$ = ratio of forward to total scattering.

The aerosol transmittance components due to scattering ($T_{as}(\lambda)$) and absorptance ($T_{aa}(\lambda)$), the aerosol single-scattering albedo($\omega(\lambda)$), and the ratio of forward to total scattering are given by:

$$T_{as}(\lambda) = \exp\left(-\omega(\lambda) \cdot \tau_a(\lambda) \cdot m\right) \quad (2\text{-}65)$$

$$T_{aa}(\lambda) = \frac{T_a(\lambda)}{T_{as}(\lambda)} \quad (2\text{-}66)$$

$$\omega(\lambda) = \omega_{0.4} \cdot \exp\left(-\omega' \cdot \left[\ln\left(\tfrac{\lambda}{0.4}\right)\right]^2\right) \quad (2\text{-}67)$$

$$F_s(z) = 1 - \tfrac{1}{2} \cdot \exp\left(\left(AFS + BFS \cdot \cos(z)\right) \cdot \cos(z)\right) \quad (2\text{-}68)$$

where

$\tau_a(\lambda)$ = aerosol turbidity (page 22)

m = air mass

$T_a(\lambda)$ = total aerosol transmittance (page 22)

$\omega_{0.4}$ = aerosol single scattering albedo at 0.4 μm wavelength (assuming rural model, use 0.945)

ω' = single scattering wavelength variation factor (assuming rural model, use 0.095)

and

$$AFS = ALG \cdot (1.459 + ALG \cdot (0.1595 + ALG \cdot 0.4129)) \quad (2\text{-}69)$$

$$BFS = ALG \cdot (0.0783 + ALG \cdot (-0.3824 - ALG \cdot 0.5874)) \quad (2\text{-}70)$$

$$ALG = \ln(1 - ASF) \quad (2\text{-}71)$$

where

ASF = aerosol symmetry factor (for rural model, assume 0.65)

The sky reflectivity is computed using:

$$r_s(\lambda) = T'_u(\lambda) \cdot T'_w(\lambda) \cdot T'_{aa}(\lambda) \cdot \left[\frac{1 - T'_r(\lambda)}{2} + (1 - F'_s) \cdot T'_r(\lambda) \cdot (1 - T'_{as}(\lambda))\right] \quad (2\text{-}72)$$

where the primed transmittances are the regular atmospheric transmittance terms evaluated at air mass 1.8, and

$$F'_s = 1 - \tfrac{1}{2} \cdot \exp\left(\frac{AFS + \frac{BFS}{1.8}}{1.8}\right) \quad (2\text{-}73)$$

Table 2-2. Standard spectrum and atmospheric optical characteristics.

λ	H0	Aw	Ao	Au	λ	H0	Aw	Ao	Au	λ	H0	Aw	Ao	Au
300	535.9	0	10	0	740	1298	0.061	0.01	0	1520	292.8	0.16	0	0
305	558.3	0	4.8	0	752.5	1269	0.0008	0.008	0	1539	275.5	0.002	0	0.005
310	622	0	2.7	0	757.5	1245	0.0001	0.007	0	1558	272.1	0.0005	0	0.13
315	692.7	0	1.35	0	762.5	1223	0.00001	0.006	4	1578	259.3	0.0001	0	0.04
320	715.1	0	0.8	0	767.5	1205	0.00001	0.005	0.35	1592	246.9	0.00001	0	0.06
325	832.9	0	0.38	0	780	1183	0.0006	0	0	1610	244	0.0001	0	0.13
330	961.9	0	0.16	0	800	1148	0.036	0	0	1630	243.5	0.001	0	0.001
335	931.9	0	0.075	0	816	1091	1.6	0	0	1646	234.8	0.01	0	0.0014
340	900.6	0	0.04	0	823.7	1062	2.5	0	0	1678	220.5	0.036	0	0.0001
345	911.3	0	0.019	0	831.5	1038	0.5	0	0	1740	190.8	1.1	0	0.00001
350	975.5	0	0.007	0	840	1022	0.155	0	0	1800	171.1	130	0	0.00001
360	975.9	0	0	0	860	998.7	0.00001	0	0	1860	144.5	1000	0	0.0001
370	1119.9	0	0	0	880	947.2	0.0026	0	0	1920	135.7	500	0	0.001
380	1103.8	0	0	0	905	893.2	7	0	0	1960	123	100	0	4.3
390	1033.8	0	0	0	915	868.2	5	0	0	1985	123.8	4	0	0.2
400	1479.1	0	0	0	925	829.7	5	0	0	2005	113	2.9	0	21
410	1701.3	0	0	0	930	830.3	27	0	0	2035	108.5	1	0	0.13
420	1740.4	0	0	0	937	814	55	0	0	2065	97.5	0.4	0	1
430	1587.2	0	0	0	948	786.9	45	0	0	2100	92.4	0.22	0	0.08
440	1837	0	0	0	965	768.3	4	0	0	2148	82.4	0.25	0	0.001
450	2005	0	0.003	0	980	767	1.48	0	0	2198	74.6	0.33	0	0.00038
460	2043	0	0.006	0	993.5	757.6	0.1	0	0	2270	68.3	0.5	0	0.001
470	1987	0	0.009	0	1040	688.1	0.00001	0	0	2360	63.8	4	0	0.0005
480	2027	0	0.014	0	1070	640.7	0.001	0	0	2450	49.5	80	0	0.00015
490	1896	0	0.021	0	1100	606.2	3.2	0	0	2500	48.5	310	0	0.00014
500	1909	0	0.03	0	1120	585.9	115	0	0	2600	38.6	15000	0	0.00066
510	1927	0	0.04	0	1130	570.2	70	0	0	2700	36.6	22000	0	100
520	1831	0	0.048	0	1145	564.1	75	0	0	2800	32	8000	0	150
530	1891	0	0.063	0	1161	544.2	10	0	0	2900	28.1	650	0	0.13
540	1898	0	0.075	0	1170	533.4	5	0	0	3000	24.8	240	0	0.0095
550	1892	0	0.085	0	1200	501.6	2	0	0	3100	22.1	230	0	0.001
570	1840	0	0.12	0	1240	477.5	0.002	0	0.05	3200	19.6	100	0	0.8
593	1768	0.075	0.119	0	1270	442.7	0.002	0	0.3	3300	17.5	120	0	1.9
610	1728	0	0.12	0	1290	440	0.1	0	0.02	3400	15.7	19.5	0	1.3
630	1658	0	0.09	0	1320	416.8	4	0	0.0002	3500	14.1	3.6	0	0.075
656	1524	0	0.065	0	1350	391.4	200	0	0.00011	3600	12.7	3.1	0	0.01
667.6	1531	0	0.051	0	1395	358.9	1000	0	0.00001	3700	11.5	2.5	0	0.00195
690	1420	0.016	0.028	0.15	1442.5	327.5	185	0	0.05	3800	10.4	1.4	0	0.004
710	1399	0.0125	0.018	0	1462.5	317.5	80	0	0.011	3900	9.5	0.17	0	0.29
718	1374	1.8	0.015	0	1477	307.3	80	0	0.005	4000	8.6	0.0045	0	0.025
724.4	1373	2.5	0.012	0	1497	300.4	12	0	0.0006					

2.1.4 Module Thermal Model

Another explicit input to several of the contemplated PV performance models is module temperature. Module output power varies by roughly 0.5%/°C change in temperature. This module temperature coefficient is less for most thin-film devices and for higher

efficiency devices[1]. The temperature of a PV module depends on module construction, module mounting, ambient conditions (in order of decreasing importance: ambient temperature, irradiance, wind speed, wind direction, humidity, barometric pressure, elevation, etc.), and conversion efficiency (solar power converted to electricity is unavailable for heating up the module).

The thermal model used in PVFORM [Fuentes, 1987] was developed and evaluated using measured array data and takes into account module construction, mounting, and operation in a term called Installed Nominal Operating Cell Temperature, INOCT. INOCT is based on JPL's NOCT which is defined as the cell temperature of the module under conditions of 800 W/m^2 irradiance, 20 °C ambient temperature, 1 m/s wind speed, with a single open-circuited module mounted in an open rack (or per the manufacturer's requirements). INOCT has the same ambient conditions, but the module is mounted and operated per the system designer's intention. As such, one module can have a wide range of INOCTs because of the possibility of different mounting configurations and operating points (peak power, fixed voltage, etc.)

2.1.4.1 General Approach

The Fuentes model uses a simplified heat balance approach. Convective and radiative heat transfer equations are developed and a number of assumptions are made. Included in these assumptions are a tilt angle of 30° (for convective heat transfer coefficient), module efficiency of 8%, reflectance of 0.10, absorptance of 0.83, emittance of 0.84, a thermal mass (m·c) of 11 kJ/m^2 °C, and a convection distance of 0.5m (enough to allow turbulence to occur, but a small value relative to an array). Also, Fuentes assumes that modules with INOCT > 48°C are thermally coupled to a roof or some other structure and increases the thermal mass proportional to INOCT.

The heat balance with simplifying assumptions yields the following expression for module temperature:

$$Tmod = \frac{\left(hc \cdot Ta + hr_s \cdot Ts + hr_g \cdot Tg + \alpha \cdot H_0 + \alpha \cdot \Delta H / L\right) \cdot \left(1 - e^L\right) + \alpha \cdot \Delta H}{hc + hr_s + hr_g} + Tmod_0 \cdot e^L \quad (2\text{-}74)$$

[1] The absolute value in Watts/°C or Volts/°C can decrease and the divisor, reference Watts or Volts, increases. Therefore the %/°C is reduced.

where

Tm	=	module temperature, K
Ta	=	ambient temperature, K
Ts	=	sky temperature, K
Tg	=	ground or roof temperature, K
hc	=	overall convective heat transfer coefficient (W/m^2-K)
hr_s	=	radiative h/t coefficient to the sky, (W/m^2-K)
hr_g	=	radiative h/t coefficient to the ground or roof, (W/m^2-K)
α	=	module absorptivity (<3.5 µm)
H_0	=	plane of array irradiance from previous time step, W/m^2
ΔH	=	change in POA irradiance from previous time step, W/m^2

and

$$L = -\left(hc + hr_s + hr_g\right) \Delta t / (m \cdot c) \tag{2-75}$$

where

m	=	module mass per unit surface area (kg/m2)
c	=	overall module specific heat (J/kg-K)
$m{\cdot}c$	=	11,000 J/m^2-K (for INOCT • 48 °C), 1.1E4·[1+(INOCT-48)/12] (for INOCT > 48°C)
Δt	=	time step (s)

The overall convection coefficient is calculated as the cube root of the sum of the cubes of the forced and free convection coefficients:

$$hc = \left(h_{forced}{}^3 + h_{free}{}^3\right)^{1/3} \tag{2-76}$$

For forced convection the following equations are used:

$$h_{forced} = \mathrm{St} \cdot \rho \cdot c_p \cdot wm \tag{2-77}$$

$$\mathrm{St} = \frac{b \cdot \mathrm{Re}^c}{\mathrm{Pr}^a} \tag{2-78}$$

$$\mathrm{Re} = \frac{wm \cdot D_h}{v} \tag{2-79}$$

$$\rho = \frac{0.0003484 \cdot 101325}{T_{film}} \tag{2-80}$$

$$\nu = 2.4237 \cdot 10^{-7} \cdot \frac{T_{film}^{0.76}}{\rho} \tag{2-81}$$

$$T_{film} = \frac{Tm + Ta}{2} \tag{2-82}$$

where

St	=	Stanton number
Pr	=	Prandtl number ($=\frac{c_p \cdot \mu}{k}$ = 0.71 for air)
Re	=	Reynolds number
ρ	=	density of air
c_p	=	specific heat of air (=1007 J/kg-°C)
wm	=	wind speed at the module height (m/s)
D_h	=	module hydraulic diameter[1] (=0.5m)
ν	=	kinematic viscosity of air
T_{film}	=	film temperature

and

Re	a	b	c
$\leq 1.2 \cdot 10^5$	0.67	0.86	-0.5
$> 1.2 \cdot 10^5$	0.4	0.028	-0.2

For free convection,

$$h_{free} = \frac{\mathrm{Nu} \cdot k}{D_h} \tag{2-83}$$

$$\mathrm{Nu} = 0.21 \cdot (\mathrm{Gr} \cdot \mathrm{Pr})^{0.32} \tag{2-84}$$

[1] Strictly speaking, the hydraulic diameter is intended to be used for fluid flow in a tube with a non-circular cross section. Fuentes assumed typical module dimensions of 1.2m x 0.3m. Using the standard $D_h = 4A/P = 4*(1.2*.3)/(2*1.2+2*0.3) = 0.48$m ±0.5m gives the stated value. For convection on a flat surface, D_h is replaced with x, the distance from the leading edge. Since it is unclear from which direction the wind is coming (wind direction was not incorporated into this model) and the module orientation is unspecified, it appears from the validation results that a value of 0.5 m is a good approximation.

$$\mathrm{Gr} = \frac{g \cdot (Tm - Ta) \cdot D_h^3 \cdot \sin(\varphi)}{\nu^2 \cdot T_{film}} \tag{2-85}$$

$$k = 2.1695 \cdot 10^{-4} \cdot T_{film}^{0.84} \tag{2-86}$$

where

Nu	=	Nusselt number
Gr	=	Grashof number
g	=	gravitational constant (=9.8 m/s^2)
φ	=	module tilt angle, assumed to be 30°
k	=	thermal conductivity of air

For front surface radiation, sky temperature is estimated from ambient temperature using

$$Ts = 0.68 \cdot \left(0.0552 \cdot Ta^{1.5}\right) + 0.32 \cdot Ta \tag{2-87}$$

which assumes the sky is clear 68% of the time and cloudy 32% of the time.

The model assumes that the roof or ground temperature under the array is somewhere between module and ambient temperatures. Ratios for the total to front surface convection coefficients and, subsequently, the ratio of the roof or ground to module temperature rise above ambient are calculated.

Wind speed is corrected from the measurement height (typically 10m) to the average array height using

$$w_m = w_a \cdot \left(\frac{y_m}{y_a}\right)^{0.2} \tag{2-88}$$

where

w_m	=	wind speed at module height (m/s)
w_a	=	wind speed at anemometer height (m/s)
y_m	=	average module height (m)
y_a	=	anemometer height (m)

The Sandia report provides source code for calculating module temperature based on weather data and the input parameters described in the following sections.

2.1.4.2 Module INOCT (°C)

As discussed previously, the INOCT is the NOCT in its installed configuration. The Sandia document provides code for estimating INOCT from a set of measured data. This routine starts with a guess for INOCT, uses the model and the measured ambient data to estimate module temperature for each point in the data set, calculates the residual (weighted with irradiance), adds the weighted residual to the INOCT guess and repeats until the residual is less than 0.1°C. This approach will probably give the best INOCT value since it is based on measured data and optimizes for the model's assumptions.

For the module energy rating, we have assumed the same mounting configuration as assumed for the standard NOCT measurement—open rack, or per manufacturer's specifications. However, NOCT is based on open circuited modules, which will tend to run hotter than modules under operation. The temperature difference due to operating the module is proportional to the irradiance level and the module operating efficiency. We can estimate the temperature difference by starting out with a very simple energy balance:

$$H \cdot \overline{\tau\alpha} - Um \cdot (Tm - Ta) - H \cdot \eta = 0 \qquad (2\text{-}89)$$

where

H = plane of array irradiance, W/m^2

$\overline{\tau\alpha}$ = module effective transmittance-absorptance product

Um = overall module heat loss coefficient, W-m^2/°C

η = module efficiency at H and Tm

Assuming a $\overline{\tau\alpha}$ of 0.9, plugging in the NOCT conditions (800 W/m^2 irradiance, 20°C ambient temperature, wind speed is ignored, 0.0% module efficiency), and solving for Um gives

$$Um = \frac{800 \cdot 0.9}{NOCT - 20} \qquad (2\text{-}90)$$

Finally, substituting Eqn. (2-89) and NOCT conditions into Eqn. (2-89) and solving for Tm (=INOCT) gives

$$INOCT = (NOCT - 20) \cdot \frac{0.9 - \eta}{0.9} + 20 \qquad (2\text{-}91)$$

Equation (2-91) provides the INOCT given measured values of NOCT and η at NOCT. Note that these results will be somewhat conservative for fixed voltage operation.

2.1.4.3 Module and Anemometer Heights (m)

We need to make an assumption regarding module height for consistency and comparative purposes. A module height of 2m might be an appropriate compromise between ground mounted and rooftop arrays. The anemometer height for the National Solar Resource Database (NSRDB) is 10 m.

2.1.4.4 Irradiance (W/m^2)

The full spectrum plane of array irradiance (the output of the irradiance model described in section 3.2.6) is used for the thermal model.

2.1.4.5 Ambient Temperature (°C)

One of the specified input weather parameters.

2.1.4.6 Wind Speed (m/s)

One of the specified input weather parameters.

2.1.4.7 Date and Time

The Fuentes thermal model is dynamic in the time domain. The date and time are used to determine the time interval from the last reading.

2.1.4.8 Limitations

This model was developed using typical 1980-vintage flat plate modules. It was verified using various residential roof-mounted arrays—from direct mount to standoff (1-9 inches between the roof and array for airflow) to rack mount.

While the basic approach wouldn't obviate its use for concentrator modules, some of the simplifying assumptions and generalized heat transfer parameters might be inappropriate. A concentrator module is typically designed to transfer most of its heat through the back (i.e. a heat sink), whereas a flat plate module loses a significant amount of it's heat from the front surface. The model ignores module conductivity and assumes that the front and rear surfaces are at the temperature of the cell. This is, at best, less true with a concentrator module. There can be a 5 to 30 C difference between cell and rear surface temperature in a concentrator module.

The model starts with a "measured" module temperature under fairly typical peak conditions and adjusts it based on actual ambient conditions. In general, a concentrator module will respond in the same manner as a flat plate module to changes in ambient conditions. A separate thermal model for concentrators may be required.

2.1.5 Optical Model

The reflectivity model uses the plane-of-array beam irradiance incidence angle to obtain an incidence angle modifier (IAM) which accounts for reflection and other effects. Reflectivity may be affected by conditions other than the incidence angle, such as module materials, soiling and incident spectrum. Of these additional effects, only module materials (as represented by module test data) were considered for this application.

For best accuracy, this effect should be applied to the beam component separately from the diffuse component. For an isotropic diffuse component[1], the effect of reflection may be integrated over the field of view to obtain a constant net effect. Depending on how the diffuse value is obtained, this constant may already be accounted for by instrument calibration. Deriving coefficients to match the measured effect on total plane-of-array irradiance is equivalent to assuming a fixed ratio of beam to diffuse irradiance. Such an assumption cannot be supported for application to both clear and cloudy days.

The IAM may be computed using the empirical curve fit suggested by Gaul and Rabl [Wenger, personal communication; see also Whitaker et. al. (1991)]:

---

[1] Note that the Perez model assumes the diffuse component includes circumsolar and horizon components. While the circumsolar component will vary along with the beam component, for fixed orientation the horizon component will also integrate to a constant.

$$IAM = a + b\theta + c\theta^2 + d\theta^3 + e\theta^4 \quad (2\text{-}92)$$

where

θ = Plane-of-array incidence angle (radians)

a-e = Empirical curve-fit coefficient

Based on PVUSA data, Wenger suggests:

a = 90.8392

b = 2.2081E-2

c = -1.13092E-3

d = 2.5439E-5

e = -2.1088E-7

However, the TRC pointed out that since these coefficients were obtained using global plane-of-array pyranometer data and maximum power point data, they suffer from confounding of the irradiance components (as described above), incidence angle effects on the pyranometer itself, and confounding of irradiance and power model effects (since I_{sc} was not used).

An alternative approach to quantifying the incidence angle effect was developed by D. King [King, 1996]. This technique involved the use of an azimuth/altitude type two-axis tracker whose azimuth was varied to obtain I_{sc} data for a range of incidence angles while keeping the diffuse component essentially constant. Attempts to reproduce this procedure at NREL yielded unsatisfactory results, so no IAM function was used in this document.

2.1.6 Irradiance Model

The irradiance model transforms commonly available time-correlated irradiance and other weather measurements and plane-of-array orientation into incidence angle and full-spectrum incident beam and diffuse irradiance estimates using astronomical solar position equations and the Perez diffuse radiation model. The steps in these computations are the determination of the true local solar time, computation of the local solar position, computation of the plane-of-array beam irradiance and incidence angle, and the evaluation of the Perez diffuse radiation model. With the exception of azimuth

angle (Equation (2-98)), these equations were extracted from source code provided by Daryl Myers of NREL and represented the "NREL consensus" method for this type of application. Equation (2-98) [Meeu, 1982] was chosen because it handles the full range of azimuth angles in a more concise form.

2.1.6.1 True Local Solar Time

The true local solar time (ω; radians) is given by:

$$\omega = E + \tfrac{\pi}{12} \cdot (t + t_{zl}) \tag{2-93}$$

$$\begin{aligned} E = {} & 0.000075 \\ & +0.001868 \cdot \cos(\alpha_D) - 0.032077 \cdot \sin(\alpha_D) \\ & -0.014615 \cdot \cos(2 \cdot \alpha_D) - 0.040849 \cdot \sin(2 \cdot \alpha_D) \end{aligned} \tag{2-94}$$

$$\alpha_D = \frac{2\pi}{365} \cdot (D - 1) \tag{2-95}$$

$$t_{zl} = \frac{L}{15} - Z \tag{2-96}$$

where

E = Equation of time (radians)
α_D = Day angle (radians); position of sun relative to stars
D = Day number (1 Jan = 1; 31 Dec = 365 or 366 in leap year)
t = Time at which ω is to be computed (hours past midnight)
t_{zl} = Local standard to local sidereal time correction (hours)
L = Site latitude (degrees; positive east of Greenwich)
Z = Time zone (hours to be added to GMT for local standard time)

2.1.6.2 Local Solar Position

The local solar position (zenith angle z and azimuth angle A in radians) is given by:

$$z = \cos^{-1}(\cos(\phi) \cdot \cos(\delta) \cdot \cos(\omega) + \sin(\phi) \cdot \sin(\delta)) \tag{2-97}$$

$$A = ATAN2(\cos(\omega) \cdot \sin(\phi) - \cos(\phi) \cdot \tan(\delta), \sin(\omega)) \tag{2-98}$$

$$\begin{aligned}\delta = {} & 0.006918 \\ & -0.399912 \cdot \cos(\alpha_D) + 0.070257 \cdot \sin(\alpha_D) \\ & -0.006758 \cdot \cos(2\alpha_D) + 0.000907 \cdot \sin(2\alpha_D) \\ & -0.002697 \cdot \cos(3\alpha_D) + 0.00148 \cdot \sin(3\alpha_D)\end{aligned} \qquad (2\text{-}99)$$

where

ϕ = Site latitude (radians)

δ = Sun declination (radians)

ω = True local solar time (radians; see Equation (2-93))

ATAN2(x,y) = four quadrant arctangent function

α_D = Day angle (radians); position of sun relative to stars

2.1.6.3 Plane-of-Array Incidence Angle

The plane-of-array (beam irradiance) incidence angle on a fixed tilted surface is given by:

$$\theta = \cos^{-1}(\cos(z) \cdot \cos(\varphi) + \sin(z) \cdot \cos(A - A_\varphi) \cdot \sin(\varphi)) \qquad (2\text{-}100)$$

where

z = Sun zenith angle (radians)

A = Sun azimuth (radians, measured from north, positive toward east)

A_φ = Azimuth toward which plane-of-array is facing (radians)

φ = Angle of tilt of plane-of-array relative to horizontal (radians; positive in northern hemisphere, negative in southern hemisphere)

Note that for a fixed latitude-tilt surface, the MER methodology assumes A_φ will be π in the northern hemisphere, and 0 in the southern hemisphere.

For two-axis tracking structures, the incidence angle is assumed to be zero. Alternate tracking position algorithms are not considered here because the rating procedure is not anticipated to allow for them.

2.1.6.4 Plane-of-Array Incident Beam and Diffuse Irradiance

The primary inputs to the power model are plane-of-array (POA) beam and diffuse irradiance. Unfortunately, these values are not normally available in weather data, so an

irradiance model is needed. The contribution of the beam irradiance to the POA irradiance may be computed as:

$$H_{POA,B} = H_B \cdot \cos(\theta) \tag{2-101}$$

where

H_B = Beam irradiance (W/m^2)

θ = Plane-of-array incidence angle (radians)

The contribution of the diffuse irradiance to the POA irradiance is somewhat more complex. Including an assumed uniform ground albedo and a uniform sky brightness excepting a circumsolar region and a horizon band, Perez et al. developed the model given below [6] for the diffuse POA irradiance:

$$H_{POA,D} = H_D \cdot \left((1 - F_1) \cdot \frac{1 + \cos(\varphi)}{2} + F_1 \cdot \frac{a}{b} + F_2 \cdot \sin(\varphi) \right) \tag{2-102}$$

$$a = \max(0, \cos(\theta)) \tag{2-103}$$

$$b = \max(\cos(85^\circ), \cos(z)) \tag{2-104}$$

$$F_1(\varepsilon) = \max(0, F_{11}(\varepsilon) + F_{12}(\varepsilon) \cdot \Delta + F_{13}(\varepsilon) \cdot z) \tag{2-105}$$

$$F_2(\varepsilon) = F_{21}(\varepsilon) + F_{22}(\varepsilon) \cdot \Delta + F_{23}(\varepsilon) \cdot z) \tag{2-106}$$

$$\varepsilon = \frac{\frac{H_D + H_B}{H_D} + \kappa \cdot z^3}{1 + \kappa \cdot z^3} \tag{2-107}$$

$$\Delta = \frac{H_D \cdot m}{H_o} \tag{2-108}$$

$$m = \frac{1}{\cos(z) + 0.00094 \cdot (1.6389 - z)^{-1.253}} \tag{2-109}$$

where

H_D = Diffuse horizontal irradiance (W/m^2)

φ = Angle of tilt of plane-of-array relative to horizontal (radians; always positive)

a,b = terms describing the incidence-weighted solid angle sustained by the circumsolar region as seen respectively by the tilted surface and the horizontal (unitless)

$F_1(\varepsilon)$ = circumsolar "reduced" brightness coefficient (unitless)

$F_2(\varepsilon)$ = horizon "reduced" brightness coefficient (unitless)

F_{1i}, F_{2i} = Coefficients for computing brightness coefficients, see Table 2-3.

ε = sky clearness (unitless)

κ = a constant: 1.041 (1/radians^3)

z = Sun zenith angle (radians)

Δ = Sky brightness (unitless)

m = Air mass (unitless)

H_o = Extraterrestrial normal incident beam irradiance (W/m^2)

Table 2-3. Perez Model Brightness Coefficients

	F_{11}	F_{12}	F_{13}	F_{21}	F_{22}	F_{23}
1≤ε≤1.065	-0.0083117	0.5877285	-0.0620636	-0.0596012	0.0721249	-0.0220216
1.065<ε≤1.23	0.1299457	0.6825954	-0.1513752	-0.0189325	0.065965	-0.0288748
1.23<ε≤1.5	0.3296958	0.4868735	-0.2210958	0.055414	-0.0639588	-0.0260542
1.5<ε≤1.95	0.5682053	0.1874525	-0.295129	0.1088631	-0.1519229	-0.0139754
1.95<ε≤2.8	0.873028	-0.3920403	-0.3616149	0.2255647	-0.4620442	0.0012448
2.8<ε≤4.5	1.1326077	-1.2367284	-0.4118494	0.2877813	-0.8230357	0.0558651
4.5<ε≤6.2	1.0601591	-1.5999137	-0.3589221	0.2642124	-1.127234	0.1310694
6.2<ε	0.677747	-0.3272588	-0.2504286	0.1561313	-1.3765031	0.2506212

2.2 Required Input Data

This section describes the input data required by the various modeling components described in section 2.1. While input requirements were discussed briefly with each algorithm, this section discusses the specific parameters that need to be available.

These parameters are subdivided here into module characteristics and evaluation characteristics. The module characteristics must be obtained by reduction of module test data, while the evaluation characteristics specify the common conditions under which all modules should be compared. The latter values are fixed as detailed by this rating procedure.

2.2.1 Module Characteristics

The module characteristic input parameters are listed in Table 2-4 below.

Table 2-4. MER Required Module Characteristics

Parameter	Units	Model Use	Notes
Incidence Angle Modifier Coefficients		Reflectivity	1
Spectral Response Function	A/W	Spectral	2
Nominal Operating Cell Temperature	°C	Thermal	
Efficiency at NOCT	%	Thermal	
Power Model Coefficients		Power	3
Effective Fixed Voltage	V	Power	4

1 The coefficients for the IAM equation are described in Section 2.1.5.
2 The SR function represents the response of the particular cell technology to spectrum with as many points as necessary or feasible to characterize the response.
3 The coefficients for the power model are described in Section 2.1.2.
4 Since the fixed 14.4 V value may be modified by assuming a recommended number of batteries and modules, this value is somewhat adjustable.

The spectral response and quantum efficiency of a module both quantify how a module responds to various wavelengths of incident light. The spectral response is typically presented as a function of wavelength with units of A/W, and the quantum efficiency is also presented as a function of wavelength but with units of electrons/photon. Quantum efficiency may be converted to spectral response using the equation:

$$SR(\lambda) = \frac{q}{h \cdot c} \cdot \lambda \cdot QE(\lambda) \qquad (2\text{-}110)$$

where

q = Electron charge constant ($1.60219 \cdot 10^{-19}$ A·s)
h = Planck's constant ($6.6262 \cdot 10^{-34}$ J·s)
c = Speed of light ($2.997925 \cdot 10^{8}$ m/s)

The spectral model expects the module spectral response represented as a series of λ-SR data points over the range from 300 to 1100 nm. For the purposes of the MER, scaling need not be accurate, as only the shape of the response function is needed. Therefore, a relative SR obtained by multiplying a relative QE by λ is adequate.

The specific characteristics required will depend on the power model chosen, but in all cases the characteristics will be available from the results of the module testing.

2.2.2 Evaluation Characteristics

The evaluation characteristics are module load type, location and environmental data. These parameters are defined by the MER, and applied, as appropriate, to all modules. The latter two characteristics are interrelated by the selection of specific actual days at specific locations to represent the various conditions under which the module is to be evaluated.

2.2.2.1 Module Load Type

The power output of any module depends on the voltage or current at which it is operated. Two load types representative of typical installations are specified.

The first load type is an ideal maximum power tracker. This load varies the voltage and current as necessary to maximize the power output of the module. This load represents the ideal behavior of a grid-connected dc to ac power inverter, and represents the best energy production output obtainable from the module under the given environmental conditions.

The second load type is an ideal voltage source. This load maintains fixed voltage representing a battery charging application. The voltage specified for this load type is 14.4 V, which is a common upper voltage limit for 12 V lead-acid batteries. This voltage was not universally accepted by the TRC. It was suggested that a time-varying voltage profile might be more useful for comparative rating and as an estimate of module output. This is a topic for further development.

2.2.2.2 Location

The location is specified using the latitude, longitude and time zone. The latitude is expected in degrees north of the equator (south is negative), the longitude is expected in degrees east of Greenwich Observatory (west is negative), and the time zone is expected in hours earlier than GMT (time zones for the United States are negative).

2.2.2.3 Environmental Data

The environmental conditions described in Table 2-5 below are functions of time and location. Time is expected to be local standard time as reported in the location's time zone. Many of these parameters are available in the National Solar Resource Database (NSRDB), which is available as the Solar and Meteorological Surface Observation

Network Compact Disc, or CD-SAMSON. This database contains hourly data from 239 sites throughout the United States.

Table 2-5 MER Required Evaluation Parameters

Parameter	Units	Model Use	Notes
Site Latitude	°	Irradiance	1
Site Longitude	°	Irradiance	1
Time Zone	h	Irradiance	2
Date	yyddd	Irradiance	1
Time	hh.hh	Irradiance	1
Global Horizontal Irradiance	W/m^2	Irradiance	1
Beam (Direct Normal) Irradiance	W/m^2	Irradiance	1
Ambient Temperature	°C	Thermal	1
Dew Point Temperature	°C	Spectral	1
Barometric Pressure	mBar	Spectral	1
Wind Speed	m/s	Thermal	1
Cloud Cover Modifier Coefficients		Spectral	3
Std Solar Spectrum	$W/m^2/\mu m$	Spectral	4
Atmospheric Absorption Spectra		Spectral	4

1 These parameters are available in the National Solar Resource Database.
2 Number of hours from Greenwich Mean Time. For example, PST is -8.
3 SEDES2 provides 74 sets of 6 coefficients: A_1, A_2, B_1, B_2, C_1, and C_2 to compute cloud cover modifier values.
4 Provided with SEDES2.

3. MODULE CHARACTERIZATION PROCEDURES

The module characterization procedures consist of testing the modules and reducing the test data to the form required by the model used in the MER computations.

3.1 Module Testing

Module testing is needed to obtain model parameters that characterize the module type. These tests obtain raw data to characterize the module with respect to the power, spectral, thermal and reflection models.

3.1.1 Power Model

The testing required to characterize the module for the power model depends on the model chosen. However, parameters for each power model must be extracted from data obtained either from indoor (laboratory) or outdoor tests.

3.1.1.1 Laboratory Testing (Anderson, Blaesser, Interpolation)

The following procedure is used to determine module characteristics for use in the Anderson, Blaesser, and interpolation models.

3.1.1.1.1 Background

The temperature and irradiance dependence of a sample PV module is required to be able to translate from standard reporting conditions to any other set of reporting conditions or visa versa. There are a wide variety of translation equations that have been developed or proposed. Some translation equations only need to know the percent change per °C or per W/m^2. Other translation equations are in units of volts, amps or W per °C or per W/m^2. At least one translation method does not use any equations but relies on interpolation to a given temperature and total irradiance based upon a matrix of I-V measurements vs. irradiance and temperature. To satisfy the required data for all of these translation methods, the I-V characteristics as a function of the total irradiance and temperature must be known.

The irradiance vs. temperature dependence matrix is generated by flash testing a PV module at different temperatures and irradiances. Temperature is controlled using a heating pad. Irradiance is controlled by stacking layers of an attenuating medium (such as velum) on the module.

3.1.1.1.2 Procedures

Setup: The normal procedure of calibrating the intensity monitor using a reference device and spectral mismatch error is followed. (1000 W/m^2, ASTM E892 AM1.5 global reference.)

Mount module: Once the monitor is calibrated, attach a thermocouple to the back of the module and place the module on a heating pad. The thermocouple should have some thermal insulation between it and the heating pad so that the temperature above the heating pad is not measured. Attach the positive and negative leads from the current and voltage terminals on the flash tester to the module. The height of the monitor must be adjusted following normal procedures to be level with the front surface of the module.

Measurements: All measurements on a given sample should be performed without moving the module or resetting the monitor calibration. If the monitor is reset then a discontinuity of as much as 1% in the current readings will result. This may be a problem if the data is analyzed as a single set or the coefficients are in units of Amps or Watts per °C. Measure the I-V characteristics at STC (25°C, 1000 W/m^2, ASTM E892 global reference). Step A: Wait until the measured temperature changes by less than 1°C over a 5 minute period. This helps ensure that the measured temperature is close to the space-charge region temperature and the temperature gradients across the module have stabilized. Step B: Measure the I-V characteristics and record the temperature as measured with the insulated thermocouple and number of velum sheets along with the usual information. Step C: Place the plastic velum diffuser sheets over the module (but not the monitor), and repeat Step B at increasing or decreasing intensity as the sheets are removed or added. The efficiency reported by the simulator will be wrong for these measurements because the simulator still thinks that the module is seeing one-sun. Choose the number of sheets for each step such that about 6 irradiance levels are tested in the range from 0.15-1 sun (for example, 0 sheet, 1 sheet, 3 sheets, etc., to 9 sheets). The temperature should not be changing as Steps B and C are repeated so measurements are taken at a fixed temperature with varying irradiance. Step D: Increase the temperature 10°C. Repeat steps A, B, C and D until the maximum desired temperature is reached. Step E: Decrease the temperature and measure only the 1-sun I-V characteristics following steps A and B until room temperature is reached. Note that only 3 points are needed for this step. The purpose of this step is to verify that the IV

vs. temperature characteristics are not a function of whether the temperature is increasing or decreasing.

Data Quality Control: Prior to release of the data, the I-V curves must be analyzed. This constitutes performing a linear least squares fit to the Voc, Isc, Pmax and FF vs. temperature. The data should be linear for the single-junction PV technologies. The temperature coefficient in ppm/°C or %/°C should be computed so that the temperature coefficient for this sample can be directly compared with other samples of the same and different technologies. This data should be saved with the file name linked to a test report number and sample ID or the manufacturer, and sample ID. It is also useful if the technology is in the sample name. The data in the file and record book should be commented sufficiently to be able to recover the raw data (filename or manufacturer, sample ID, and date).

3.1.1.1.3 Assumption and Sources of Uncertainty

This method assumes that I_{sc} is linear with total irradiance. That is, incident irradiance is estimated based on the ratio of the I_{sc} measured with n velum sheets to the I_{sc} measured with no velum sheets times the irradiance measured with no velum sheets. If the 1000 W/m^2 point is used in translation equations involving irradiance coefficients, then a plot of I_{sc} vs. irradiance must be linear and the 1000 W/m^2 point must be the greatest irradiance on the graph. This is because the spectral mismatch error is changed between no velum sheets on the module and one or more sheets, so the spectral calibration must be performed with no velum sheets. It is believed that the spectral mismatch error does not change between one and more than one sheet because the velum acts as a scattering medium with almost no specular transmittance. This method assumes that the space-charge region temperature has been measured and that the temperature is uniform across the module surface. Note that, substantial additional time may be required if temperature coefficients measurements below 20°C are required because of the time required to control the room temperature. These additional points should not be required if the coefficients are linear with temperature.

3.1.1.2 Outdoor Testing (Blaesser, Myers)

The Blaesser and Myers models have built-in thermal models and, therefore, need to be characterized under actual conditions. In general, this means outdoors. Data should be collected over a 4 week period that is characterized by diverse weather conditions

including a high percentage of clear days. Testing should be done at locations and times of year where the noon-time air mass is less than 3.

The following items must be addressed:

- module mounted at latitude tilt, facing due south.
- monitor back of module temperature, H_{POA}, T_{amb}, WS, V and I.
- measure IV curves every 30-180 seconds, average values of I_{sc}, V_{oc}, I_{pp}, V_{pp}, P_{pp} I_{fo} along with ambient conditions every 10-15 minutes, and record a snapshot IV curve along with the averaged data. Maintain module at peak power conditions between IV curves.

3.1.2 Spectral Model

Typically, a sample cell from the module's technology will be tested by exposing it to a series of monochromatic light sources and measuring its short circuit current output. This will yield a Relative (external) Spectral Response curve.

3.1.3 Thermal Model

The Fuentes model requires the module's Nominal Operating Cell Temperature. A procedure for measuring and calculating NOCT is provided by ASTM E1036/Annex A1, "Test Method for Electrical Performance of Non-Concentrator Terrestrial PV Modules and Arrays Using Reference Cells." If the test is performed per the specification (i.e. with the module open circuited), the resulting module temperature will have to be corrected to account for operation. Alternatively, the module can be operated at its peak power point during the test so that the correction does not have to be applied.

3.1.4 Optical Model

Several approaches have been suggested for testing the influence of solar angle-of-incidence on a module. The approach favored by the Technical Review Committee was developed by David King of Sandia [King, 1996]. It consists of mounting the module on an azimuth-elevation type controllable 2-axis solar tracker, tracking the sun in elevation. The tracker orientation is varied in azimuth only to maintain (approximately) constant diffuse irradiance and albedo while varying the incidence angle of the beam irradiance.

The test is performed under a very clear sky with high direct-to-global irradiance ratio. This the AOI influence is at its peak. The other extreme would be isotropically diffuse irradiance where the module would exhibit no AOI sensitivity.

This test does not account for the effects of soiling on the reflectivity of the modules, since it is performed quickly with clean modules. Other approaches that used longer-term data were considered to be subject to an uncontrollable variation in soiling, which would complicate reproducibility of the results. Since the MER is specified for clean modules, this should not be an issue.

3.2 Data Reduction

Data acquired by testing the modules must, in most cases, be used to compute estimates of model parameters. This section describes the key calculations to be performed on test data for the models described in this report.

3.2.1 Power Model

The choice of power model used in the MER computation determines the parameters that must be computed. Since errors introduced in this model by inaccurate parameters or inappropriate models tend to dominate the error in the final result, the determination of the appropriate parameters should be undertaken very carefully.

3.2.1.1 Anderson Model

Solving the Anderson I_{sc} and V_{oc} translation equations for the temperature and irradiance coefficients α, β, and δ:

$$\alpha = \frac{\left(H_2 Isc_1 / H_1 Isc_2\right) - 1}{T_1 - T_2} \tag{3-1}$$

$$\beta = \frac{\left[Voc_1 / Voc_2\left(1 + \delta \ln\left(H_1/H_2\right)\right)\right] - 1}{T_1 - T_2} \tag{3-2}$$

$$\delta = \frac{\left[Voc_1 / Voc_2\left(1 + \beta\left(T_1 - T_2\right)\right)\right] - 1}{\ln\left(H_1/H_2\right)} \tag{3-3}$$

Equations (3-2) and (3-3) are not independent, but if data are selected where $H_1=H_2$, then the δ term in equation (3-2) drops out leaving

$$\beta = \frac{\left(Voc_1/Voc_2\right)-1}{T_1-T_2}_{H_1=H_2} \tag{3-4}$$

Similarly, if the data are such that $T_1 = T_2$ then the β term drops out of equation (3-3) resulting in

$$\delta = \frac{\left(Voc_1/Voc_2\right)-1}{\ln\left(H_1/H_2\right)}_{T_1=T_2} \tag{3-5}$$

These equations should be applied to the results of an IV vs. irradiance and temperature indoor test. While an average of all combinations of pairs of different test points may be chosen to compute α (as well as β and δ subject to the stated constraints), averaging only a selection of test points with widely differing inputs is likely to be most accurate. Computation of the variance and examination of a residual plot should be used to avoid errors due to outliers or systematic errors.

3.2.1.2 Myers Model

This model does not use the laboratory test procedures described in Section 2.1 to obtain its coefficients. Instead, a set of measured data points must be collected from a field test, including plane-of-array irradiance, maximum power output, and power output at the appropriate fixed voltage conditions. This information can be extracted from full IV curve data, though averaging may be advisable to reduce the data storage requirements without undersampling. For the fixed voltage condition, the module may be assumed to never draw current if the open circuit voltage is below the specified fixed voltage. This assumption is justified if a charge controller disconnects the battery under low irradiance conditions.

Two linear least-squares regressions of a quality-checked subset of the field data (P_m vs. H; P_{fv} vs. H) can be performed to obtain the appropriate equation parameters. To check the quality of the data, the irradiance must be greater than 0 (value subject to change?) and less than 1425 W/m^2, and the power values should be greater or equal to 0. No fewer than (200?) values should be used for the regression.

3.2.1.3 Interpolation Model

The only data reduction required for this model is the extraction of the maximum power and fixed voltage power for each of the IV curves obtained from testing, with the corresponding irradiances and temperatures.

3.2.1.4 Blaesser Model

Equation (2-17) of the Blaesser model contains the regression coefficients a, b, and c.

$$Dv = a \cdot \ln(H_r / H) + b \cdot (T_{amb} - T_r) + c \cdot H \qquad (3\text{-}6)$$

$$Dv = DV / V_{oc,r}; \qquad DV = V_r - V = V_{oc,r} - V_{oc} \qquad (3\text{-}7)$$

Combining these three equations results in

$$1 - V_{oc} / V_{oc,r} = a \cdot \ln(H_r / H) + b \cdot (T_{amb} - T_r) + c \cdot H \qquad (3\text{-}8)$$

A linear regression can be performed using this equation and measured values of V_{oc}, H, and T_{amb}, along with the reference values $V_{oc,r}$, T_r, and H_r. Since the Blaesser model is used to adjust a reference curve to actual conditions, the above reference values should correspond to the reference IV curve to be used. Best results will most likely be obtained using one of the IV curves obtained during the outdoor testing representing the average conditions. It is also possible to use an IV curve measured indoors for the reference.

3.2.2 Spectral Model

If relative quantum efficiency data must be used, multiply each RQE value by its corresponding wavelength to obtain relative spectral response. Also, to simplify computations, the SR should be interpolated to obtain data at the wavelengths at which the extraterrestrial (AM0) spectrum, H_0, used by the SEDES2 spectral model is specified.

3.2.3 Thermal Model

Once the NOCT is obtained using ASTM E1036, equation 2-37 is used along with the reference module efficiency to estimate INOCT.

3.2.4 Optical Model

No data reduction procedures have been defined for this model, because no model has been selected.

4. WEATHER DATA

One of the key ingredients in the Module Energy Rating is the selection of appropriate weather data. The weather data should define extreme conditions that will allow differences in module design and performance to be discernible. It would be fairly easy to define the reference days by arbitrarily assigning hourly values for each parameter. However, it was felt that users might find real data from specific dates and locations a bit more descriptive, i.e. a "summer day in Phoenix". To emphasize the standardization of the weather, the National Solar Radiation Database (NSRDB) was selected as the source of the data. These data comply with the parameter requirements stipulated in section 2.2, and are available on CD-ROM from NREL. Thus, a complete set of hourly weather data is specified by a site (city name) and date.

Subjective criteria for the reference days were developed as shown in Table 4-1. Data from the NSRDB were summarized and reviewed by Daryl Myers of NREL. He then developed a list of days generally meeting each set of criteria, though primarily based on the time of year, irradiance and temperature criteria. From this list, Myers selected sites providing some geographic diversity. A summary of the selected days are provided in Table 4-2 and Figure 4-1. According to Myers, these days are representative of extreme conditions that can actually be achieved without being artificially extreme or unique in themselves.

Table 4-1 Criteria for Reference Days

	Month	Day Hrs	GHI		DNI		Tamb		Wind Speed		Rel Hum Wtd (%)
			Peak† (W/m^2)	Total (kWh/m^2)	Peak (W/m^2)	Total (kWh/m^2)	Peak (°C)	Wtd (°C)	Peak (m/s)	Wtd (m/s)	
Hot Sunny	Sum		>1000	10-12			>35			Low	Low
Cold Sunny	Wint		>900				0.0			Avg	Low
Hot Cloudy	Sum		<400				>35			Avg	High
Cold Cloudy	Wint		200 - 400				0.0			High	High
NICE	Sprg		800	6			20			Avg	Avg

† - Did not consider latitude and time of year.

Table 4-2 Selected Reference days

Day	Location	Month	Day Hrs	GHI		DNI		Tamb		Wind Speed		Rel Hum
				Peak† (W/m^2)	Total (kWh/m^2)	Peak (W/m^2)	Total (kWh/m^2)	Peak (°C)	Wtd‡ (°C)	Peak (m/s)	Wtd‡ (m/s)	Wtd‡ (%)
Hot Sunny	Phoenix, AZ	Jun	15	1080	9.14	1003	11.9	39.4	36.3	9.8	3.9	6.3
Cold Sunny	Alamosa, CO	Feb	11	671	4.34	1032	9.4	3.3	-0.6	4.6	2.2	50.9
Hot Cloudy	Brownsville TX	Jul	15	480	3.47	81	0.3	33.3	32.1	9.3	7.9	59.8
Cold Cloudy	Buffalo, NY	Dec	10	237	1.32	2	0.0	0.0	-0.1	4.6	3.7	93.4
NICE	Sacramento, CA	May	14	905	7.12	846	8.3	19.4	17.3	5.7	5.0	65.4

‡ - Values are weighted with GHI

During the evaluation of the NSRDB, it became obvious that the subjective criteria were somewhat self-contradictory. For example, the hot sunny day had higher wind speed than desired. Data for Phoenix, Bakersfield, Dagget, and Las Vegas all showed relatively high wind speed trends at temperatures above 40 °C. Similarly, the humidity on the Hot Cloudy day seemed low. However, high humidity is accompanied by either low temperature (relative humidity goes up as temperature decreases) or by high irradiance (probably driving evaporation).

Note that comparing MER values from different days can be a bit misleading. One of the main reasons PV systems provide less energy in the winter than in the summer is the shorter winter day, not necessarily worse weather. Latitude exacerbates this situation: as latitude increases the differences between summer and winter day lengths increase.

The following figures show the weather data graphically. Tabular data for each of the selected reference days are presented in the following sections. Tables in each section provide the actual data from the NSRDB. Only selected parameters are presented: hour (time of day) global horizontal irradiance (GHI), direct normal irradiance (DNI), diffuse horizontal irradiance (Diff), ambient temperature (Tamb), wind speed (WS) and relative humidity (RH).

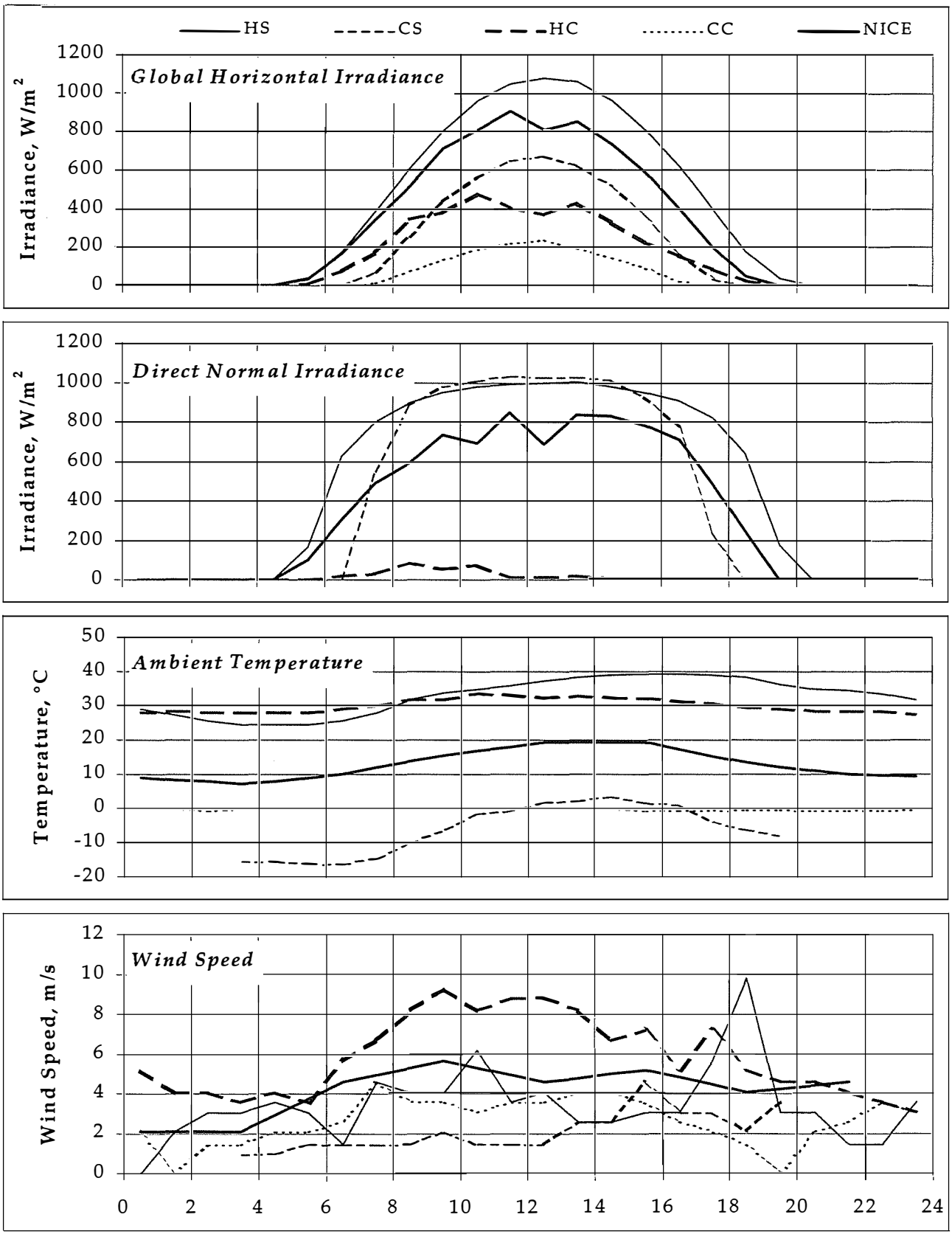

Figure 4-1 Reference Day Weather Data Plots

4.1 Hot Sunny: Phoenix, AZ, June 15, 1976

This day exemplifies the summer in the desert southwest: hot, dry, and clear. Modules with good thermal characteristics or low temperature coefficients should do relatively well on this day.

Hour	GHI (W/m^2)	DNI (W/m^2)	Diff (W/m^2)	Tamb (°C)	WS (m/s)	RH (%)
0.5	0	0	0	28.9	0	15
1.5	0	0	0	27.2	2.1	15
2.5	0	0	0	25.6	3.1	21
3.5	0	0	0	24.4	3.1	18
4.5	0	0	0	24.4	3.6	20
5.5	32	166	15	24.4	3.1	16
6.5	172	624	35	25.6	1.5	15
7.5	388	802	53	27.8	4.6	16
8.5	608	893	70	31.7	4.1	11
9.5	805	949	84	33.9	4.1	7
10.5	959	982	93	35	6.2	5
11.5	1049	992	98	36	3.6	6
12.5	1080	995	101	37.2	4.1	6
13.5	1061	1003	99	38.3	2.6	4
14.5	960	982	93	38.9	2.6	5
15.5	807	950	84	39.4	3.1	5
16.5	617	906	71	39.4	3.1	4
17.5	397	821	53	38.9	5.7	5
18.5	175	636	35	38.3	9.8	5
19.5	34	175	15	36.1	3.1	7
20.5	0	0	0	35	3.1	8
21.5	0	0	0	34.4	1.5	10
22.5	0	0	0	33.3	1.5	12
23.5	0	0	0	31.7	3.6	15

4.2 Cold Sunny: Alamosa, CO, February 11, 1961

With the extremely high DNI and low temperature, this day should produce peak power values. However, since it is in the winter, the short day length will limit module energy.

Hour	GHI (W/m^2)	DNI (W/m^2)	Diff (W/m^2)	Tamb (°C)	WS (m/s)	RH (%)
0.5	0	0	0			
1.5	0	0	0			
2.5	0	0	0			
3.5	0	0	0	-15.6	1	79
4.5	0	0	0	-15.6	1	79
5.5	0	0	0	-16.1	1.5	75
6.5	0	0	0	-16.1	1.5	75
7.5	67	548	12	-14.4	1.5	76
8.5	251	882	22	-10	1.5	73
9.5	434	979	31	-6.1	2.1	68
10.5	566	1008	38	-1.7	1.5	53
11.5	650	1032	42	-0.6	1.5	56
12.5	671	1027	49	1.7	1.5	47
13.5	624	1027	41	2.2	2.6	48
14.5	523	1012	35	3.3	2.6	32
15.5	357	925	31	1.7	4.6	42
16.5	165	774	20	1.1	3.1	38
17.5	34	226	9	-3.9	3.1	62
18.5	0	0	0	-6.1	2.1	71
19.5	0	0	0	-7.8	3.6	70
20.5	0	0	0			
21.5	0	0	0			
22.5	0	0	0			
23.5	0	0	0			

4.3 Hot Cloudy: Brownsville, TX, July 4, 1983

The medium irradiance levels and high temperatures of these conditions will emphasize low temperature sensitivity.

Hour	GHI (W/m^2)	DNI (W/m^2)	Diff (W/m^2)	Tamb (°C)	WS (m/s)	RH (%)
0.5	0	0	0	27.8	5.2	82
1.5	0	0	0	28.3	4.1	80
2.5	0	0	0	27.8	4.1	82
3.5	0	0	0	27.8	3.6	82
4.5	0	0	0	27.8	4.1	82
5.5	5	2	5	27.8	3.6	79
6.5	71	16	68	28.9	5.7	77
7.5	172	27	162	30.0	6.7	72
8.5	340	81	294	31.7	8.2	63
9.5	381	51	343	31.7	9.3	63
10.5	480	69	419	33.3	8.2	56
11.5	405	12	393	32.8	8.8	56
12.5	367	9	358	32.2	8.8	59
13.5	426	15	411	32.8	8.2	56
14.5	329	5	325	32.2	6.7	54
15.5	225	2	223	32.2	7.2	57
16.5	152	1	151	31.1	5.2	65
17.5	88	1	88	30.6	7.2	70
18.5	24	1	24	29.4	5.2	75
19.5	1	1	1	28.9	4.6	74
20.5	0	0	0	28.3	4.6	80
21.5	0	0	0	28.3	4.1	80
22.5	0	0	0	28.3	3.6	80
23.5	0	0	0	27.2	3.1	85

4.4 Cold Cloudy: Buffalo, NY, December 6, 1985

Cold and cloudy conditions are particularly severe for photovoltaic power generation because of the generally lower irradiance levels. These conditions will allow performance comparisons for wintertime carry-through capability.

Hour	GHI (W/m^2)	DNI (W/m^2)	Diff (W/m^2)	Tamb (°C)	WS (m/s)	RH (%)
0.5	0	0	0	0.0	2.1	100
1.5	0	0	0	0.0	0.0	96
2.5	0	0	0	-0.6	1.5	100
3.5	0	0	0	0.0	1.5	96
4.5	0	0	0	0.0	2.1	100
5.5	0	0	0	0.0	2.1	96
6.5	0	0	0	0.0	2.6	100
7.5	12	0	12	0.0	4.6	100
8.5	73	1	73	0.0	3.6	100
9.5	134	0	134	0.0	3.6	96
10.5	187	2	187	0.0	3.1	96
11.5	221	2	220	0.0	3.6	92
12.5	237	0	237	0.0	3.6	92
13.5	196	1	196	0.0	4.1	92
14.5	146	1	145	0.0	4.1	92
15.5	91	1	91	-0.6	3.6	92
16.5	22	0	22	-0.6	2.6	89
17.5	0	0	0	-0.6	2.1	89
18.5	0	0	0	-0.6	1.5	89
19.5	0	0	0	-0.6	0.0	85
20.5	0	0	0	-0.6	2.1	85
21.5	0	0	0	-0.6	2.6	89
22.5	0	0	0	-0.6	3.6	89
23.5	0	0	0	-0.6	3.1	89

4.5 NICE: Sacramento, CA, May 4, 1967

NICE is an acronym for Normal Irradiance-Cool Environment, a phrase coined by Jerry Anderson of Sunset Technology. This is intended to be the "Goldilocks" day: not too hot and not too cold.

Hour	GHI (W/m^2)	DNI (W/m^2)	Diff (W/m^2)	Tamb (°C)	WS (m/s)	RH (%)
0.5	0	0	0	8.9	2.1	89
1.5	0	0	0	8.3	2.1	90
2.5	0	0	0	7.8	2.1	92
3.5	0	0	0	7.2	2.1	93
4.5	0	0	0	8.1	2.9	92
5.5	38	101	28	9.1	3.8	90
6.5	163	303	85	10.0	4.6	89
7.5	344	491	123	11.9	5.0	83
8.5	513	594	145	13.7	5.3	78
9.5	708	732	151	15.6	5.7	72
10.5	811	693	214	16.9	5.3	68
11.5	905	846	132	18.1	5.0	65
12.5	811	689	179	19.4	4.6	61
13.5	854	833	132	19.4	4.8	59
14.5	733	832	91	19.4	5.0	56
15.5	588	785	91	19.4	5.2	54
16.5	400	712	69	17.4	4.8	61
17.5	200	491	64	15.3	4.5	67
18.5	49	245	25	13.3	4.1	74
19.5	0	0	0	12.2	4.3	79
20.5	0	0	0	11.1	4.4	84
21.5	0	0	0	10.0	4.6	89
22.5	0	0	0	9.6		89
23.5	0	0	0	9.3		89

5. RESULTS

This section describes the testing of a set of five sample modules, model validation analysis, and MER results for the sample modules. For all of these activities, the same sample modules and calculation database are used. These common elements are presented briefly in the following paragraphs.

The basic characteristics of the sample modules are given in Table 5-1. These modules represent a variety of single-bandgap technologies and a range of manufacturing dates (1988-1994). Note that in some cases 1 or more modules (N_{mod}) and batteries (N_{bat}) were combined to obtain effective per-module fixed-voltage load values that would be near the peak power point for the module. Due to the broad range of manufacturing dates and the fact that our choices of numbers of batteries and modules have not been approved by the manufacturers, the data presented here are for illustrative purposes only. So while ultimately, MER results for commercial modules are intended to be used to compare one technology to another, these results are for model validation only.

Table 5-1. Basic Characteristics of Tested Modules

Module	Technology	$V_{oc,STC}$ (V)	$V_{mp,STC}$ (V)	N_{bat}	N_{mod}	V_{fb} (V)	Eff. (%)	P_{STC} (W)
1	c-Si	21.7	17.4	1	1	14.4	12.5	53.0
2	mc-Si	21.3	16.9	1	1	14.4	9.8	55.0
3	a-Si	14.9	10.3	2	3	9.6	3.6	13.7
4	CdS/CdTe	90.2	67.7	4	1	57.6	6.4	53.7
5	$CdS/CuInSe_2$	22.6	16.1	1	1	14.4	6.2	31.4

Most data reduction and model validation calculations were performed with Microsoft Access. Access Basic functions were developed and used in database queries that serve as a simple method of applying these calculations to data in interactive or automated modes as desired. This approach proved very beneficial for evaluating individual models, by providing the complete results of each step and allowing for the substitution of measured data as the input to each model. Once models are finalized, this database could provide the basis for a user-friendly MER calculation tool.

5.1 Testing

Two types of tests were performed on the five sample modules. Indoor flash tests were performed to obtain irradiance/temperature cross sensitivity data for determining the

interpolation and Anderson model parameters. Outdoor testing was performed primarily for validating the various models, but some of this data was used as well for generating parameters for the Myers and Blaesser models. The following sections describe the tests performed and present the parameters obtained for the models.

5.1.1 Laboratory Testing

The laboratory testing was performed on the five sample modules at NREL on the 17th through 20th of July 1995. A Spire flash tester, heating pad, thermocouple, and velum were used as described in the Laboratory Testing subsection of the Module Testing section of this document to obtain irradiance/temperature cross sensitivity data.[1] Tables in Appendix A summarize the indoor data collected using the Spire.

Representative spectral response data from technologically similar PV cell specimens were used because obtaining spectral response characteristics from entire modules is technically difficult. These data are discussed in the Spectral Model validation section.

The points extracted from the IV curves for the interpolation model are presented in Table 5-2 and 5-3.

To compute the coefficients for the Anderson model, all possible pairs of appropriate data points were extracted from the summary IV curve data and the equations described in the Data Reduction section were applied to those pairs. The minimum, average, and maximum values of these computations are shown in Table 5-4. There is a fairly wide variation in these values, though the averages for the first three modules are similar to the sample values quoted by J. Anderson. A brief investigation into the origins of this variation showed some patterns that could indicate problems in the data set, although the sources of these problems were unclear.

---

[1] It is interesting to note that for both this data and earlier test results, the open-circuit voltage extracted from the IV curve data by the Spire data system was found to be inaccurate for several curves. It was suggested that a blocking diode could create this problem, but the presence of such a diode was never confirmed. The Voc data used in this analysis was estimated with the Access database using linear least-squares fit to IV data points near Voc.

Table 5-2. Maximum Power Interpolation Table (Watts)

Temperature (°C)	Irradiance (W/m^2)			
Module 1	253	487	773	1000
20.00	12.80	26.03	42.20	54.13
30.29	12.42	25.10	40.36	51.78
40.45	11.70	23.87	38.20	49.78
50.18	11.53	23.23	36.97	47.95
Module 2	257	485	762	1000
19.63	13.69	26.93	43.34	56.40
30.43	13.14	25.82	41.16	53.60
40.18	12.57	24.60	39.43	51.13
50.13	12.11	23.75	37.65	48.57
Module 3	205	443	741	1000
20.10	2.35	6.04	10.20	13.69
29.28	2.54	5.99	10.25	13.64
40.08	2.52	5.98	10.15	13.61
50.13	2.45	5.90	10.07	13.46
Module 4	237	456	741	1000
19.43	12.94	25.39	41.07	54.34
30.05	12.57	24.72	40.20	53.02
40.10	12.09	23.93	38.85	51.43
50.10	11.74	23.27	37.77	50.26
Module 5	255	485	767	1000
19.90	7.10	14.61	24.25	32.19
30.88	6.54	13.76	22.85	30.66
40.20	6.09	12.75	21.52	28.79
50.58	5.56	11.99	19.98	27.07

Table 5-3. Fixed Voltage Interpolation Table (Amperes)

Temperature (°C)	Irradiance (W/m^2)			
Module 1	253	487	773	1000
20.00	0.77	1.53	2.45	3.20
30.29	0.78	1.53	2.45	3.17
40.45	0.75	1.50	2.40	3.17
50.18	0.77	1.53	2.42	3.17
Module 2	257	485	762	1000
19.63	0.84	1.60	2.57	3.40
30.43	0.84	1.60	2.56	3.39
40.18	0.83	1.60	2.56	3.39
50.13	0.82	1.59	2.56	3.34
Module 3	205	443	741	1000
20.10	0.24	0.61	1.04	1.40
29.28	0.25	0.61	1.04	1.40
40.08	0.25	0.61	1.05	1.40
50.13	0.25	0.61	1.05	1.39
Module 4	237	456	741	1000
19.43	0.21	0.40	0.65	0.87
30.05	0.20	0.40	0.65	0.87
40.10	0.20	0.40	0.64	0.86
50.10	0.20	0.39	0.63	0.85
Module 5	255	485	767	1000
19.90	0.49	0.99	1.61	2.12
30.88	0.45	0.95	1.56	2.08
40.20	0.39	0.88	1.48	1.98
50.58	0.29	0.80	1.37	1.87

Table 5-4. Ranges of Anderson Coefficients Found

	α ($°C^{-1}$)			β ($°C^{-1}$)			δ (--)		
Module	Min	Avg	Max	Min	Avg	Max	Min	Avg	Max
1	-0.003718	0.000066	0.003769	-0.0038	-0.0033	-0.0029	0.0405	0.0496	0.0689
2	-0.0004	0.000333	0.000986	-0.0041	-0.0034	-0.003	0.0391	0.0536	0.0612
3	-0.000437	0.000895	0.00178	-0.0033	-0.0018	0.0045	0.0474	0.0588	0.0895
4	-0.000585	0.000167	0.000596	-0.0029	-0.0023	-0.0017	0.0349	0.0458	0.0545
5	-0.001349	-0.000021	0.001067	-0.0056	-0.0047	-0.0039	0.0888	0.1134	0.1315

The average values of the computed Anderson coefficients were used for subsequent modeling. Table 5-5 presents these values, along with the corresponding reference point data that was used. The IV curves from which these points were derived were used as the basis for translation to other conditions.

Table 5-5. Chosen Anderson Model Parameters

Module	α ($^{\circ}C^{-1}$)	β ($^{\circ}C^{-1}$)	δ (--)	H_1 (W/m^2)	T_1 ($^{\circ}C$)	V_{oc1} (V)	I_{sc1} (A)	P_{mp1} (W)
1	0.000066	-0.00326	0.0496	1000	20.0	22.0	3.32	54.1
2	0.000333	-0.00336	0.0536	1000	19.7	21.6	3.57	56.4
3	0.000895	-0.00176	0.0588	1000	20.1	15.1	1.76	13.7
4	0.000167	-0.00232	0.0458	1000	19.2	91.0	0.92	54.3
5	-0.000021	-0.00474	0.1134	1000	20.0	23.1	2.33	32.2

5.1.2 Outdoor Testing

The outdoor test consisted of installing the sample modules in a latitude tilt configuration and simultaneously recording module IV curves, weather parameters, and global plane-of-array spectral characteristics. Data collection was performed at the NREL Outdoor Test Facility in Golden, Colorado, from the July 28 through 31, 1995.

The weather parameters were sampled at 5-second intervals and averaged every 10 minutes. These parameters included beam irradiance (cavity radiometer), diffuse horizontal irradiance (shaded thermopile pyranometer), plane-of-array irradiance (thermopile pyranometer), wind speed, barometric pressure, relative humidity. Figure 5-1 shows selected parameters for the four days of testing. Note that data collection commenced mid-morning on the 28th and only a few data points were collected in late afternoon of the 31st.

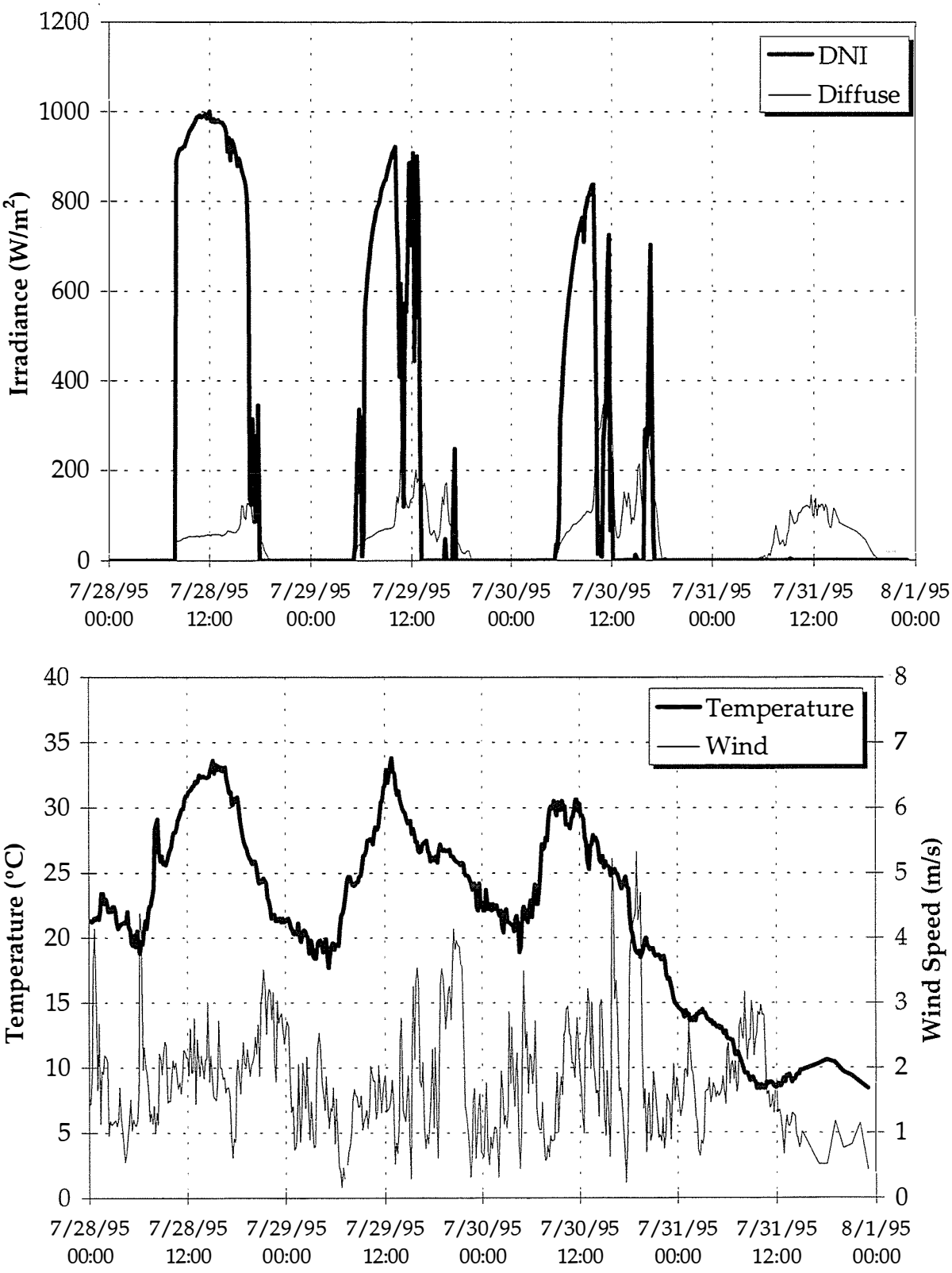

Figure 5-1 Validation Weather Data

Module measurements, for each module, included maximum power and module back temperature sampled at 5 second intervals and averaged at 10 minute intervals, as well as complete IV curves sampled at 10 minute intervals.

Finally, a LI-COR spectroradiometer was configured to sample in-plane global spectra every two minutes during daylight hours in the 300 to 1100 nm wavelength band. For the purposes of validation computations, these spectra were subsequently averaged point-by-point at 10 minute intervals.

This rather extensive data set was primarily collected for validation purposes, but data from the 28th was also used to obtain model parameters for all five modules. While some outdoor data from earlier testing was available, it only included data for the first three modules. The parameters obtained for the Myers and Blaesser models are given in Table 5-6 and Table 5-7.

Table 5-6. Linear Irradiance-Only (Myers) Model Parameters

Module	a (m^2)	b (W)
1	0.0547	0.0481
2	0.1435	0.0485
3	0.0164	0.0135
4	-0.0674	0.0429
5	-0.1111	0.0245

Table 5-7. Blaesser Model Parameters

Module	a (--)	b ($°C^{-1}$)	c (m^2/W)	$H_{1,r}$ (W/m^2)	T_1 (°C)	$V_{oc,r}$ (V)	$I_{sc,r}$ (A)
1	0.0562	0.00250	0.0000733	1000	20.0	22.0	3.32
2	0.0486	0.00383	0.0000716	1000	19.7	21.6	3.57
3	0.0408	0.00423	0.0000368	1000	20.1	15.1	1.76
4	0.0483	0.00483	0.0000892	1000	19.2	91.0	0.92
5	0.1079	0.00578	0.0001251	1000	20.0	23.1	2.33

5.2 Validation Analysis

A crucial aspect of this project was the validation of the various models used to estimate module performance under the prescribed MER conditions. A significant effort was expended generating the required validation data. Because of the need to evaluate each model, extensive measurements were made.

At the outset of the project, the intent was to use existing module and array performance data from NREL's outdoor test facility in Golden, Colorado, PG&E's Photovoltaic Test Facility in San Ramon, CA, and the Photovoltaics for Utility Scale Applications project in Davis, CA. Initial validation results presented to the TRC in March 1995 suggested that the irradiance measurements from these projects, based solely on global in-plane thermopile pyranometers, and the lack of measured spectra would not provide the required accuracy or level of detail necessary to fully evaluate the models. Thus, the outdoor measurements described in the Testing Section were made.

5.2.1 Power Models

The four power models described in the DC Power Model section were evaluated using results from the precursor models (irradiance, spectral, etc.), as well as using various measured parameters from the validation tests.

Models were evaluated by comparing integrated modeled power over each of four validation days to measured integrated power (daily energy), as well as comparing individual modeled power values to measured 10-minute averages. The results of the analysis, discussed below, are based on measured inputs: module temperature, POA irradiance, and spectral content/correction. A comparison of measured POA irradiance to DNI/diffuse derived irradiance is discussed in the Irradiance Model Section.

Peak power results for four models, five modules and four days are shown in Figure 5-2. Similar fixed voltage results for Anderson, Blaesser, and Interpolation models are shown in Figure 5-3. (We did not attempt to generate fixed-voltage coefficients for the Myers model.) Though there are a few bright spots, these results are generally unsatisfactory. Depending on the model and module, peak power model error ranged from 2% to 48% as shown in Figure 5-4. This chart shows the aggregate error for the

four days of validation data (sum of estimated energy for all four days divided by the measured energy, quotient minus 1).

Figure 5-5 and Figure 5-6 compare modeled to measured power and model error as a function of irradiance for each 10-minute average point for module 1. Figure 5-7 and Figure 5-8 show similar data for fixed voltage operation. The corresponding plots for modules 2 through 5 are provided in Appendix B.

These results show that overall, the Anderson model performed the worst and the Myers model performed the best for peak power prediction. Note that both the Blaesser and Myers model coefficients were generated based on the July 28 data set, so we would expect them to predict that day fairly well. Conversely, data for the Interpolation model and the coefficients for the Anderson model were based on indoor measurements.

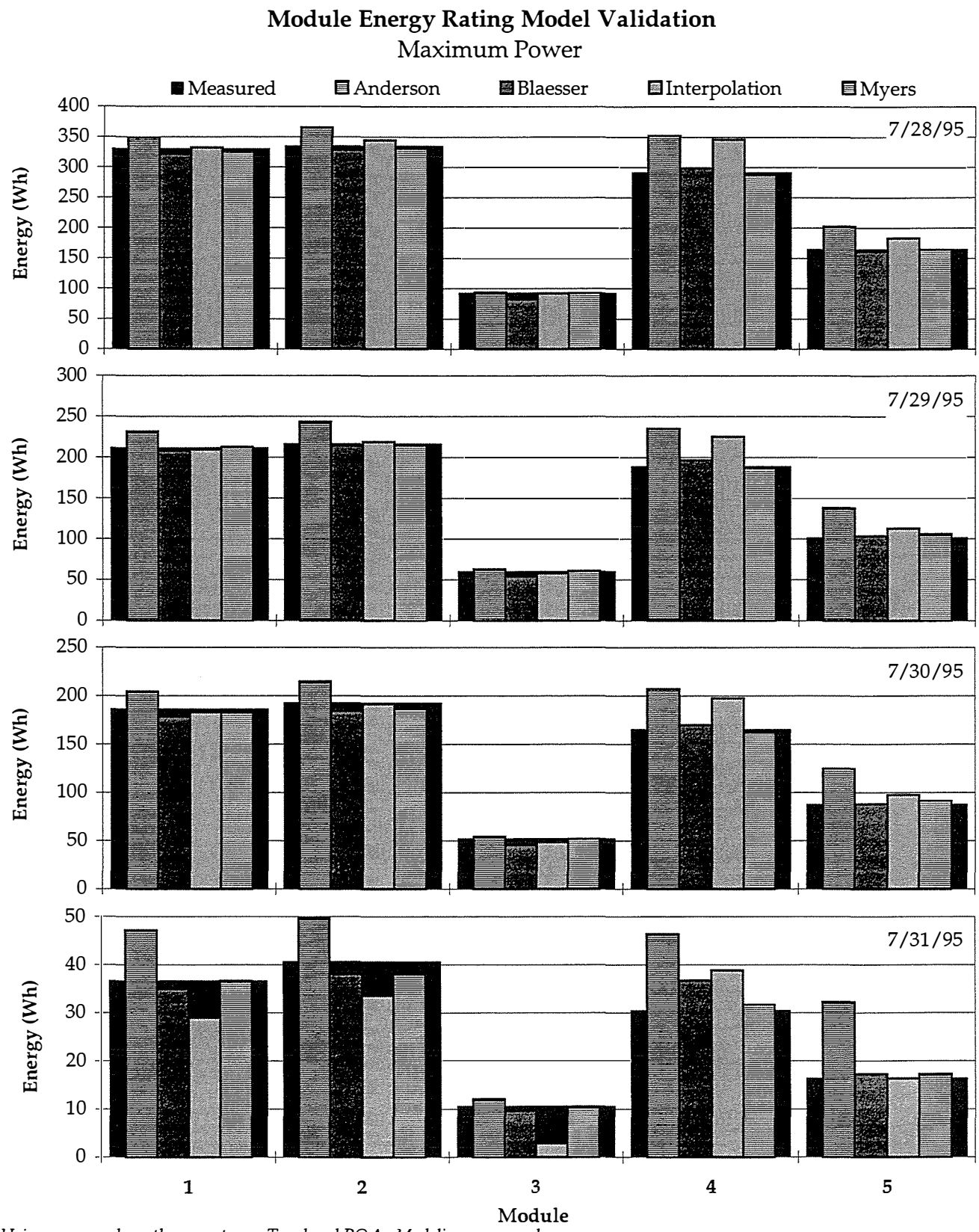

Figure 5-2 MER Power Model Validation, Maximum Power

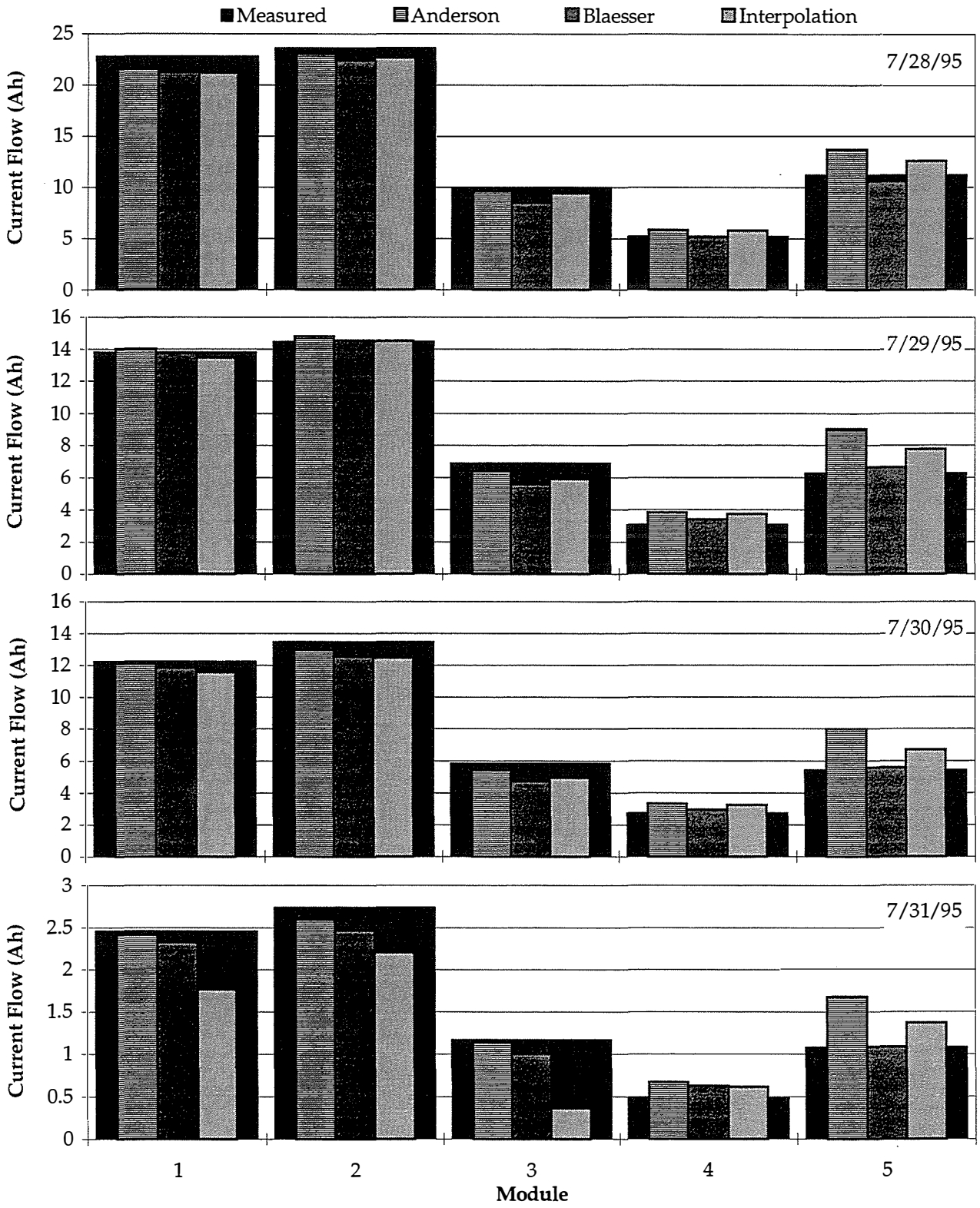

Using measured weather, spectrum, Tmod and POA; Modeling power only

Figure 5-3 MER Power Model Validation, Fixed Voltage

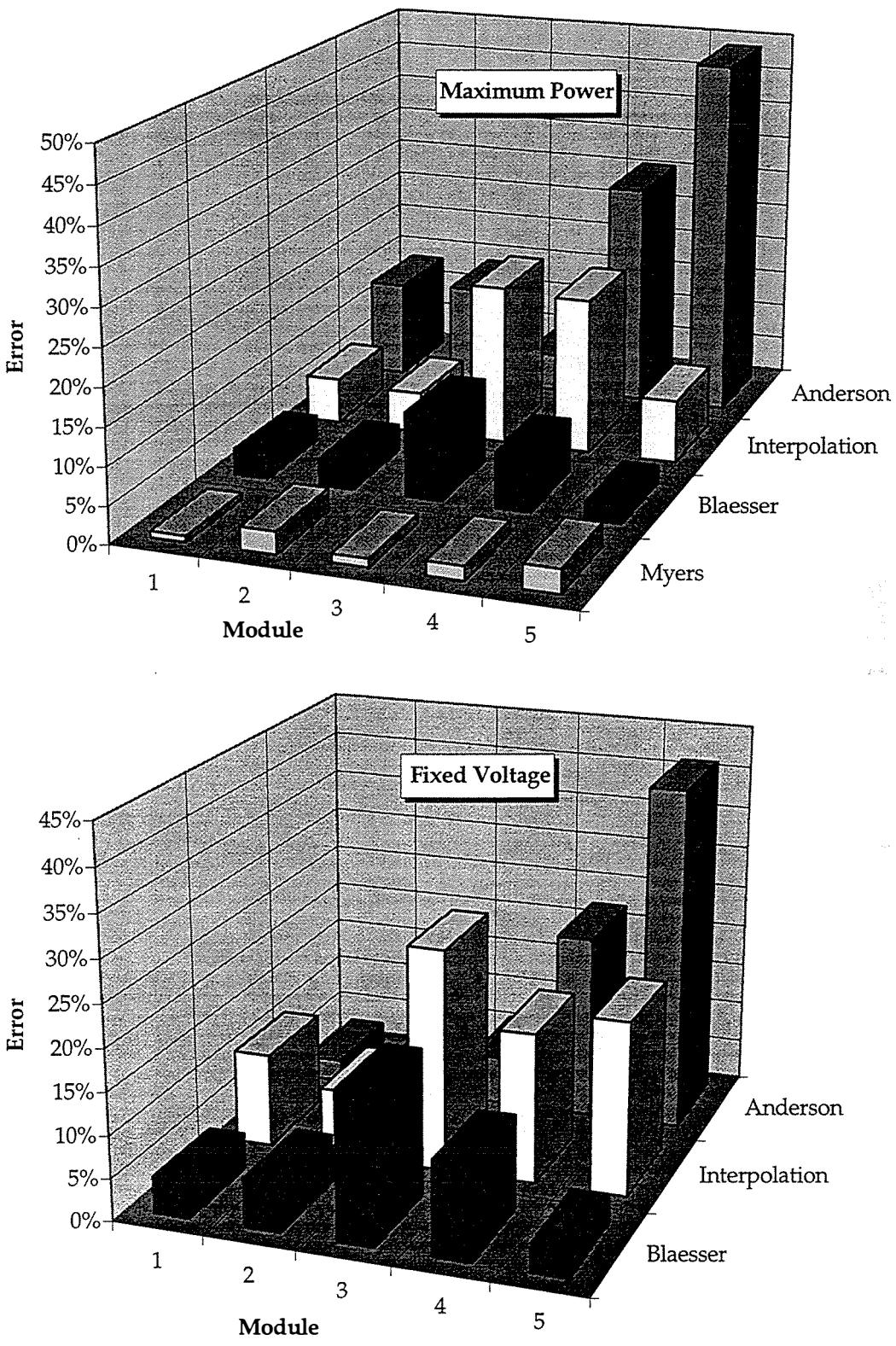

Figure 5-4 MER Power Model Error, Maximum Power and Fixed Voltage

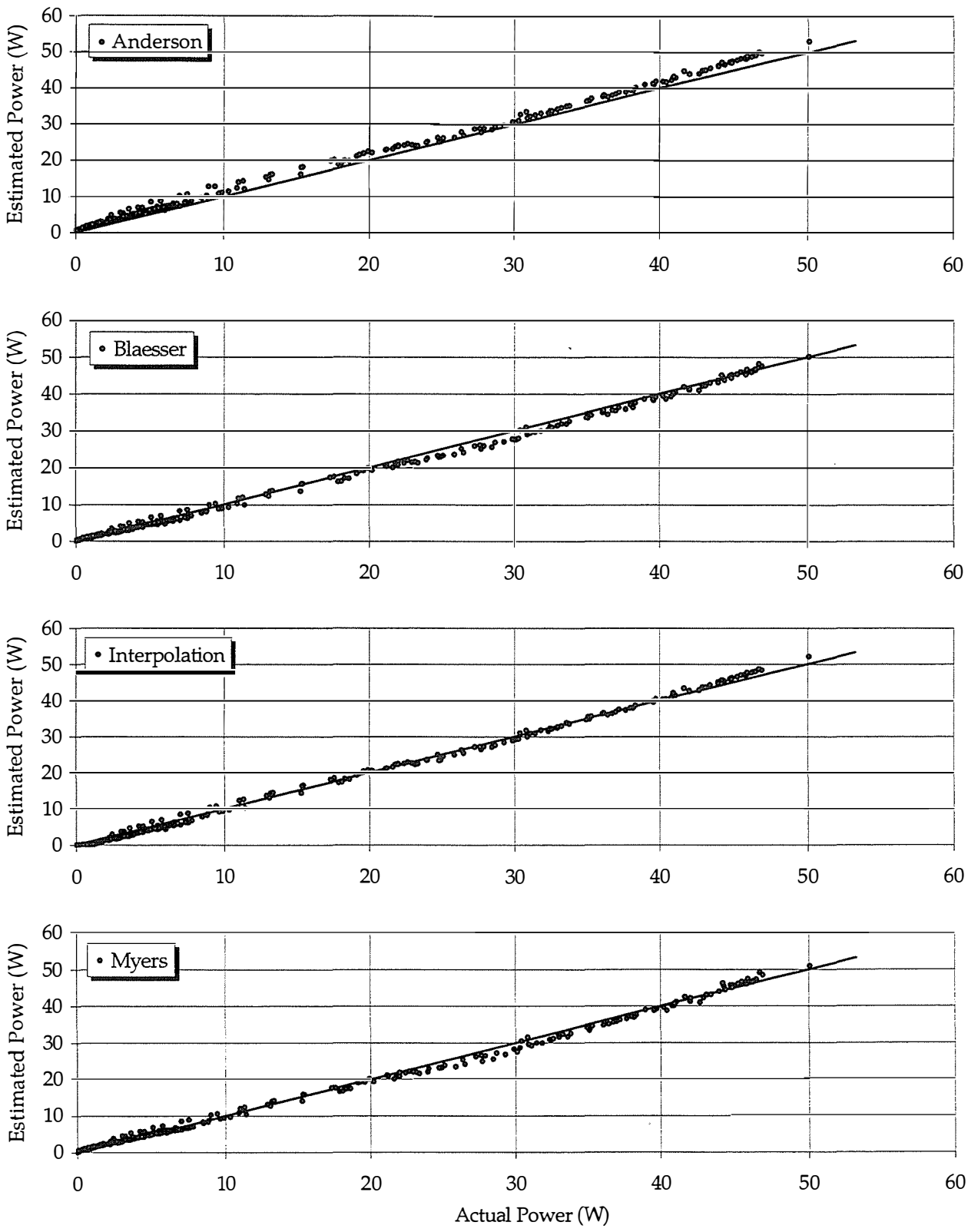

Figure 5-5 MER Power Model Comparison, Estimated Max. Power vs Actual

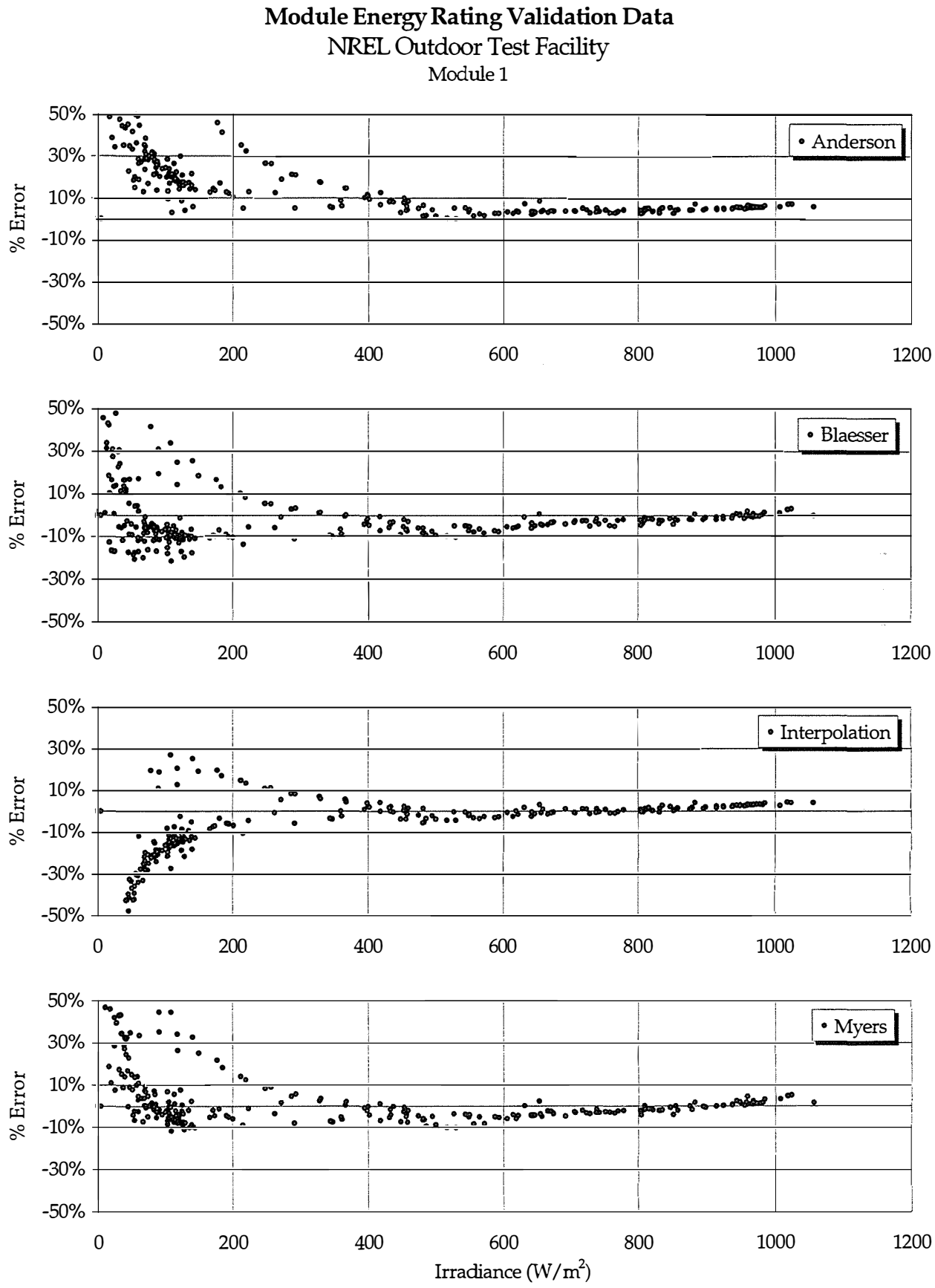

Figure 5-6 MER Power Model Comparison, Max. Power Error vs Irradiance

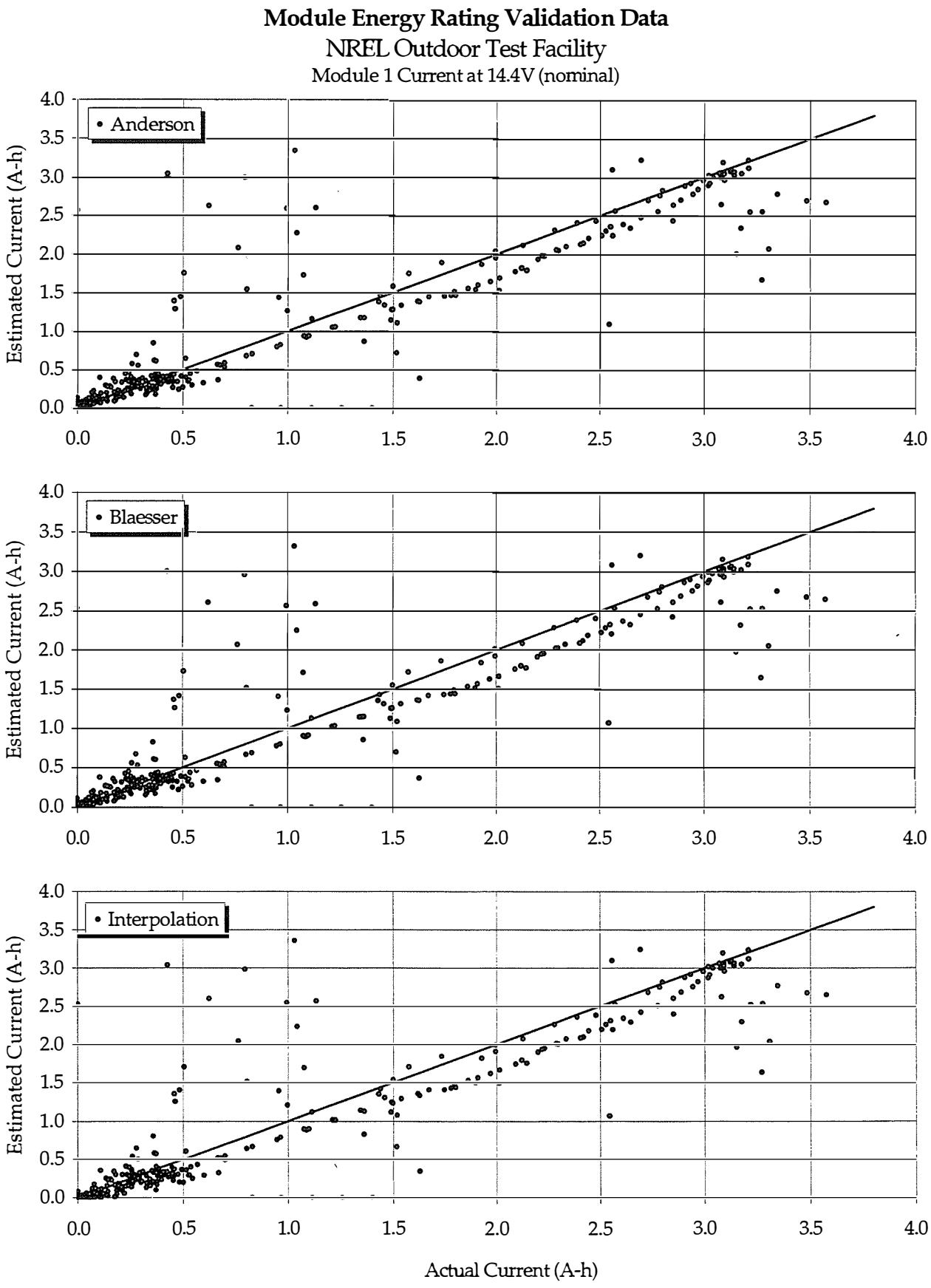

Figure 5-7 MER Power Model Comparison, Model Estimated A-H vs Actual

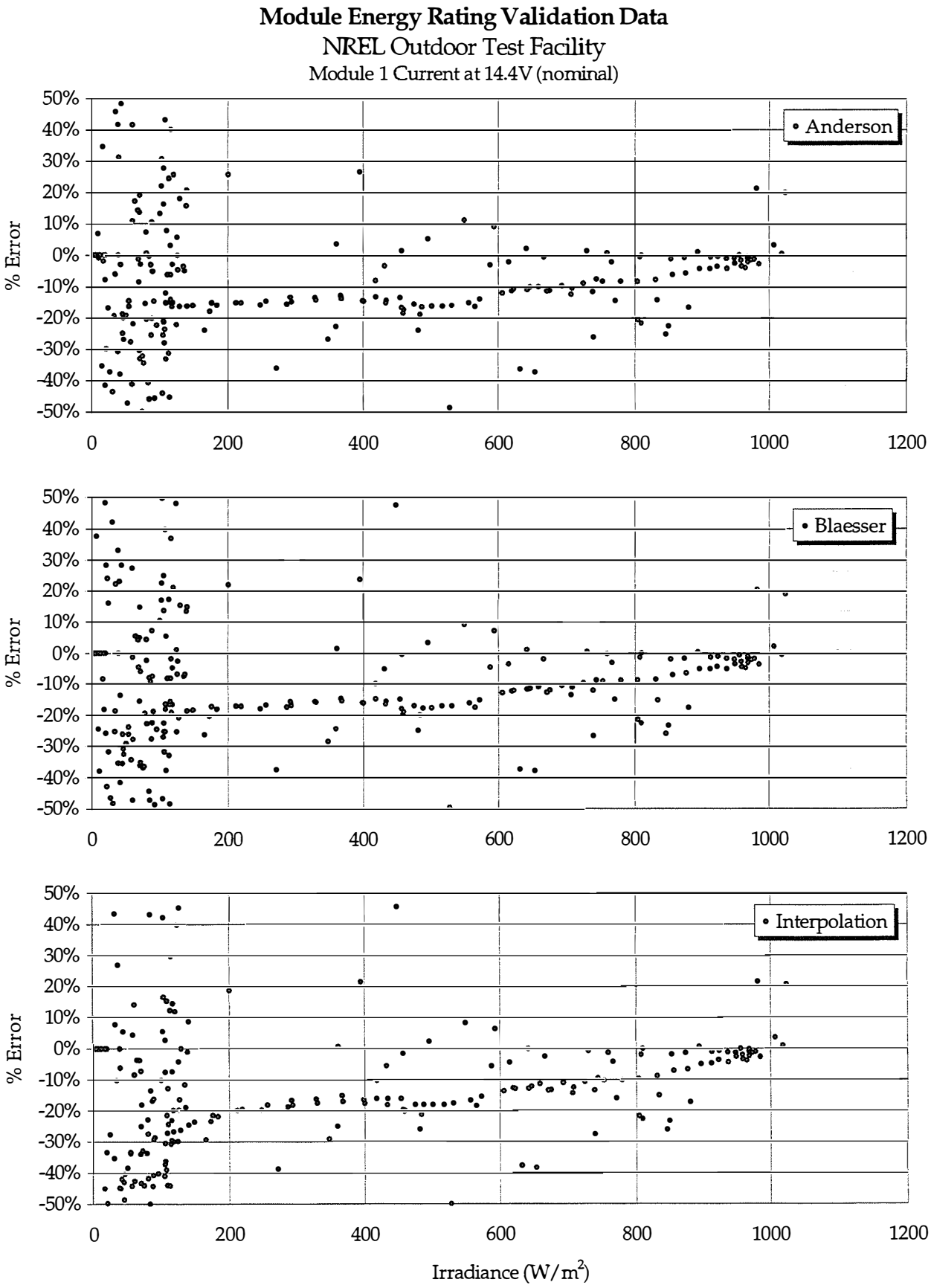

Figure 5-8 MER Power Model Comparison, Model A-h Error vs Irradiance

The Anderson model proved to be more competitive with the other models in predicting fixed voltage performance. Figures 5-7 and 5-8 show that the integrated results are a bit misleading. Both of these plots suggest all of the models tend to slightly under-predict current at moderate irradiance levels. However, at low irradiance they tend to significantly over-predict. For example, at a measured current of 1 A the estimated current can be as much as 3.5 A high. Over a day, that +2.5A absolute error from one low-irradiance value offsets ten of the more typical -0.25A moderate irradiance errors.

A final general result is that, as expected, all of these models are better at predicting module performance under high irradiance conditions than low irradiance conditions. They also tend to be more accurate for crystalline silicon modules than for thin film modules.

5.2.1.1 Anderson Model

A rather unexpected result was the relatively poor performance of the Anderson model. Despite its use of measured module temperature and a derivation very similar to the Blaesser model, it did not fair as well. The primary difference between these two models is the use of indoor flash test data vs. outdoor data for coefficient derivation. The Blaesser and Myers models also benefited from the use of nearly the same data for both coefficient derivation and model validation

Simply because of the model's poor performance here, we suspect these results. The fact that it tends to predict the highest energy (both peak power and fixed voltage) suggests that this model is not capturing all of the "losses" outdoors. The one parameter that we elected to ignore was the incidence angle modifier. The IAM reduces the irradiance input to the power model as a function of incidence angle to account for the modules front surface reflectivity. Since the Anderson and Interpolation models are based on flash tests done at normal incidence, they would tend to over-predict power at high incidence angles. The use of pyranometer measured POA irradiance rather than DNI/Diffuse derived irradiance would reduce that error somewhat because of the pyranometers own attenuation at high incidence angle. However, Figure 5-6 shows consistent over prediction under high irradiance, low incidence angle conditions as well as overcast, "no" incidence angle conditions.

Another potential source of error is in the characterization data. Any spectrum or uniformity errors associated with the sheets of velum used to attenuate the flash intensity will be accentuated at the lowest irradiance levels where module performance becomes non-linear. The velum used was selected because of its uniformity and some testing was done to insure that spectral changes were minimal.

Any model can be quite sensitive to the procedures used to generate and evaluate the data for the coefficients. This comment appears to be especially true of the Anderson model. The procedures used here should, therefore, be further reviewed and refined. Also, additional validation data are necessary to evaluate each of these models under the broad range of conditions with which they are intended to be used.

5.2.1.2 Blaesser Model

Both the Blaesser and Myers model coefficients were generated based on the July 28 data using the measured POA irradiance without spectral correction. In spite of these simplifications, the Blaesser model performs relatively well coming in a close second to the Myers model in overall peak power performance. Fixed voltage estimates are lower than Anderson estimates in all cases and are lower than the Interpolation model in most cases.

5.2.1.3 Interpolation Model

The most notable behavior of the Interpolation model is its error at low irradiance (Figure 5-6). While the error for the other modules becomes more positive at low irradiance, the Interpolation model error becomes more negative. The weakness of the interpolation model is that you must actually extrapolate to obtain points beyond its measurement range. At the low irradiance end, linear extrapolation is used where the performance is becoming non linear. Any error in the four points used for extrapolation will be magnified for large extrapolation. Thus, a requirement for use of the Interpolation model is the to have measurements covering the entire range of expected weather conditions.

5.2.1.4 Myers Model

Equally unexpected to the Anderson's poor results were the Myer's relatively good results. Myer's contention—if the error associated with measuring and characterizing a given parameter is greater than the contribution of that parameter, don't include it in

the model—appears to ring true. Since the model is based on a regression analysis of one of the validation days, July 28, it's not surprising that it works well for that day. However, July 28 was the clearest day and the model works equally well for the July 31 which had roughly 1/10 the insolation. Since the module only takes into account irradiance, we would expect it to show some error on days with similar irradiance levels but different ambient temperatures. For the data set utilized, lower irradiance levels tend to occur at lower temperatures, so this effect is masked. Again, a wider range of validation data is necessary to reach a supportable conclusion.

5.2.2 Spectral Model

A validated spectral model was not absolutely required in order to compute the MER, because it is used to *define* the (otherwise unavailable) spectrum for the reference days. The spectral model must generate reasonable spectra, but once the spectra for each reference day are specified, the model is no longer needed[1].

However, to most accurately characterize the input conditions for validating the power models, measured spectra were used. Measured spectra and individual spectral response characteristics were combined to obtain spectral correction factors (SCF) for each data sample. The SCF is then combined with measured irradiance to obtain effective irradiances for each of the modules, which were in turn used as inputs to the power model along with measured module temperature. The spectral correction factor computed from the measured spectral data is shown in Figure 5-9. These spectral correction calculations were limited to the measured bandwidth, which implicitly assumes that the actual spectra at unmeasured wavelengths were no different than the corresponding reference spectra.

As part of the investigation of spectral effects in the modeling process, a number of additional plots were generated. Figure 5-10 includes plots of spectral responses for the sample modules, sample spectral shapes, and a comparison of the predicted spectrum and measured spectrum for one sample on the cloudiest outdoor test date. For example, comparing the spectral response shape of module 3 (a-Si) with the noon and evening spectral shapes, one can see that the lower proportion of energy in the higher wavelengths in the evening will make the module appear to be more efficient at

---

[1] In reality, the model may still be necessary since the spectra vary with orientation and it would be cumbersome to provide spectra for all conceivable orientations.

converting the available irradiance. Note that the reddening effect apparent in the evening sky is limited to direct and circumsolar diffuse irradiance. For the fixed south facing orientation used in this analysis, the spectrum is dominated by the more blue diffuse sky component (see above footnote). In addition, the comparison of estimated and measured global spectra shows that the spectral model produces reasonable data.

Figure 5-11 shows the effective irradiance for the sample modules on the MER reference days, and the net change in effective insolation ($kWh\text{-}m^2$/ $kWh\text{-}m^2$) that results from application of the spectral correction factor. Note the small rise in estimated plane-of-array irradiance near sunrise and sunset; these are artifacts of applying the Perez translation model to averaged irradiance data. These artifacts cannot be completely eliminated given that averaged data are used. The net change in effective insolation (or equivalently, change in effective efficiency) for module 3 (a-Si) shows improvement for medium and higher temperatures, with a corresponding reduction for cooler temperatures. This effect has been observed by T. Townsend in comparisons of a-Si-based PV systems in tropical and temperate climates [personal communication, September 1995]. The order of magnitude of the effect is about 4% for a-Si and 1-2% for the remaining modules. However, it is unclear from this analysis if there is a change in spectral response due to temperature, if there is simple spectrum/temperature relationship, or if there is some other mechanism acting here, such as a-Si annealing.

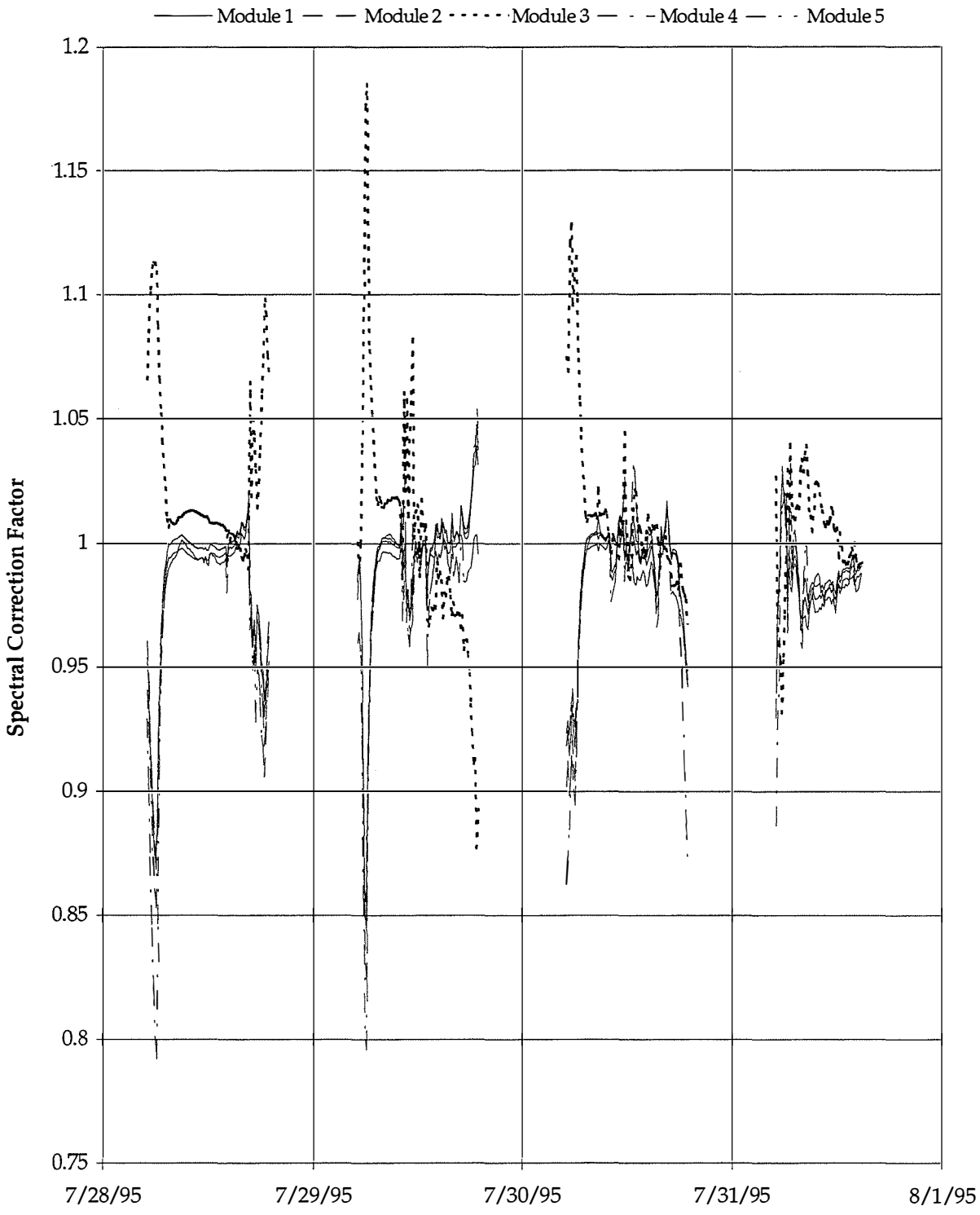

Figure 5-9 Spectral Correction Factors Based on Measured Spectra

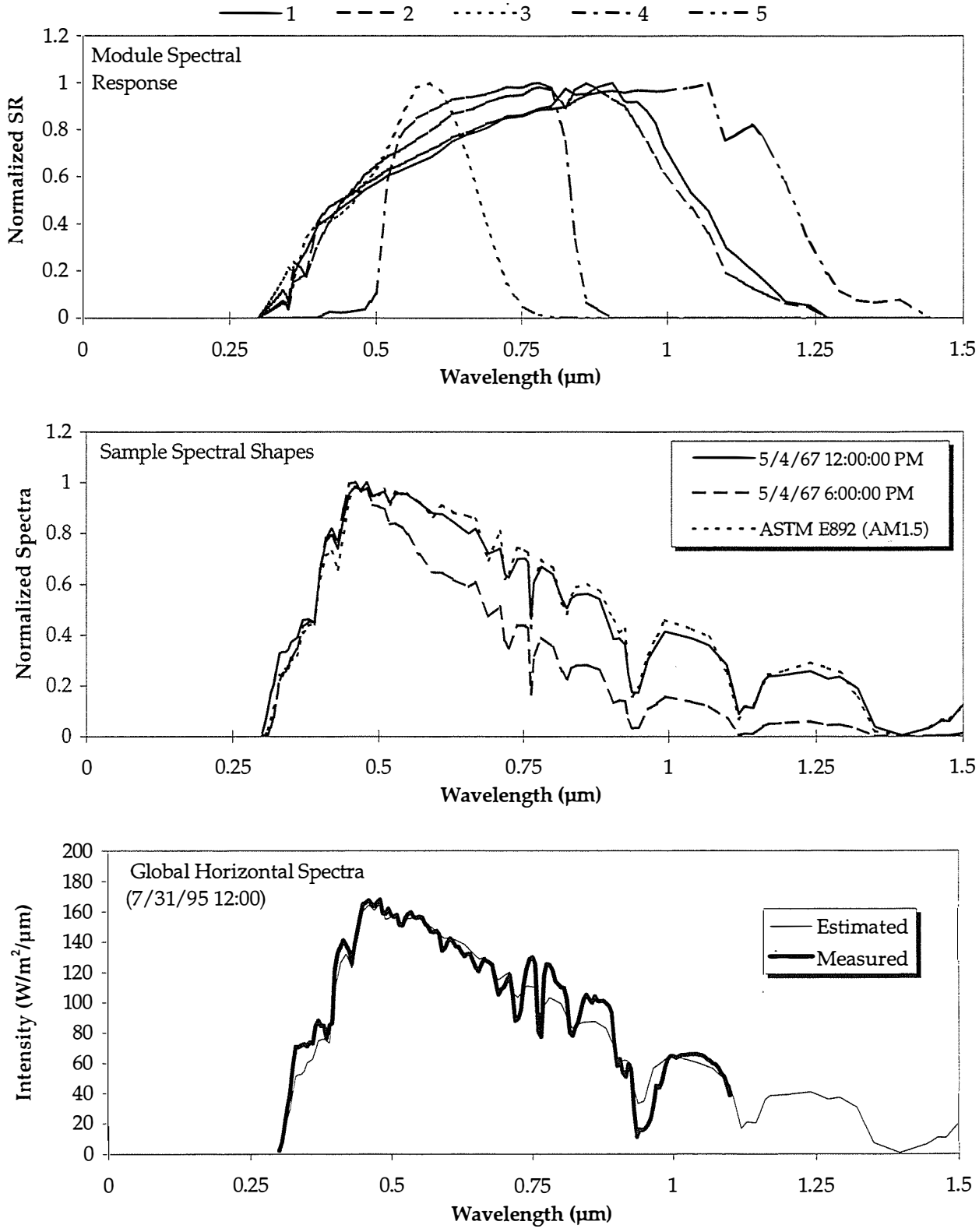

Figure 5-10 Spectral Response and Spectral Model Results

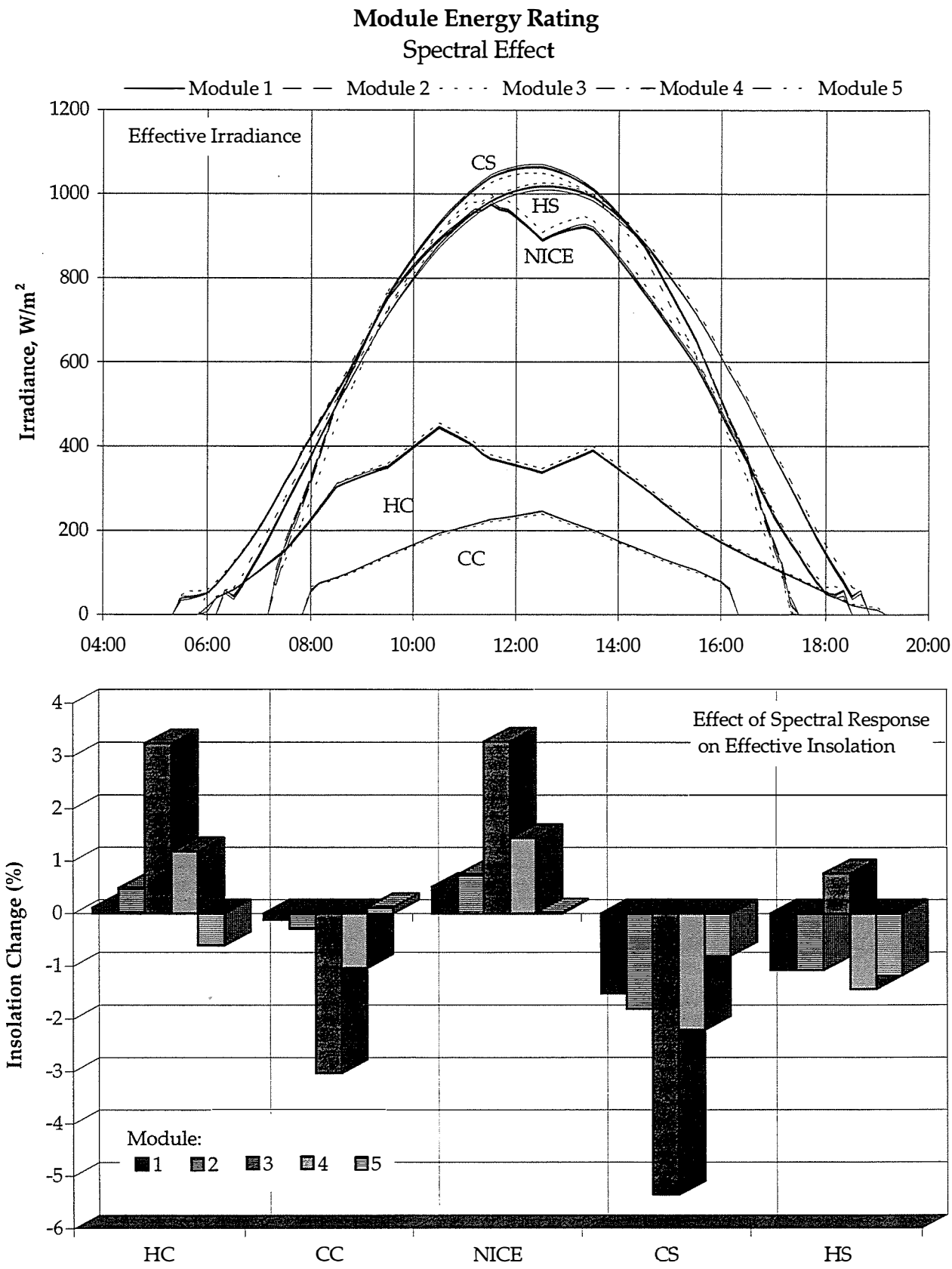

Figure 5-11 Effective Irradiance

Figure 5-12 shows the spectral correction factor for the sample modules on the MER reference days. The small spikes before and after sunset are associated with the Perez/averaged data artifacts previously discussed. Note that the a-Si module reacts more strongly than the other modules, and sometimes increases when the other modules are not affected or are decreasing.

5.2.3 Thermal Model

Though NOCT can determined using a standard ASTM-defined procedure, we did not perform that procedure nor were NOCT values available for all of the modules tested. Since the modules were relatively similar in construction a common 47 °C was used for all modules. Figure 5-13 shows the measured module temperatures for all 5 modules. The data—10-minute averages—shows little in the way of steady state performance, but there are some instances where the transients are not too severe. These instances suggest that the difference in temperature between the 5 modules is no more than about 5 °C.

Figure 5-14 and Figure 5-15 show that Fuentes model over-predicts module temperature by 10-15 °C for all modules at higher temperatures. Both absolute and relative error is lower at lower temperatures. This result is expected since, at least for this data set lower temperature is associated with lower irradiance and module temperature tends towards ambient temperature at low irradiance.

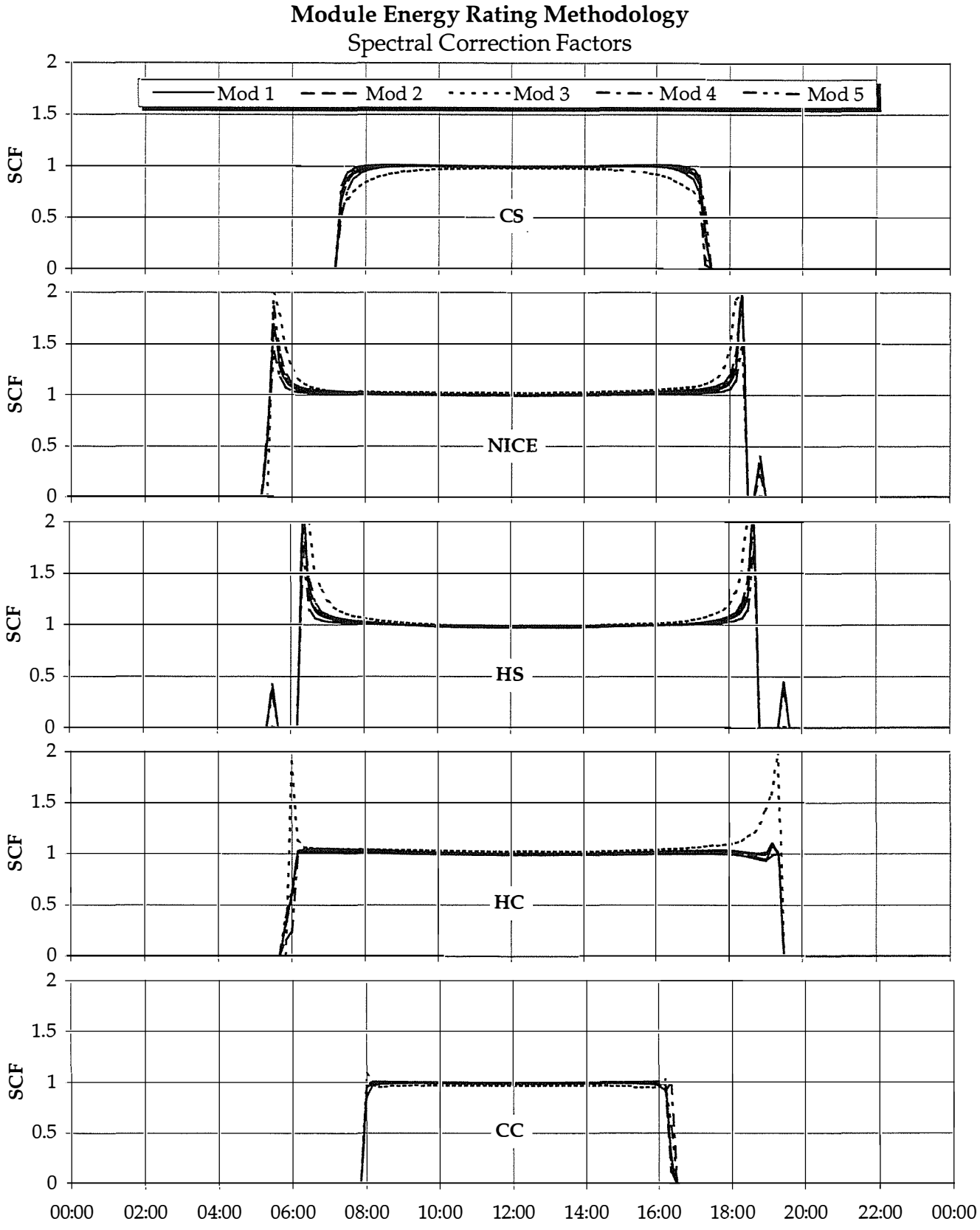

Figure 5-12 MER Reference Day Spectral Correction Factors

Module Energy Rating Methodology Model Validation
NREL Outdoor Test Facility
Measured Module Temperature

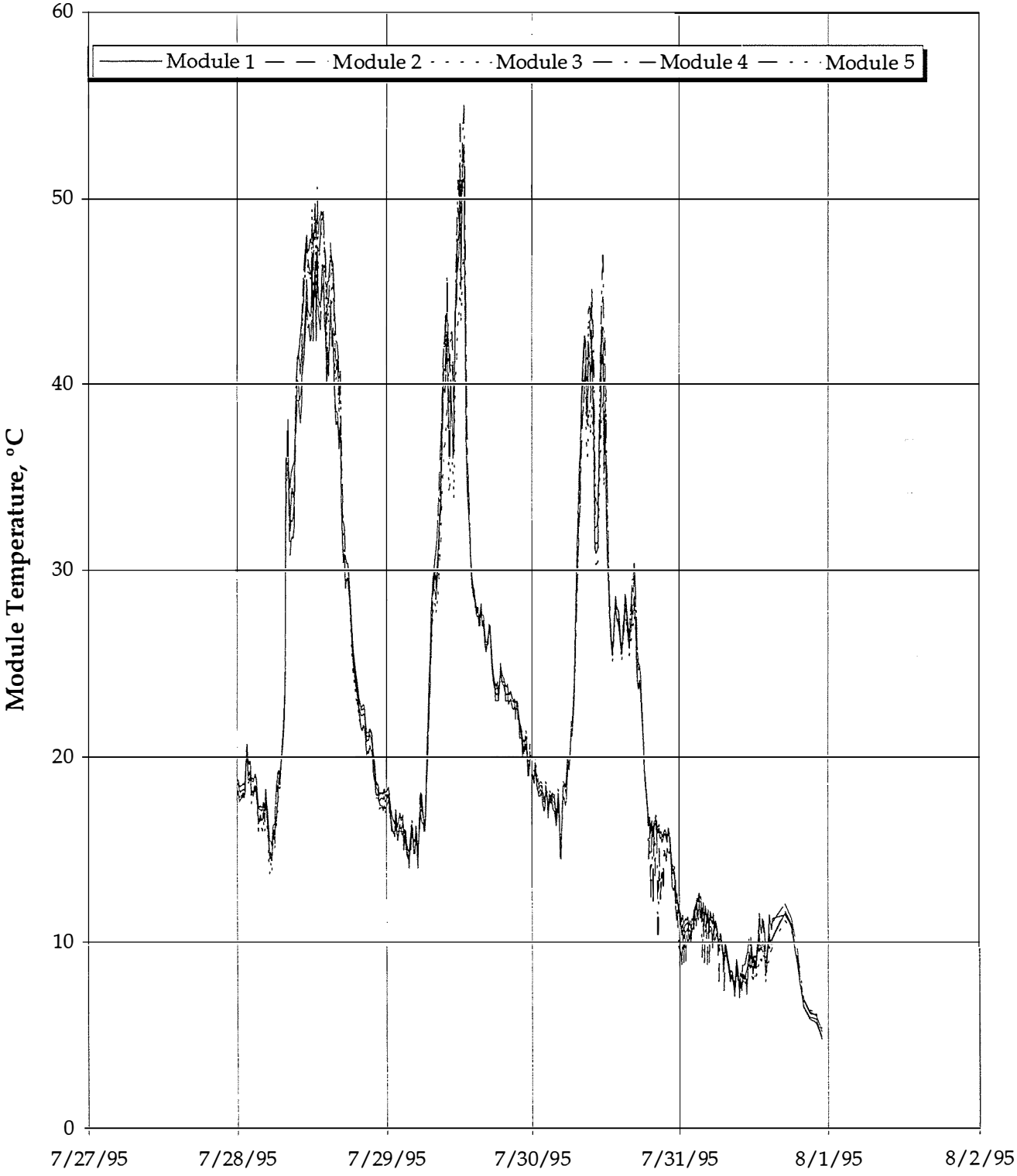

Figure 5-13 Measured Module Temperature

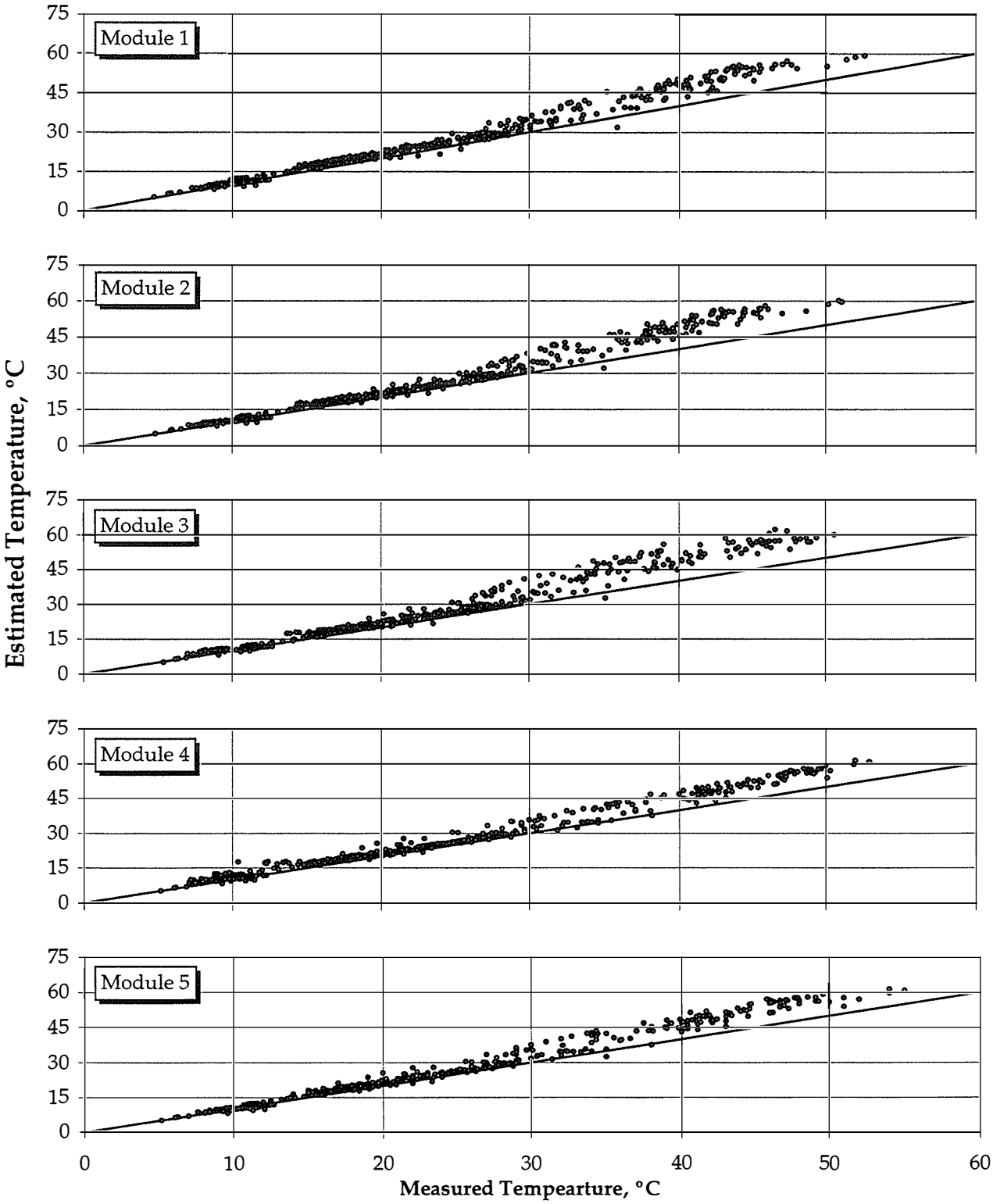

Figure 5-14 MER Thermal Model Validation, Actual Temperature vs. Estimated

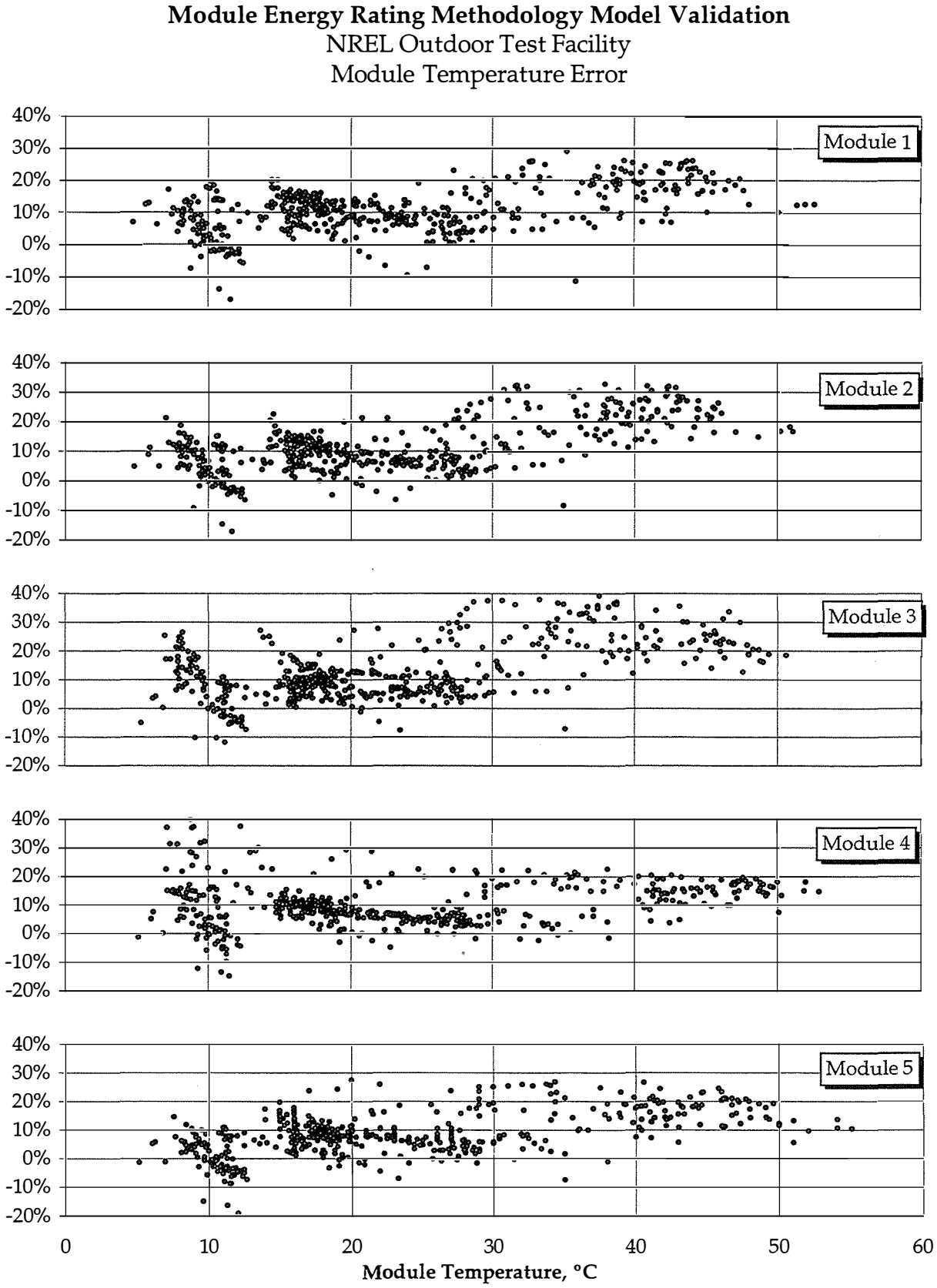

Figure 5-15 MER Thermal Model Validation, Model Error vs. Temperature

5.2.4 Reflection Model

Based on measurements made by Keith Emery of NREL and his resulting recommendations, we did not include an incidence angle correction in these validation results. As mentioned in the Power Model Section, this may have had some impact on the power model results.

5.2.5 Irradiance Model

Figure 5-16 shows a comparison between the measured POA irradiance and the value estimated from measured DNI and diffuse using the Perez model. For the sunny day, the calculated irradiance is consistently high, though the relative error shows a consistent decrease until late in the afternoon. A similar trend is apparent in the second and third days, though the random error seems to increase as the cloud cover increases.

With random errors up to 50%, the final day shows clearly that the irradiance model is not working very well at all for cloudy conditions. This may be attributable to poorer accuracy under cloudy conditions, or to more variable conditions, or to inappropriate model correlation coefficients in the Perez model for overcast conditions.

5.3 Module Energy Rating Results

Using the coefficients described previously, module energy ratings were computed for the five sample modules, and are shown in Figure 5-17 and Figure 5-18. Keeping in mind that the MER results are intended primarily to support comparisons between modules and that inaccuracies in the various models have been noted, the presence of multiple model results is of secondary importance. Also, the fact that this data is only intended for illustrative purposes and does not necessarily reflect the general trends in PV technology bears repeating here.

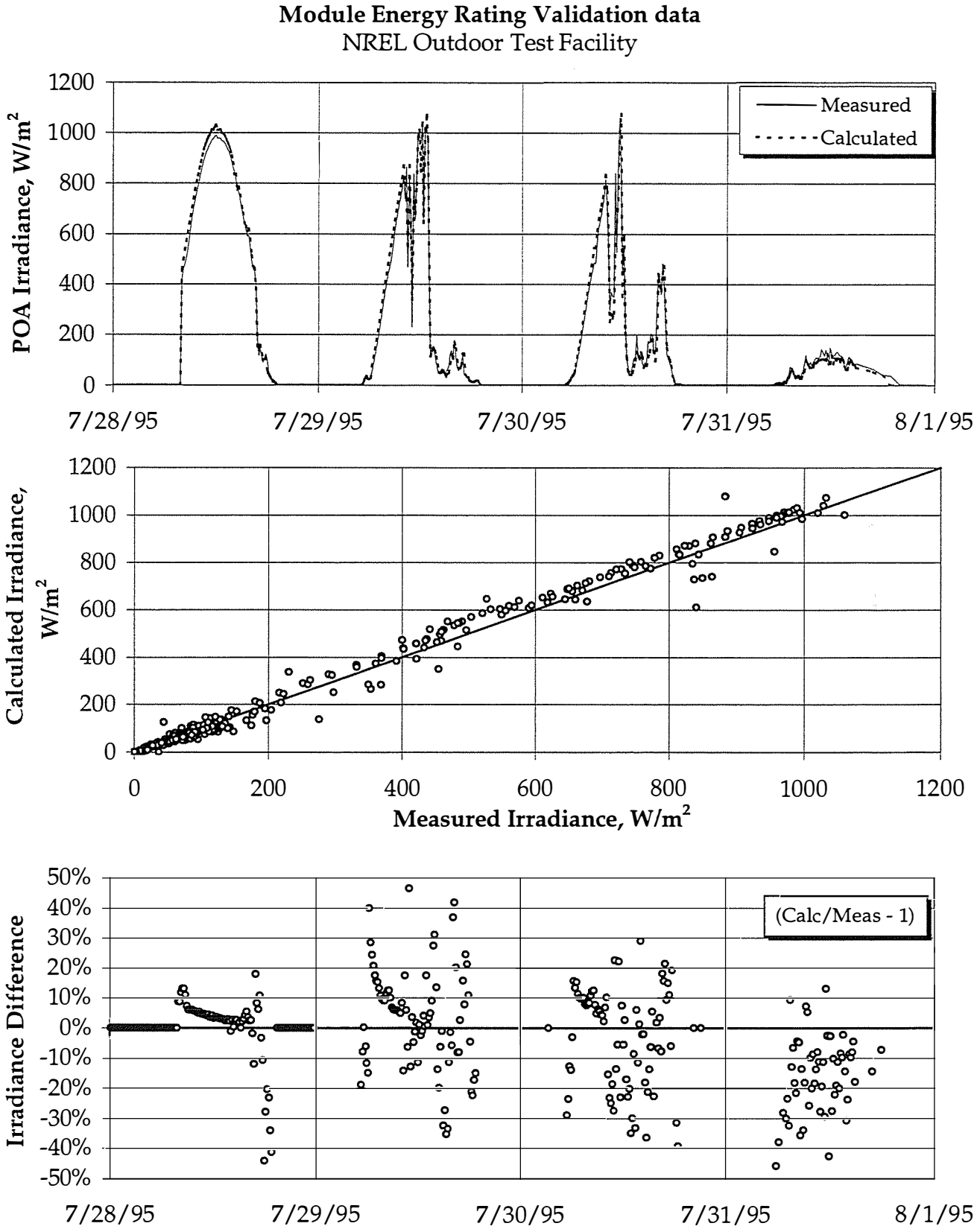

Figure 5-16 MER Irradiance Model Validation

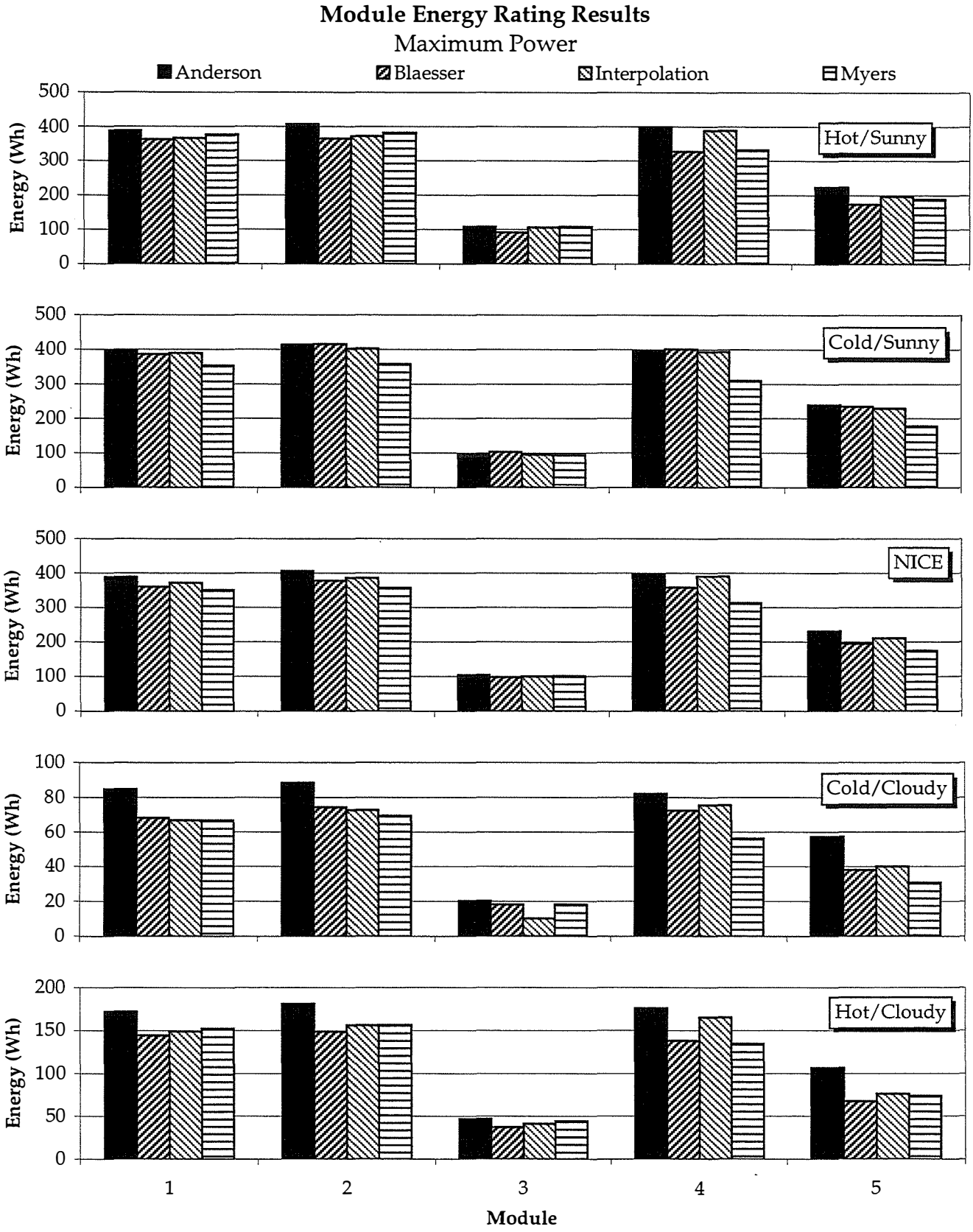

Figure 5-17 Module Energy Rating Results, Maximum Power

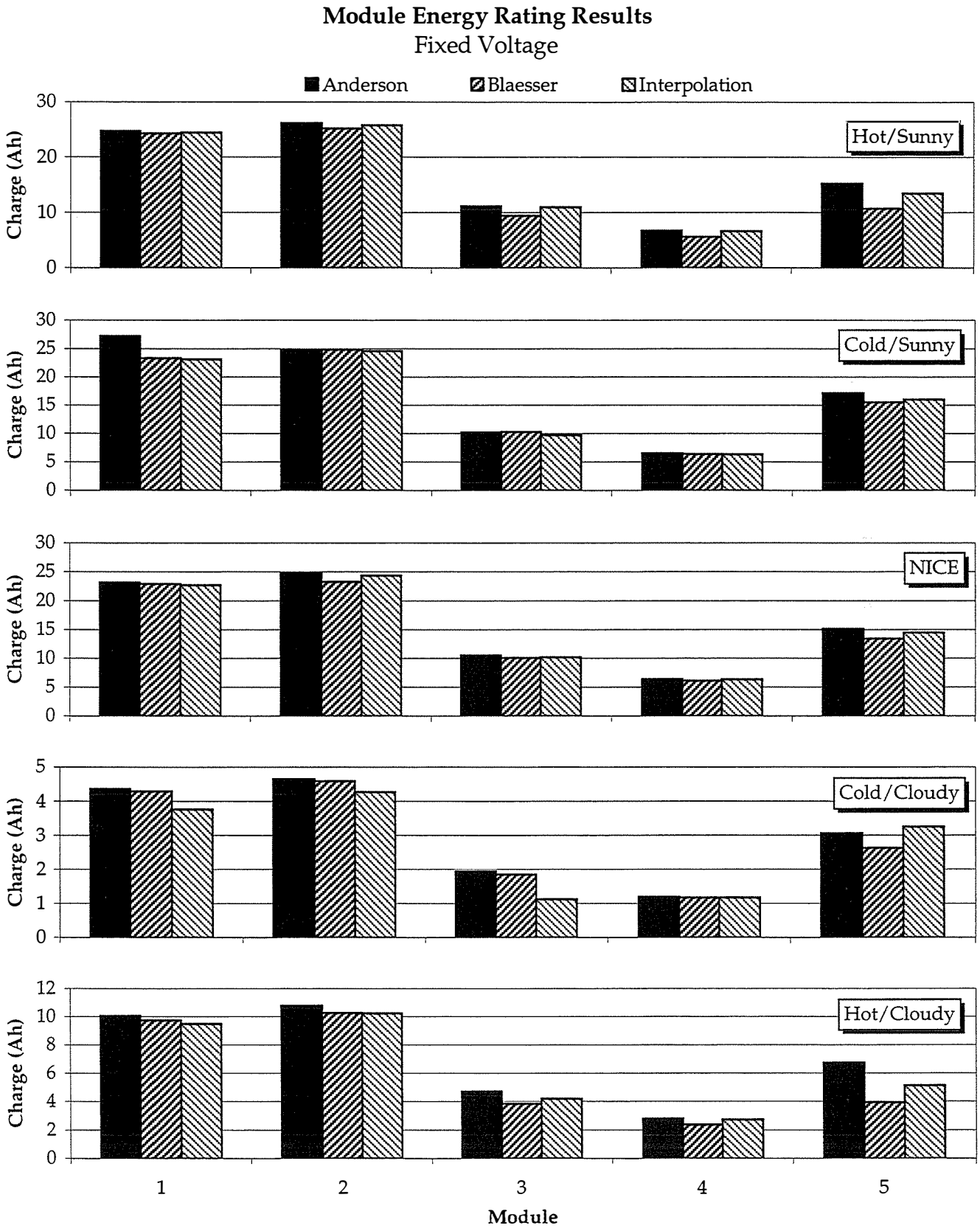

Figure 5-18 Module Energy Rating Results, Fixed Voltage

The most obvious difference between the modules is the magnitude of their production capacity. It is clear that for a given system load, the number of modules required to meet an energy demand will be different for the different module types. Since other factors (such as required Voc or economics) may also affect the system module count, these factors should be accounted for and the product of the module count and the MER values should be compared. If all other factors are equal, then the highest total MER will indicate the best alternative.

Note that the MER values for maximum power loads tend to track their STC relative power ratings, when insolation is disregarded. In theory, the advantage of the MER is that some modules will be more strongly affected by climate than others, leading to cases where a poorly performing module at STC may outperform its competitor(s) in a more realistic climate. For example, modules 1 and 2 have very similar STC ratings, but the difference between their maximum power MER ratings varies with climate. When other factors are included, this fact may change the recommended module for a particular application. While the differences between these two modules are small, comparing with a more sensitive technology like module 3 in an otherwise similar system configuration, the differences would likely be more distinct.

In contrast with the maximum power MER rating, the fixed voltage MER rating does not track the STC power rating well, unless the module is designed for this type of application. Comparing the fixed voltage and maximum power MER estimates for Module 4 shows how dramatic this effect can be. Of course, this module has an open circuit voltage of 90.2 V, so this module was probably not intended for battery charging.

6. CONCLUSIONS AND RECOMMENDATIONS

This project set out to address three specific goals:

- Define a Module Energy Rating Methodology
- Define specific conditions for evaluating module performance representative of the US climate
- Define procedures and techniques for measuring module characteristics and estimating module performance at the representative conditions

The first of these goals has been squarely met. A general method for describing a PV module energy rating has been developed and agreed upon by an industry-representative Technical Review Committee.

The second goal has been met in principle with the definition of five representative daily weather profiles. These profiles are further defined by the source of weather data (the National Solar Radiation Database) and specific locations and dates within the database. While these suggested weather profiles appear to adequately represent a broad range of geographic locations and climatic conditions, they are subject to change under further scrutiny of system owners and designers.

The third goal has not been satisfactorily met. The combined errors in characterizing module performance, in translating indoor measurements to outdoors, in measuring ambient conditions and module performance, and in accounting for all of the various parameters affecting module performance exceed the accuracy required to compare one module to another under a variety of conditions. Recommendations in the following sections are intended to address the measurement and modeling errors encountered.

A consensus was never reached as to the level of accuracy required for the overall performance modeling. We feel that to provide users with ratings that they can confidently compare and make decisions on, we need to be able to model performance to within 5 percent of actual over the full range of expected conditions. This implies that we need to account for factors that have rather small impact on module performance—as small as 1 percent—so that the combined error of all factors puts us below that 5 percent level. As we all initially suspected and have shown through this initial work, this level of accuracy will not be achieved easily.

A common complaint is that we're making this process too difficult, that it should be easy to perform and simple to calculate. While it is true that the results should be easy

to use and interpret, the steps necessary to achieve those results will likely have to be complex. The process is not intended to be an easy to use tool, only the results are. The process needs to be accurate and repeatable. An easy to use process with low accuracy will provide numbers for users to compare, but the comparisons may not be valid, may misrepresent products and will ultimately prove not useful.

While we are closer to a useful module energy rating, there is still a good deal of work to be done. The following comments are offered to help direct further work on this topic.

6.1 Testing

- Modules used for model validation should be representative of industry current production. This requirement is more difficult to implement and more critical for advanced thin film devices for which "current production" changes rapidly.

6.1.1 Indoor Tests

- Data used to characterize module performance must span the range of conditions that are to be modeled, especially for the interpolation model.

- The requirement for a broad range of measurements must be weighed against the added error of attempting to create extreme conditions, particularly irradiance. Most simulators are designed and calibrated for 1000 W/m^2 ASTM AM 1.5 spectrum based on a specific amount of power being fed to a specific light source placed a specific distance from the test device. Higher irradiances can be achieved by increasing the power to the light source, which will likely change spectral content, or by moving the light source closer to the module, which could introduce light distribution non-uniformity.

  Reducing intensity can also be done by several different methods. Reducing the power to the light source will also change the spectral content. Moving the light source away from the PV module could actually improve distribution uniformity, but may not be physically possible due to test chamber dimensions. The final option is to use neutral density filters to attenuate the light; however, all filters are somewhat wavelength dependent and may suffer from non-uniformities.

- Translation of indoor flash tests to outdoor measurements has been an ongoing battle. Confidence is fairly high if the conditions being translated from and to are not vastly different and if crystalline silicon is used. Unfortunately, our requirements are for the broadest of translation conditions and for all technologies. One thought is that modules may perform differently under direct and diffuse light conditions than they do under the direct-only conditions in a simulator.

6.1.2 Outdoor Tests

- Validation data must represent the range of climatic conditions that are to be modeled.

- Sufficient data under these various conditions must be collected to reduce statistical uncertainty.

- Highest accuracy irradiance data will likely be achieved using the cavity radiometer and *in-plane* diffuse measurements. A method for accurately measuring in-plane diffuse needs to be developed.

6.2 Validation Analysis

- All of the results presented here are based on software. There is a substantial amount of code involved in performing these calculations and, though an extensive effort was made to eliminate bugs, there is always the possibility that bugs still exist.

6.2.1 Power Models

- Model coefficients should be generated using the same types of input data as the resulting models will use. For example, spectral corrections and incidence angle modifiers should be applied to measured irradiance when outdoor data are used.

- The results tend to favor models based on outdoor characterizations when compared to outdoor validation data. This is not a wholly unexpected conclusion, however, it was anticipated that proper accounting for the differences between indoor and outdoor measurements could be made.

- It appears that, ultimately, different power models will be specified for different technologies. Though we had difficulties with the diode model analytical approach, this may prove to be the most accurate. However, these models are very technology specific and, presently, we've only found models for single and poly-crystalline silicon. Further research in this area is necessary.

- None of the modeling or validation work involved concentrator modules. There are some unique characteristics associated with concentrators that are not dealt with in the existing models. For example, under high concentration crystalline silicon efficiency changes much more dramatically with changes in irradiance than under one-sun conditions. Concentrators have to be included in this research at some point. Fortunately, the overall MER approach and the definition of weather conditions is independent of module type; only the modeling and characterization work needs to be expanded.

6.2.1.1 Anderson Model

The work performed by Sunset Technology and documented under a separate NREL report [Anderson, 1994] shows that this model should perform better than we have observed. However, Anderson's validation results in that report were based on the matrix flash simulator IV curves used to develop the coefficients, not on independent outdoor measurements. These results may not address the applicability of the model to outdoor data.

6.2.1.2 Blaesser Model

- Blaesser states that the coefficients for his model can be obtained with a few IV curves under different conditions. His intent was to provide a simple method to evaluate PV array performance by making some standard measurements and translating the results to STC. His method provides a great deal of simplicity (no module temperature measurements), and the model has more than sufficient accuracy relative to the equipment used in field testing. For our purposes, we would expect Anderson to work better as it makes no assumptions about module thermal characteristics. However, the Blaesser derivation appears to address some of those mystical outdoor characteristics that elude indoor measurement based models.

6.2.1.3 Interpolation Model

- If there are differences between indoor and outdoor measurements that we aren't accounting for, the interpolation model will be the most severely affected.
- A broader range of measurement conditions is necessary to utilize this approach.
- This model might be technology independent if the indoor vs outdoor issues are addressed. Non linearities of multi-junction thin films do not need to be characterized per se, the measurements will take them into account. However, cross dependencies, such as temperature dependence of spectral response, might require multi-dimensional test matrices.

6.2.1.4 Myers Model

- For peak power, the simplest model was as good as any.
- It needs to be evaluated under a broader range of ambient conditions.
- Application of this model to fixed voltage estimation becomes rather complex if a voltage profile is to be defined.

6.2.2 Thermal Model

- Potential areas of weakness within the Fuentes thermal model include the fixed values of emittance and thermal capacitance, the determination of the characteristic length through the use of a quasi-hydraulic diameter calculation, the sky temperature model.
- PVUSA and Sandia are looking at alternative temperature models using regression analysis. These should be compared in detail with the Fuentes model.

6.2.3 Spectral Model

- Spectral effect on insolation was in the 1 to 5% range for the sample modules. While significant, the power model accuracy will have to improve before

these effects can be distinguished. In many cases, spectral effects will not contribute significantly to the difference between modules.

- Multi-bandgap technologies will need significantly more work in order to account for spectral effects. The interactions between the junctions when spectral variation occurs can change the shape of the IV curve, necessitating an integrated power and spectral model. No attempt to handle these technologies has been attempted in this work.

6.2.4 Optical Model

- While some measurements were made, very little analysis was performed on incidence angle effects.

- Differences in albedo and diffuse sky component associated with measurements made outdoors may be of the same order of magnitude as the incidence angle effect itself. These errors can be reduced if measurements are made under very clear sky conditions, by varying only the module azimuth angle, and at locations where ground reflectance and the elevation of the horizon are constant in all directions.

- Indoor flash tests at varying incidence angles can be used to eliminate the diffuse problem, but the relative distances between the near and far edges of the module with respect to the light source become important.

- It has been suggested that laser ray tracing might provide more accurate results by eliminating the diffuse problem and the problem of one edge of the module being closer to the light source than the other edge. Care must be taken to ensure that the beam of light strikes the same area of cell as the incidence angle is varied (non-uniform response) and does not strike any inactive cell area (grid lines or interconnects).

- While it is generally agreed that an IAM should be applied to the direct component, there is less agreement as to if and how to apply an IAM to the diffuse component. One currently used application of an IAM (King, 1996) applies the correction to the global plane of array irradiance. This application under high diffuse conditions needs to be evaluated.

6.2.5 Irradiance Model

- The problems of early morning and late afternoon errors in the Perez model need to be addressed. A work around was implemented for these results, but a more thorough solution should be implemented.

6.3 MER Calculations

- For our purposes, where we are continuously changing parameters and rerunning the MER calculations for multiple modules and multiple models, the Access database is rather slow. However, it allows us to conveniently evaluate and modify intermediate results, which would be much more difficult using a traditional programming language. There are many optimizations that can be made to the final product to enhance its speed. Also, a user will typically analyze only one module at a time using one power model.

- It is clear that the fixed voltage MER will show a very different view of some modules than the maximum power MER will. This will offer manufacturers a significantly different benchmark to optimize their products for (should they so choose). The results presented here show that if an appropriate number of series modules and batteries are used, poor performance will result. The fixed voltage performance of Module 4 is an example of this behavior.

- The selection of a fixed 14.4 battery voltage is a simplification that may not be necessary and may be misrepresentative. A battery profile would be preferable, but agreeing on an appropriate profile might be difficult. Also, the difference between battery terminal voltage and the module voltage need to be accounted for (blocking diodes, charge controller losses, wiring losses, etc.).

- The TRC felt rather strongly that the MER should be presented in terms of W-h or A-h, which will vary significantly with module power but which are comprehendible by most PV buyers. Other terms such as efficiency or normalized values like W-h/W_{Rated} and A-h/A_{Rated} are more easily compared but are more obscure. Ultimately the user can divide the module's cost by appropriate MER value and compare the $/W-h or $/A-h values directly.

7. REFERENCES

A. J. Anderson, "Photovoltaic Translation Equations: A New Approach," Final Report for Task 1.0 of NREL Subcontract No. TAD-4-14166-01, November 1994.

R. E. Bird, Riordan, C., "Simple Solar Spectral Model for Direct and Diffuse Irradiance on Horizontal and Tilted Planes at the Earth's Surface for Cloudless Atmospheres," Journal of Climate and Applied Meteorology, Volume 25, Number 1, pp. 87-97, January 1986.

G. Blaesser, personal communication, November 1995.

K. Emery, Osterwald, C. R., "Efficiency Measurements and Other Performance Rating Methods," *Current Topics in Photovoltaics*, Volume 3, Academic Press Ltd., 1988.

F. Fabero, Vela, N., Chenlo, F., "Influence of Solar Spectral Variations on the Conversion Efficiency of a-Si and m-Si PV Devices: A Yearly and Hourly Study," preprint from Proceedings of the 23rd Photovoltaic Specialists European Conference, 1995.

M. K. Fuentes, "A Simplified Thermal Model for Flat-Plate Photovoltaic Arrays," Sandia Report SAND85-0330•UC--63, May 1987.

C. F.Gay, Rumberg, J. E., Wilson, J. H., "AM PM - All-Day Module Performance Measurements," Proceedings of the 16th Photovoltaic Specialists Conference, pp. 1041-1046, IEEE, 1982.

D. King, Hansen, B. R., "A Sensitivity Analysis of the Spectral Mismatch Correction Procedure Using Wavelength Dependent Error Sources," Proceedings of the 22nd IEEE Photovoltaic Specialists Conference, October 1991.

D. King, "Photovoltaic Module and Array Performance Characterization Methods for All System Operating Conditions," NREL/SNL Program Review, AIP Press, 1996, pp.347-368.

F. Kreith, Kreider, J. F., *Principles of Solar Engineering*, Hemisphere Publishing Corporation, Washington, D. C., 1978.

J. Meeus, *Astronomical Formulae for Calculators*, Second Edition, Willmann-Bell, Richmond, VA, 1982.

S. Nann, Emery, K., "Spectral Effects on PV-Device Rating," Solar Energy Materials and Solar Cells, Volume 27, pp. 189-216, 1992.

S. Nann, Riordan, C., "Solar Spectral Irradiance Under Clear and Cloudy Skies: Measurements and a Semiempirical Model," Journal of Applied Meteorology, Volume 30, Number 4, pp. 447-462, April 1991.

R. Perez, Stewart, R., Seals, R., Guertin, T., "The Development and Verification of the Perez Diffuse Radiation Model," Contractor Report SAND88-7030, Sandia National Laboratories, Albuquerque, NM, 1988.

R. Perez, Seals, R., Ineichen, P., Stewart, R., Menicucci, D., "A New Simplified Version of the Perez Diffuse Irradiance Model for Tilted Surfaces," Solar Energy, Volume 39, Number 3, pp. 221-231, 1987.

W.H. Press, Flannery, B. P., Teukolsky, S. A., Vetterling, W. T., *Numerical Recipes*, Cambridge University Press, Cambridge, 1986.

T. Townsend, "A Method for Estimating the Long-Term Performance of Direct-Coupled Photovoltaic Systems," MS Thesis, University of Wisconsin, 1989.

H. S. Rauschenbach, *Solar Cell Array Design Handbook*, Van Nostrand Reinhold, New York, 1980.

C. Seaman, "Correction for Spectral Mismatch Effects on the Calibration of a Solar Cell When Using a Solar Simulator," DOE/JPL-1012-50, January 1981.

C. M. Whitaker, Townsend, T. U., Wenger, H.J., Iliceto, A., Chimento, G., Paletta, F., "Effects of Irradiance and Either Factors on PV Temperature Coefficients," Proceedings of the 22nd IEEE Photovoltaic Specialists Conference, October 1991.

APPENDIX A INDOOR MODULE TESTING DATA

Table 0-1. Summary of Indoor Testing Data (Modules 1, 2 and 3)

Module	*T* (C)	*H* (W/m²)	Sheets	*Voc,est* (V)	*Voc,Spire* (V)	*Isc* (A)	*Vmp* (V)	*Imp* (A)	*Pmp* (W)
1	20	1000	0	22	22	3.32	17.6	3.07	54.1
1	20	773	1	21.8	21.8	2.56	18	2.35	42.2
1	20	487	3	21.4	21.4	1.62	18.1	1.44	26
1	20	253	7	20.7	20.7	0.84	18	0.71	12.8
1	30.3	1000	0	21.3	21.3	3.31	17.2	3	51.8
1	30.2	773	1	21.1	21.1	2.57	17.1	2.36	40.4
1	30.3	487	3	20.6	20.6	1.63	17	1.48	25.1
1	30.4	253	7	19.9	19.9	0.86	17.1	0.73	12.4
1	40.2	1000	0	20.7	20.7	3.33	16.3	3.05	49.8
1	40.2	773	1	20.4	20.4	2.54	16.3	2.34	38.2
1	40.5	487	3	20	20	1.61	16.6	1.44	23.9
1	40.9	253	7	19.2	19.2	0.83	16.1	0.73	11.7
1	50	1000	0	20.1	20.1	3.35	15.6	3.08	48
1	50.2	773	1	19.8	19.8	2.58	15.9	2.32	37
1	50.2	487	3	19.3	19.3	1.63	15.6	1.49	23.2
1	50.3	253	7	18.6	18.6	0.86	15.4	0.75	11.5
2	19.7	1000	0	21.6	21.6	3.57	17.4	3.24	56.4
2	19.6	762	1	21.4	21.4	2.72	17.7	2.45	43.3
2	19.6	485	3	20.9	20.9	1.73	17.7	1.53	26.9
2	19.6	257	7	20.2	21.7	0.92	17.2	0.8	13.7
2	30.5	1000	0	20.9	20.9	3.58	16.5	3.25	53.6
2	30.6	762	1	20.6	20.7	2.74	16.8	2.45	41.2
2	30.3	485	3	20	20.2	1.74	17	1.52	25.8
2	30.3	257	7	19.4	19.5	0.93	16.6	0.79	13.1
2	40.5	1000	0	20.3	20.3	3.6	15.5	3.3	51.1
2	40	762	1	19.9	20	2.75	16	2.47	39.4
2	40.1	485	3	19.4	19.5	1.75	15.9	1.54	24.6
2	40.1	257	7	18.7	18.7	0.93	15.6	0.81	12.6
2	49.9	1000	0	19.6	19.6	3.61	15	3.24	48.6
2	49.9	762	1	19.3	19.3	2.77	14.9	2.52	37.6
2	50.2	485	3	18.8	18.8	1.75	15.2	1.56	23.8
2	50.5	257	7	18	18	0.94	15	0.81	12.1
3	20.1	1000	0	15.1	15.1	1.76	10.4	1.31	13.7
3	20.1	741	1	14.9	14.9	1.31	10.7	0.95	10.2
3	20.1	443	3	14.5	14.5	0.78	10.9	0.55	6
3	20.1	205	7	13	13	0.36	9.9	0.24	2.4
3	29.5	1000	0	14.7	14.7	1.78	10.1	1.35	13.6
3	29.3	741	1	14.5	14.5	1.32	10.4	0.99	10.3
3	29.3	443	3	14.1	14.1	0.79	10.3	0.58	6
3	29	205	7	13.5	13.5	0.37	10.7	0.24	2.5
3	40	1000	0	14.3	14.3	1.8	9.8	1.39	13.6
3	40	741	1	14.1	14.1	1.33	10.2	0.99	10.1
3	40.1	443	3	13.7	13.7	0.8	9.7	0.62	6
3	40.2	205	7	13.1	13.1	0.37	10.4	0.24	2.5
3	50.1	1000	0	14	14	1.81	9.7	1.38	13.5
3	50.1	741	1	13.7	13.8	1.35	9.9	1.02	10.1
3	50.1	443	3	13.3	13.3	0.8	9.7	0.61	5.9
3	50.2	205	7	12.6	12.6	0.37	9.7	0.25	2.4

Table 0-2. Summary of Indoor Test Data (Modules 4 and 5)

Module	T (C)	H (W/m^2)	Sheets	Voc,est (V)	Voc,Spire (V)	Isc (A)	Vmp (V)	Imp (A)	Pmp (W)
4	19.2	1000	0	91	91	0.92	68.2	0.8	54.3
4	19.5	741	1	90.1	90.1	0.68	69.3	0.59	41.1
4	19.5	456	3	88.3	88.2	0.42	68.6	0.37	25.4
4	19.5	237	7	85.7	85.7	0.22	67.3	0.19	12.9
4	30	1000	0	89.4	89.4	0.92	67.2	0.79	53
4	30.1	741	1	88.3	88.3	0.68	66.7	0.6	40.2
4	30.1	456	3	86.4	86.4	0.42	68.1	0.36	24.7
4	30	237	7	83.7	83.6	0.22	65.4	0.19	12.6
4	40	1000	0	86.9	86.9	0.92	65.1	0.79	51.4
4	40.1	741	1	85.6	85.6	0.69	65.4	0.59	38.8
4	40.1	456	3	83.6	83.7	0.42	63.9	0.37	23.9
4	40.2	237	7	80.6	80.6	0.22	63.3	0.19	12.1
4	50.1	1000	0	84.7	84.8	0.92	64.2	0.78	50.3
4	50.2	741	1	83.4	83.4	0.69	63.6	0.59	37.8
4	49.9	456	3	81.2	81.2	0.42	62.1	0.37	23.3
4	50.2	237	7	78.1	78.1	0.22	60.5	0.19	11.7
5	20	1000	0	23.1	23.1	2.33	16.6	1.94	32.2
5	19.9	767	1	22.6	22.6	1.79	16.4	1.48	24.3
5	19.9	485	3	21.5	21.5	1.13	15.7	0.93	14.6
5	19.8	255	7	19.9	19.9	0.6	14.3	0.5	7.1
5	30.8	1000	0	22.2	22.2	2.34	15.5	1.98	30.7
5	30.9	767	1	21.5	21.5	1.78	15.5	1.48	22.8
5	30.9	485	3	20.4	20.4	1.13	14.6	0.94	13.8
5	30.9	255	7	18.8	18.8	0.6	13.4	0.49	6.5
5	40.3	1000	0	21.1	21.1	2.34	15	1.92	28.8
5	40.1	767	1	20.4	20.5	1.79	14.7	1.46	21.5
5	40.2	485	3	19.3	19.3	1.13	13.8	0.92	12.7
5	40.2	255	7	17.7	17.7	0.6	12.5	0.49	6.1
5	50.4	1000	0	20.1	20.1	2.33	14.5	1.86	27.1
5	50.5	767	1	19.4	19.4	1.78	13.7	1.46	20
5	50.7	485	3	18.3	18.2	1.14	13	0.92	12
5	50.7	255	7	16.5	16.5	0.6	11.5	0.48	5.6

APPENDIX B ADDITIONAL MER POWER MODEL VALIDATION AND COMPARISON PLOTS

In section 5.2.1, Figures 5-5 and 5-6 compared modeled power to measured power and model error as a function of irradiance for each 10-minute average point for module 1. Figures 5-7 and 5-8 showed similar data for fixed voltage operation. The following figures show the corresponding plots for modules 2 through 5.

Module Energy Rating Validation Data

NREL Outdoor Test Facility

Module 2

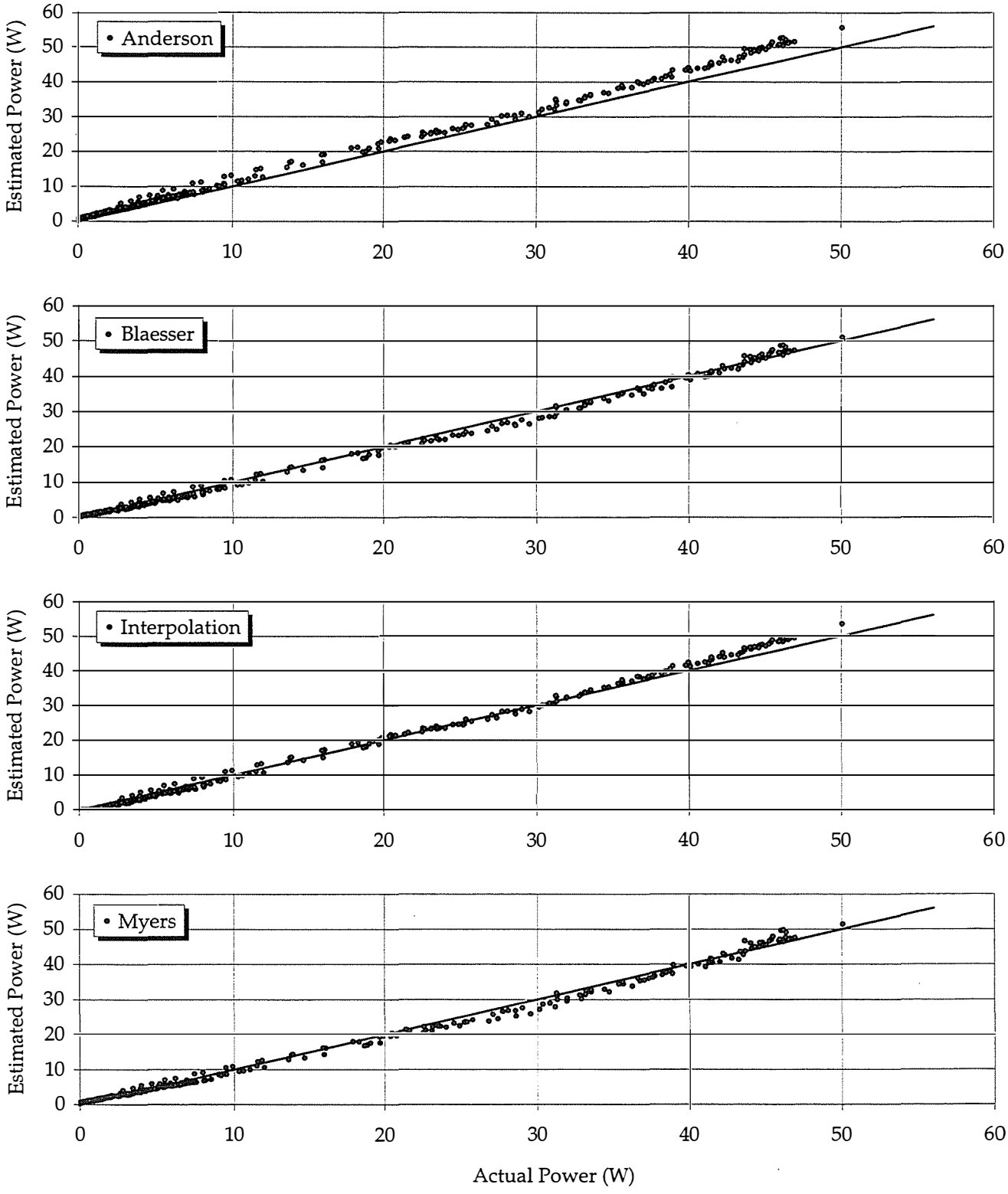

Module Energy Rating Validation Data

NREL Outdoor Test Facility

Module 2

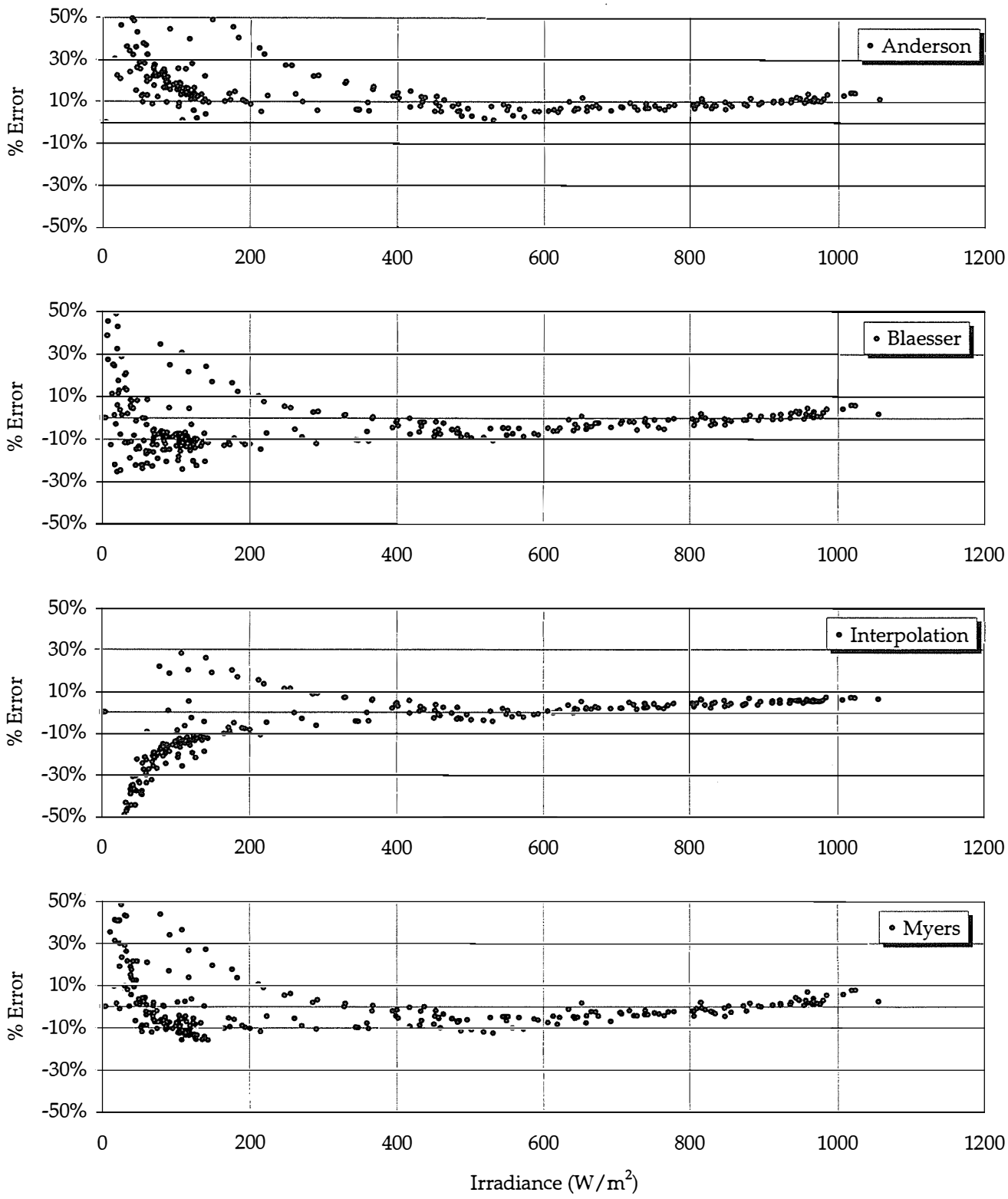

Module Energy Rating Validation Data

NREL Outdoor Test Facility

Module 2 Current at 14.4V (nominal)

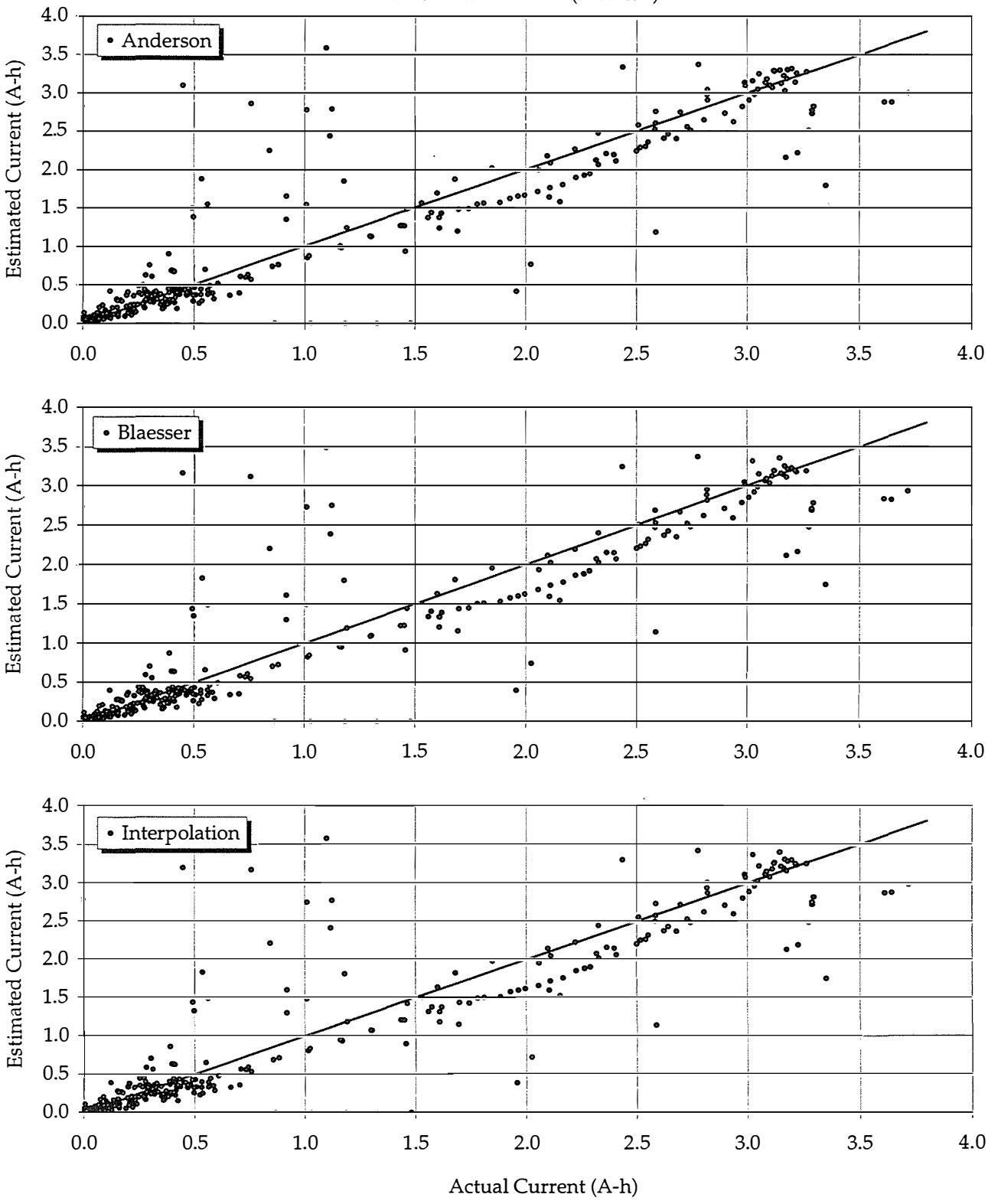

Module Energy Rating Validation Data

NREL Outdoor Test Facility

Module 2 Current at 14.4V (nominal)

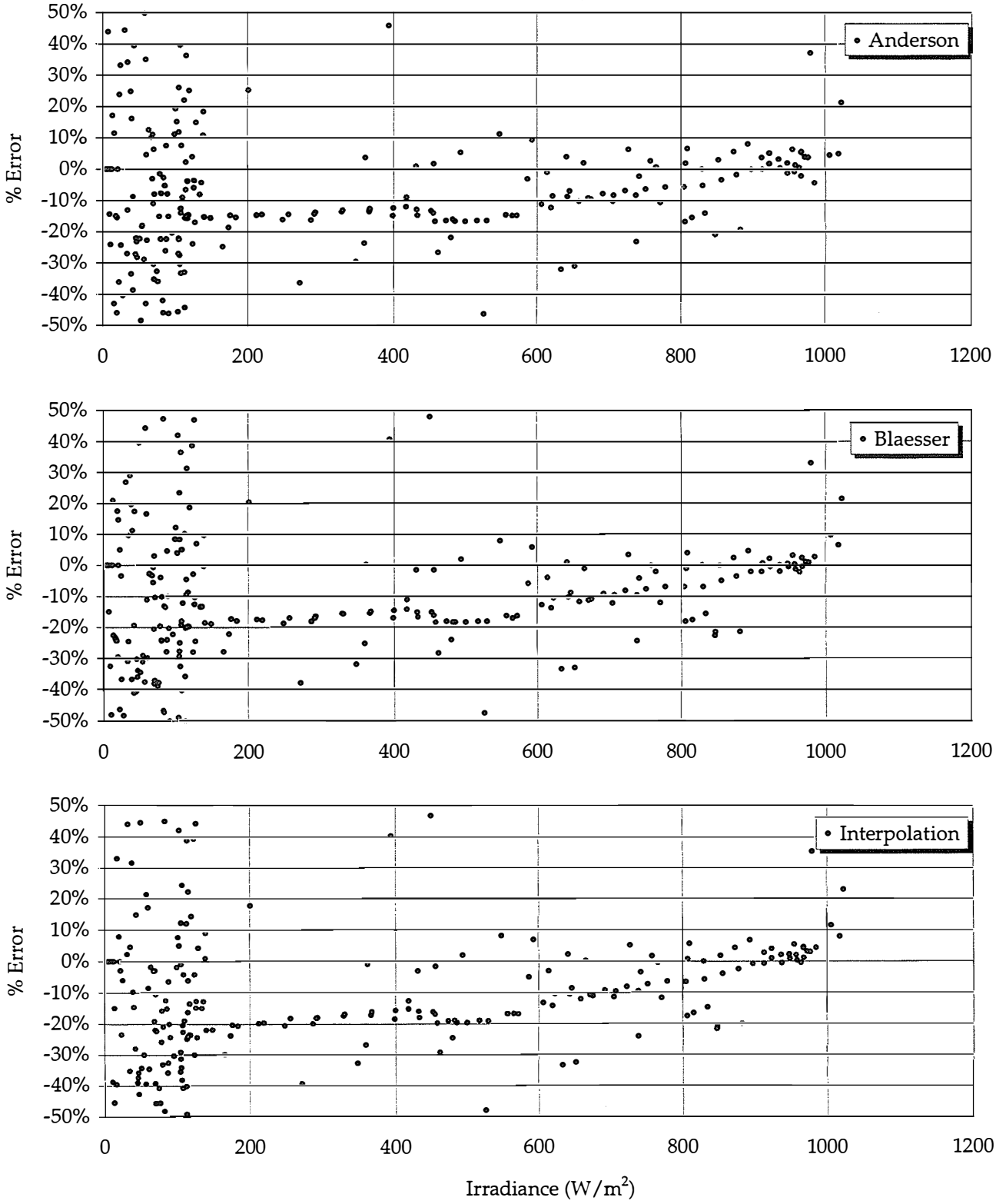

Module Energy Rating Validation Data

NREL Outdoor Test Facility

Module 3

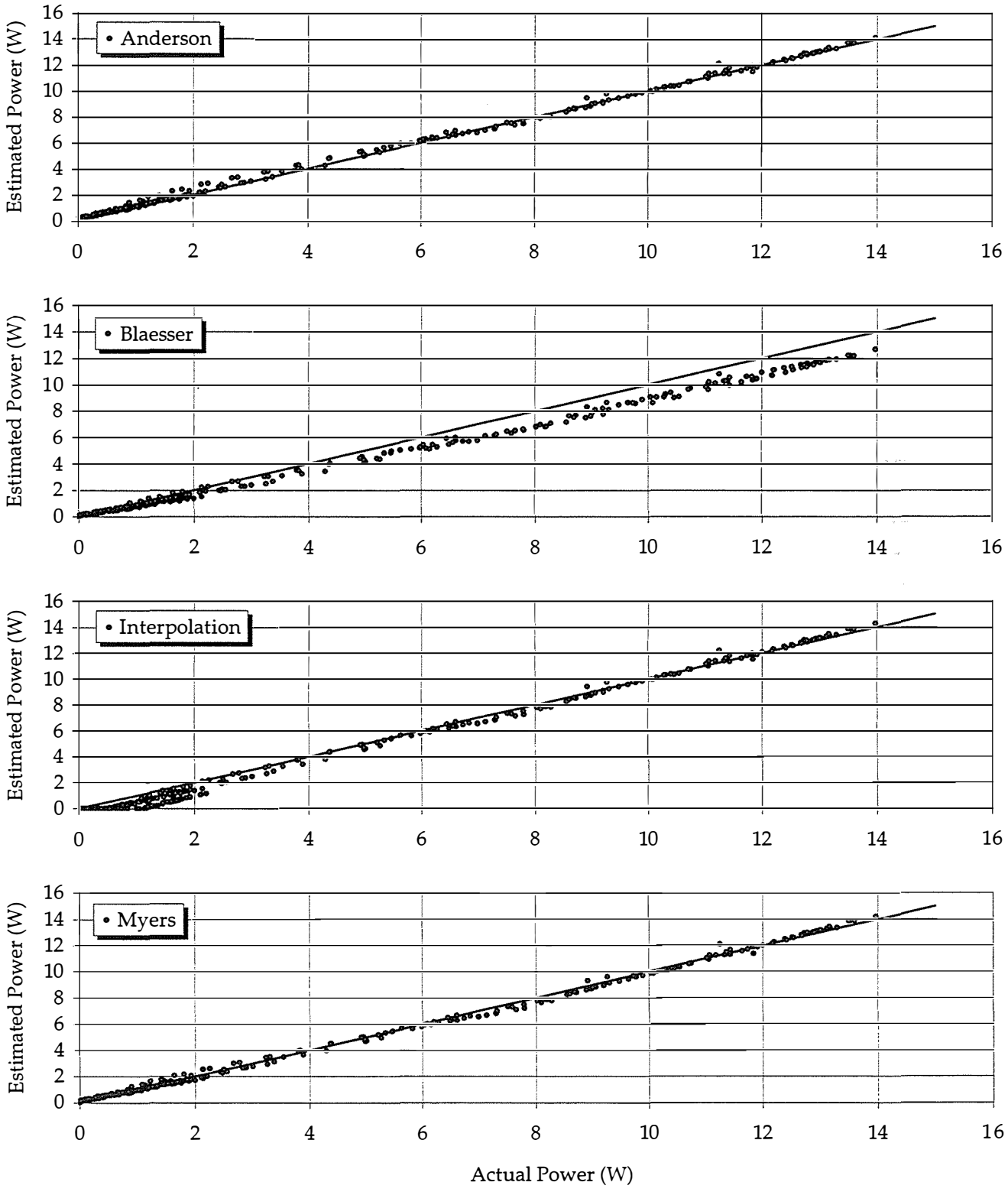

Module Energy Rating Validation Data

NREL Outdoor Test Facility

Module 3

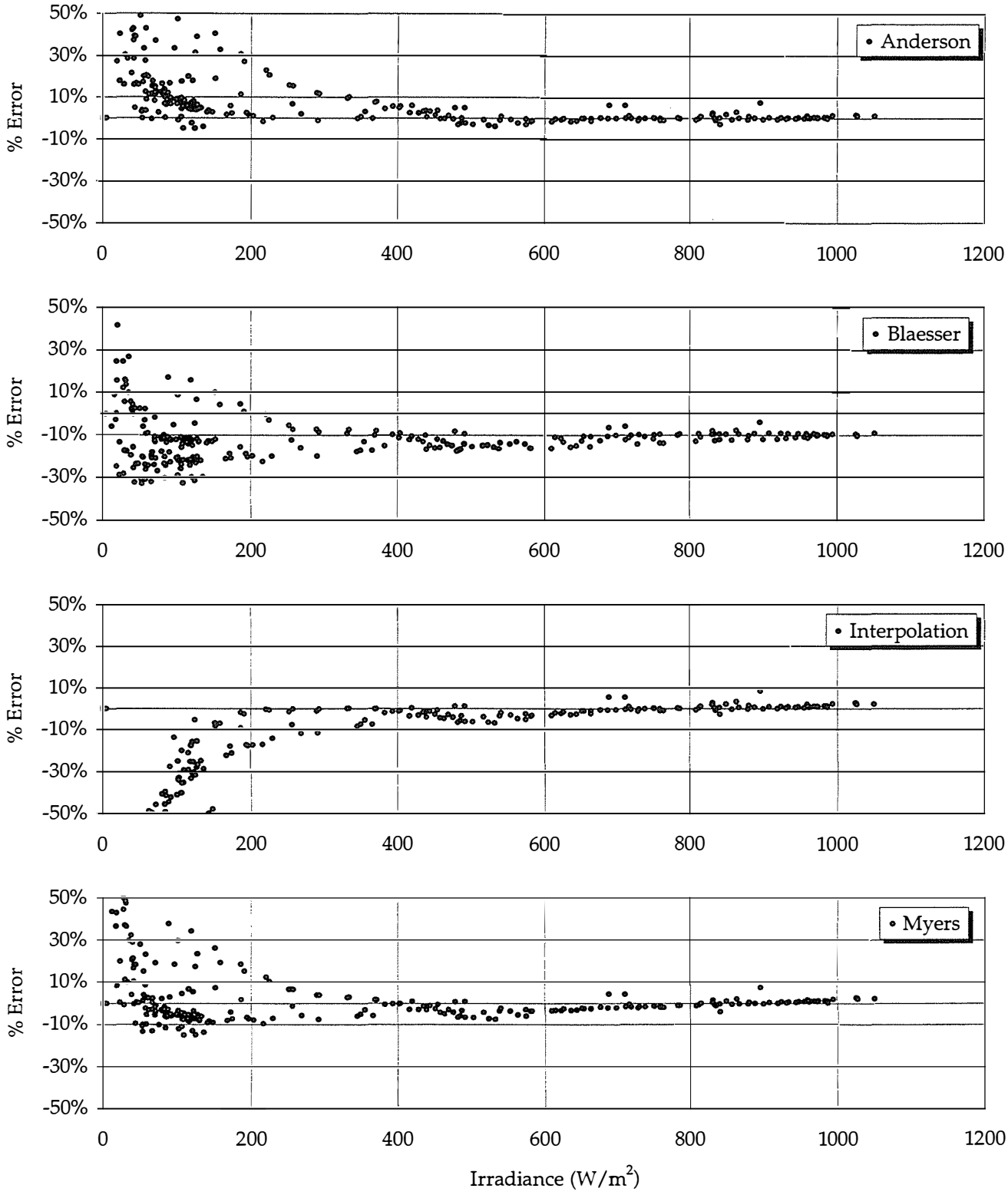

Module Energy Rating Validation Data

NREL Outdoor Test Facility

Module 3 Current at 14.4V (nominal)

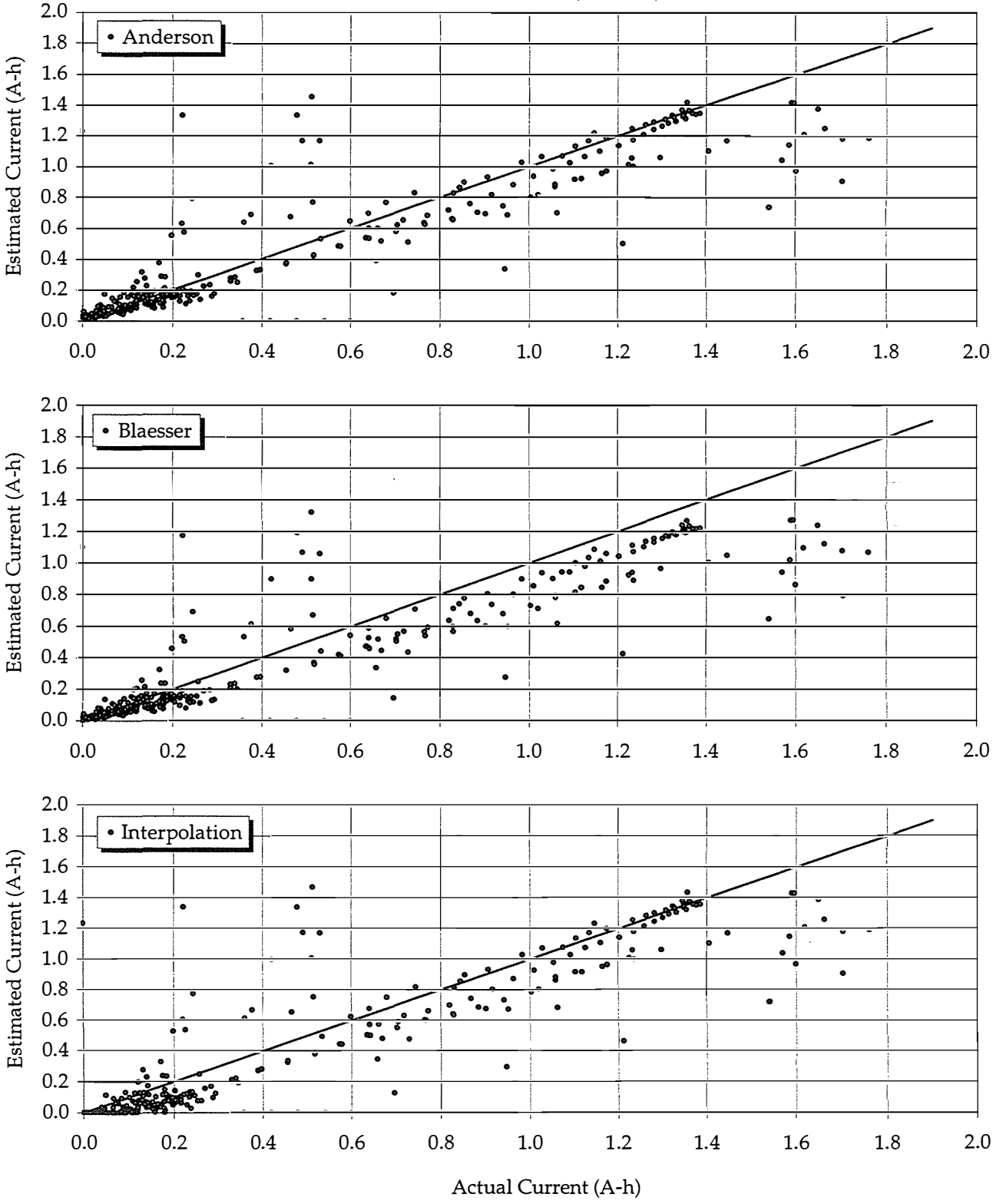

Module Energy Rating Validation Data

NREL Outdoor Test Facility

Module 3 Current at 14.4V (nominal)

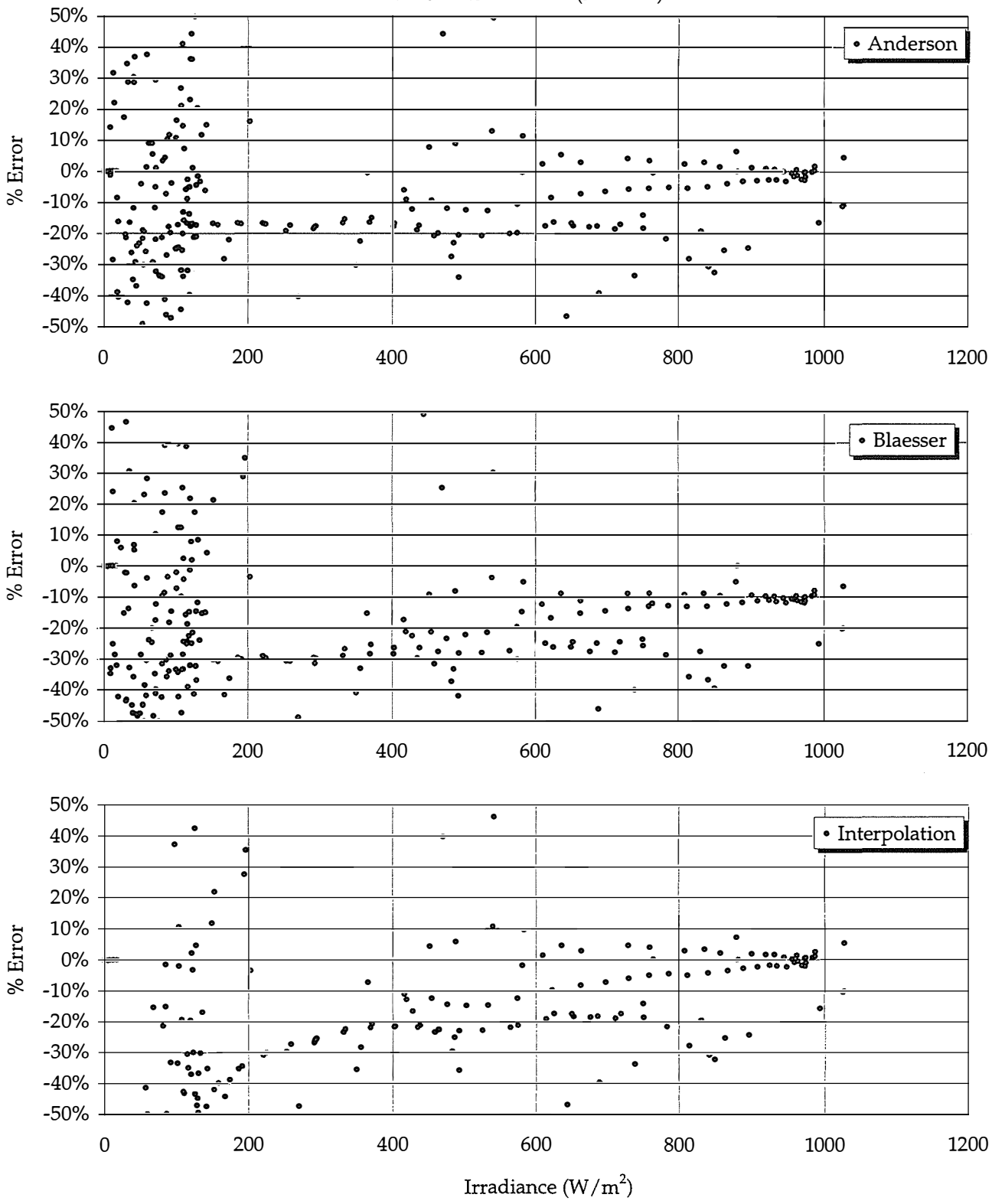

Module Energy Rating Validation Data

NREL Outdoor Test Facility

Module 4

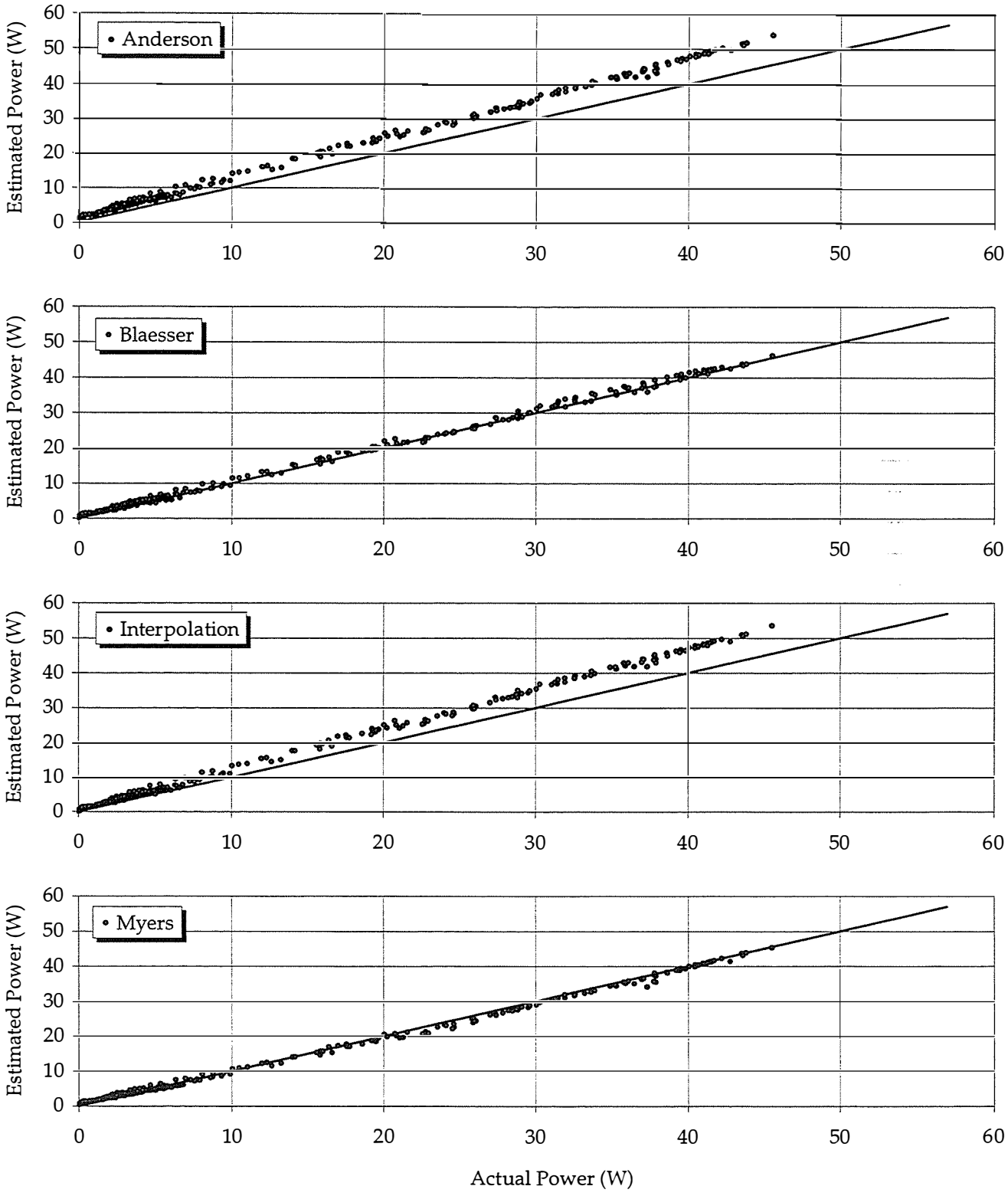

Module Energy Rating Validation Data

NREL Outdoor Test Facility

Module 4

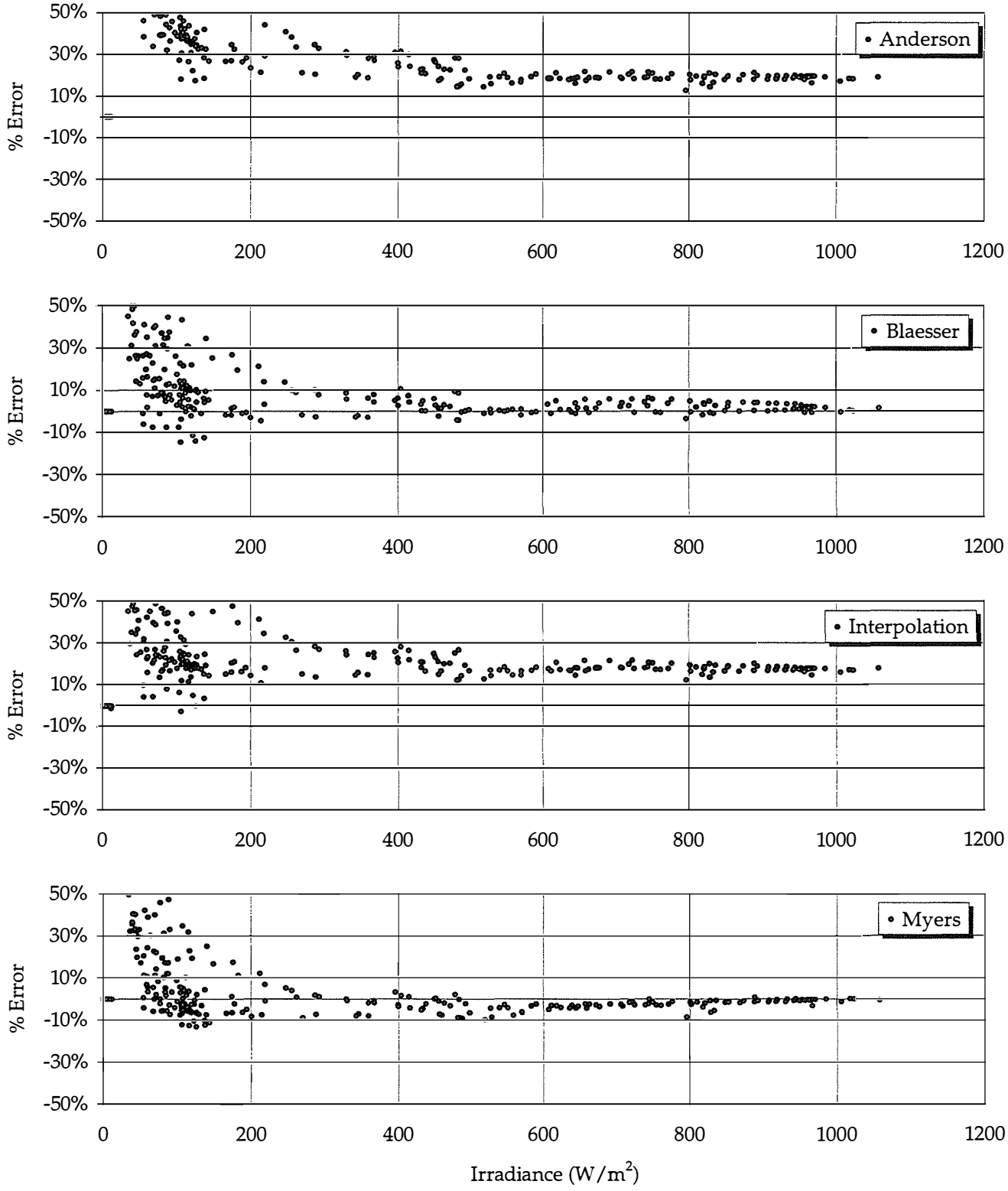

Module Energy Rating Validation Data

NREL Outdoor Test Facility

Module 4 Current at 14.4V (nominal)

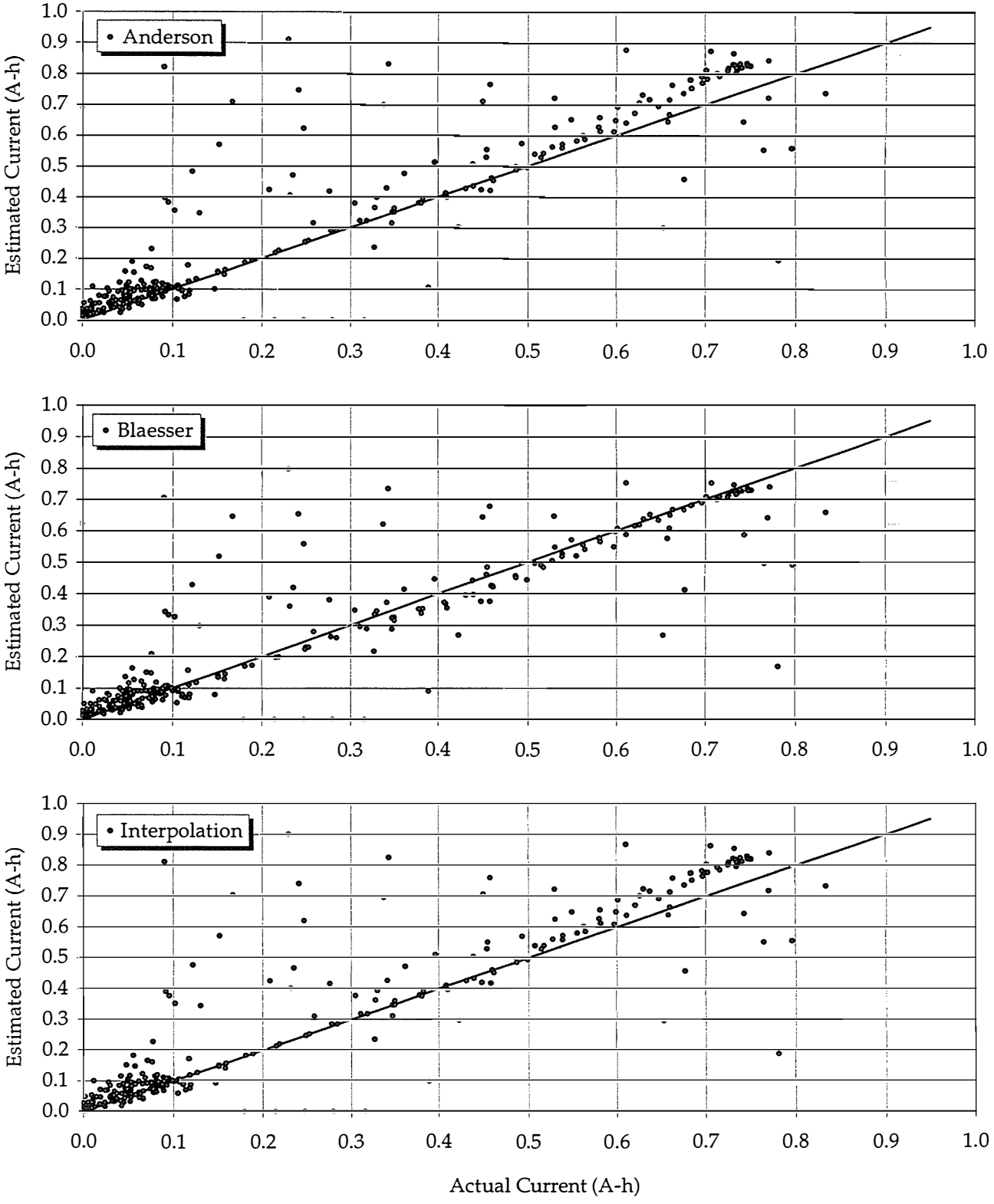

Module Energy Rating Validation Data

NREL Outdoor Test Facility

Module 4 Current at 14.4V (nominal)

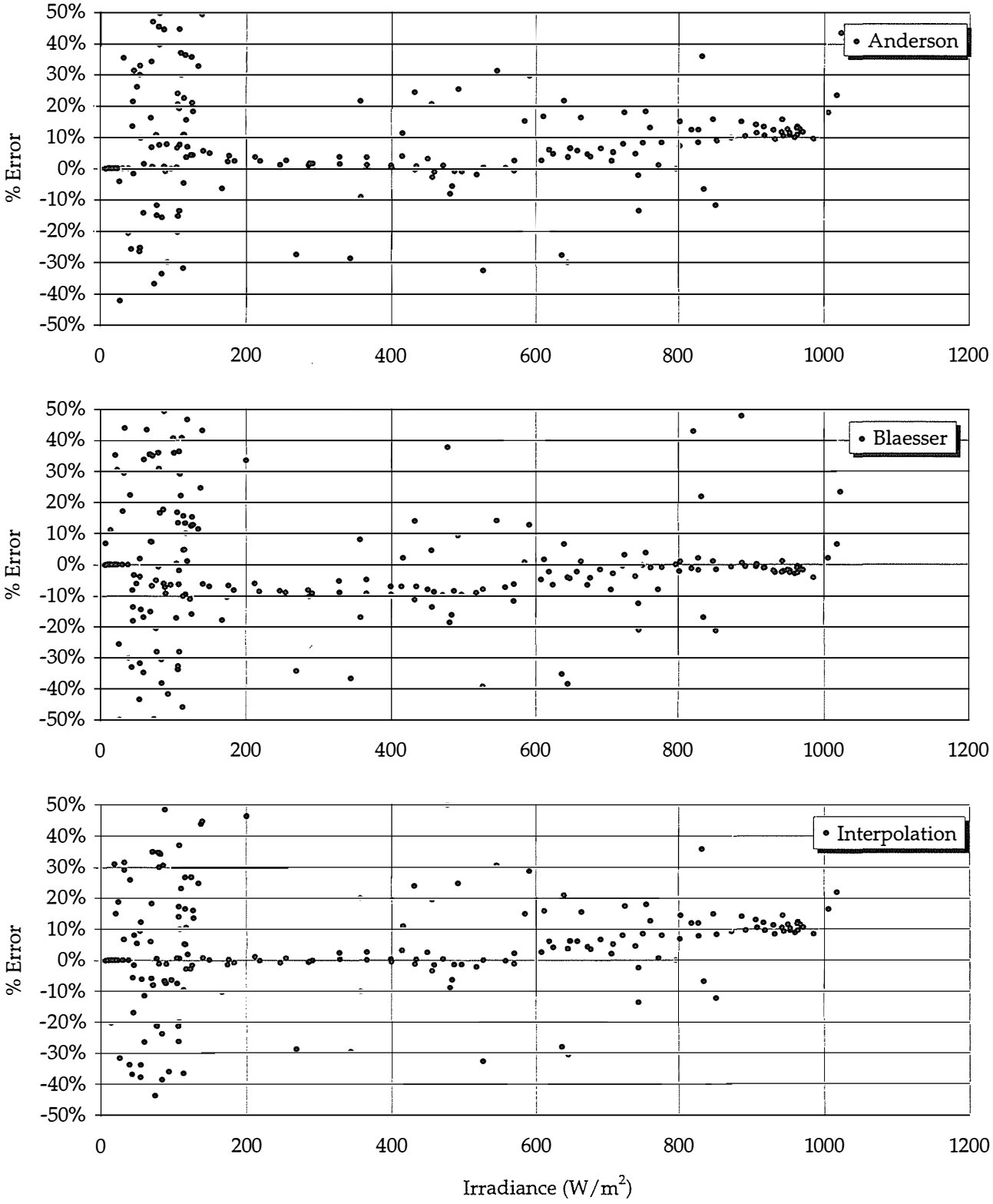

Module Energy Rating Validation Data

NREL Outdoor Test Facility

Module 5

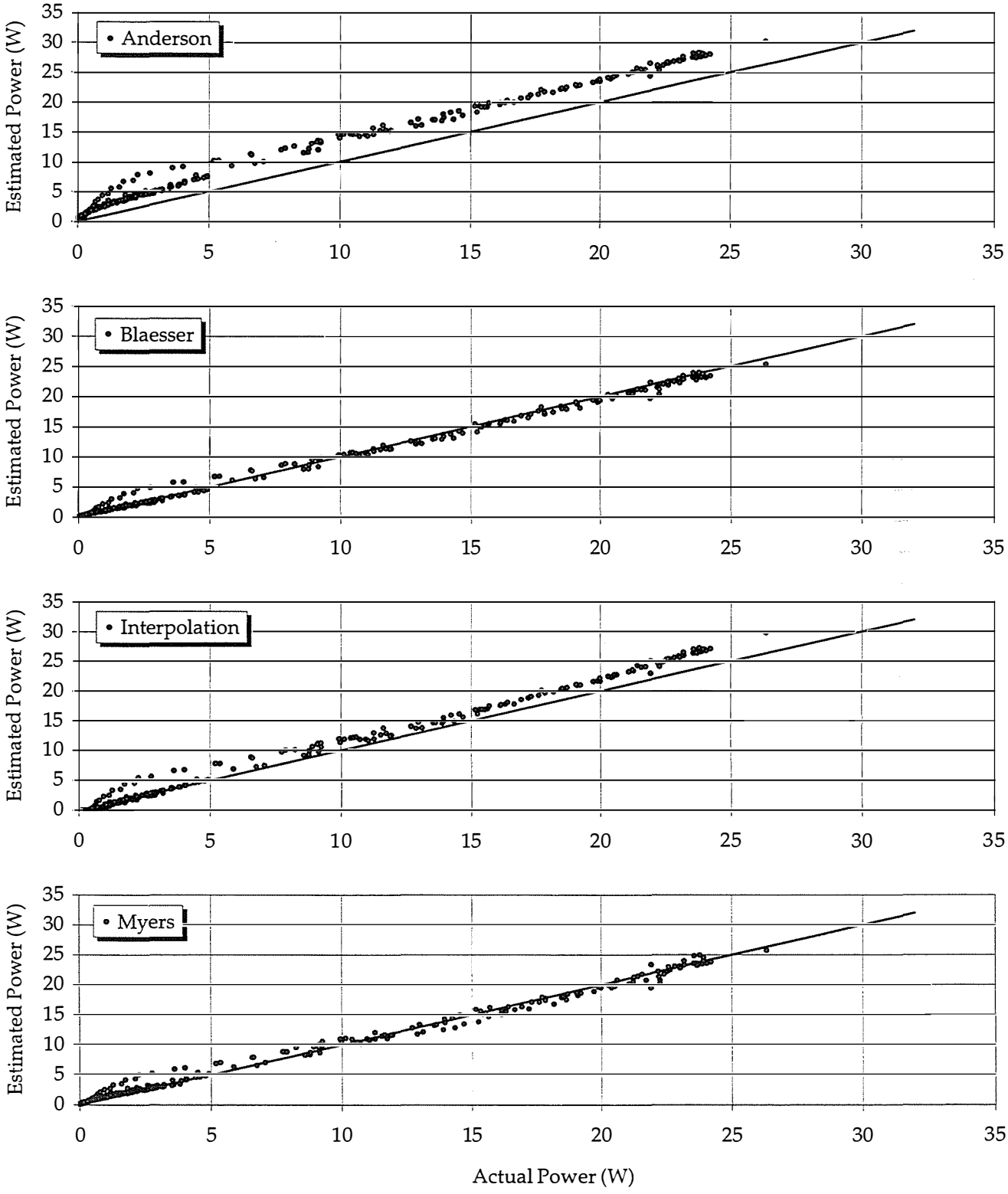

Module Energy Rating Validation Data

NREL Outdoor Test Facility

Module 5

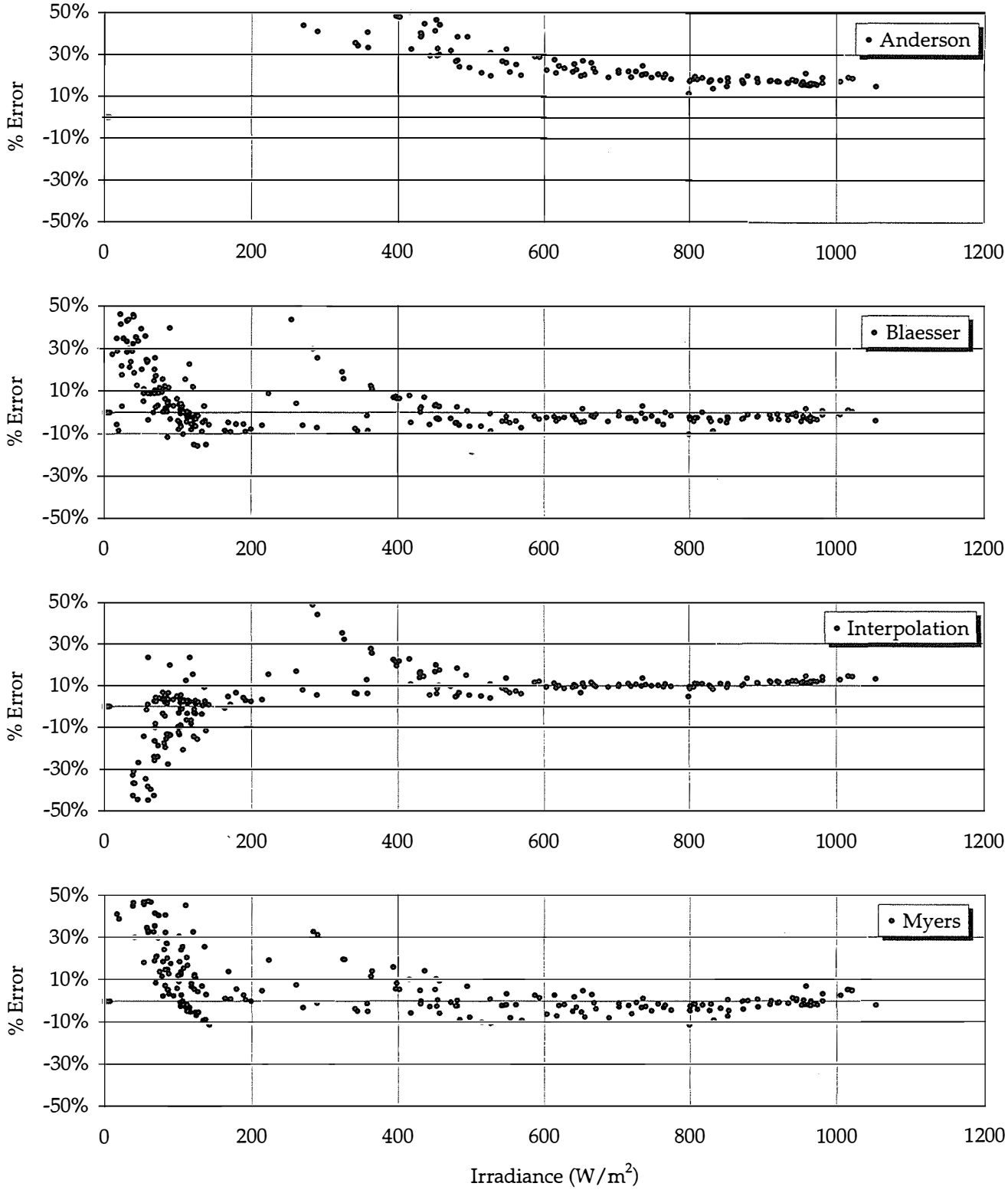

Module Energy Rating Validation Data

NREL Outdoor Test Facility

Module 5 Current at 14.4V (nominal)

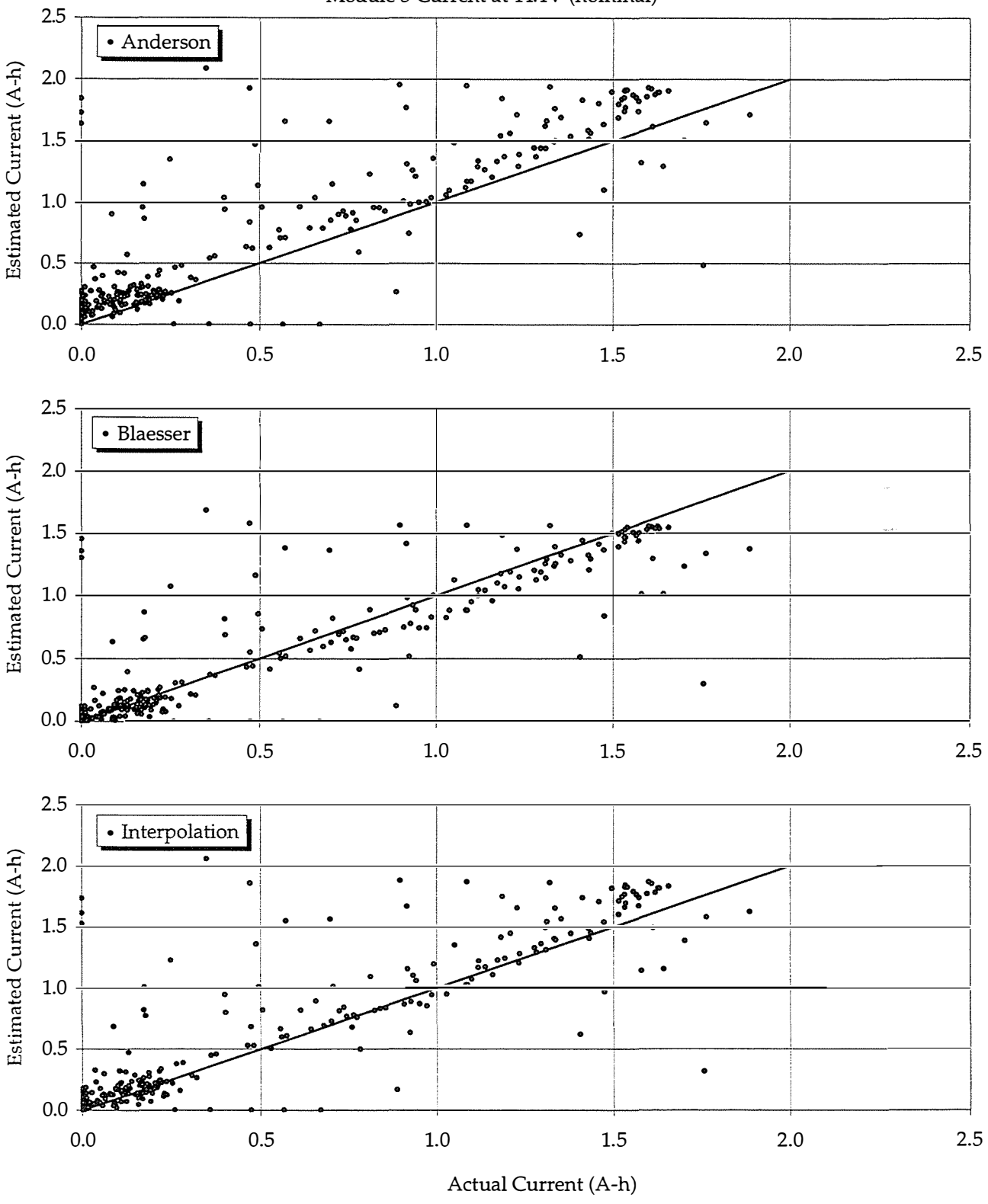

Module Energy Rating Validation Data

NREL Outdoor Test Facility

Module 5 Current at 14.4V (nominal)

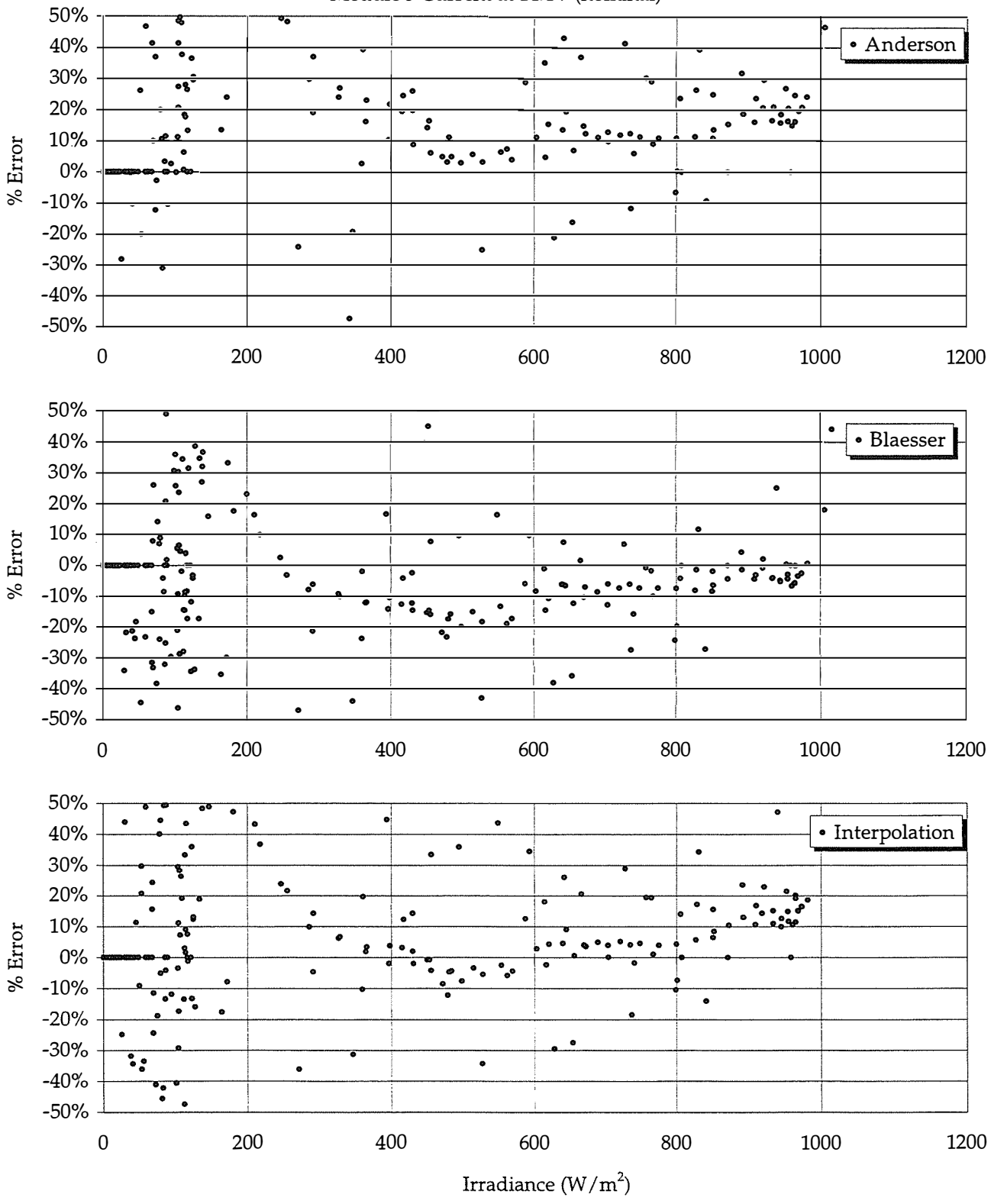

REPORT DOCUMENTATION PAGE

Form Approved
OMB NO. 0704-0188

1. AGENCY USE ONLY (Leave blank)	2. REPORT DATE	3. REPORT TYPE AND DATES COVERED
	January 1998	Final Report

4. TITLE AND SUBTITLE

Photovoltaic Module Energy Rating Procedure; Final Subcontract Report

5. FUNDING NUMBERS

C: AAI-4-14192-01
TA: PV806301

6. AUTHOR(S)

C.M. Whitaker and J.D. Newmiller

7. PERFORMING ORGANIZATION NAME(S) AND ADDRESS(ES)

Endecon Engineering
2500 Old Crow Canyon Road
San Ramon, California 94583

8. PERFORMING ORGANIZATION REPORT NUMBER

9. SPONSORING/MONITORING AGENCY NAME(S) AND ADDRESS(ES)

National Renewable Energy Laboratory
1617 Cole Blvd.
Golden, CO 80401-3393

10. SPONSORING/MONITORING AGENCY REPORT NUMBER

SR-520-23942

11. SUPPLEMENTARY NOTES

NREL Technical Monitor: B. Kroposki

12a. DISTRIBUTION/AVAILABILITY STATEMENT

12b. DISTRIBUTION CODE

UC-1270

13. ABSTRACT *(Maximum 200 words)*

This document describes testing and computation procedures used to generate a photovoltaic Module Energy Rating (MER). The MER consists of 10 estimates of the amount of energy a single module of a particular type (make and model) will produce in one day. Module energy values are calculated for each of five different sets of weather conditions (defined by location and date) and two load types. Because reproduction of these exact testing conditions in the field or laboratory is not feasible, limited testing and modeling procedures and assumptions are specified.

14. SUBJECT TERMS

photovoltaics ; module energy rating ; MER ; module characterization ; performance

15. NUMBER OF PAGES

126

16. PRICE CODE

17. SECURITY CLASSIFICATION OF REPORT	18. SECURITY CLASSIFICATION OF THIS PAGE	19. SECURITY CLASSIFICATION OF ABSTRACT	20. LIMITATION OF ABSTRACT
Unclassified	Unclassified	Unclassified	UL